Supporting Information

Tricyclic SpiroLactams Kill Mycobacteria *in vitro* and *in vivo* by Inhibiting Type II NADH Dehydrogenases

Sushovan Dam[#], Salia Tangara[#], Claire Hamela[#], Theo Hattabi, Léo Faïon, Paul Carre, Rudy Antoine, Adrien Herledan, Florence Leroux, Catherine Piveteau, Maxime Eveque, Marion Flipo, Benoit Deprez, Laurent Kremer, Nicolas Willand*, Baptiste Villemagne*, Ruben C. Hartkoorn*

[#] Joint first authors: Sushovan Dam, Salia Tangara and Claire Hamela contributed equally

*Joint last and corresponding authors: Nicolas Willand, Baptiste Villemagne and Ruben C. Hartkoorn jointly supervised this work

nicolas.willand@univ-lille.fr

baptiste.villemagne@univ-lille.fr

ruben.hartkoorn@inserm.fr

Table of Contents

Methods:

Strains and growth conditions

Mtb strain H37Rv and 18b-lux were kindly provided by Dr. R. Brosch, Paris, France, and Dr. S. Cole, Lausanne, Switzerland respectively. Other mycobacterial species used were *M. marinum* M strain, *M. abscessus* CIP104536^T (kindly provided Dr. JL Herrmann Paris, France), *M. avium* TMC724 (provided by Dr S. Canaan, Marseille, France) and *M. smegmatis* mc^{2}155. Unless otherwise indicated, all mycobacterial strains were routinely grown in complete Middlebrook 7H9 media (supplemented with 10% OADC (0.005% w/v oleic acid, 0.5% w/v albumin fraction V, 0.2% w/v dextrose, 4 mg/L catalase, and 0.95 g/L NaCl) 0.2% v/v glycerol and 0.05% v/v tween 80), or for solid medium on complete Middlebrook 7H11 agar (supplemented with 10% OADC and 0.5 % glycerol).

Mycobacterial Marinum M strain carrying pTEC15 (Addgene, plasmid 30174) to express green fluorescent protein (Wasabi) were grown under hygromycin B selection in Middlebrook 7H9 supplemented with oleic acid, albumin, dextrose, catalase (OADC), and 0.05% Tween-80. To prepare heat-killed Mycobacteria, bacteria were incubated at 80°C for 20 min.

Bacillus subtilis (ATCC-6633) was obtained from the American Tissue Culture collection (ATCC). *Pseudomonas aeruginosa* POA1 (ATCC 15692, LMG 12228), *Klebsiella pneumoniae* (ATCC 13883, LMG 2095), *Acinetobacter baumannii* (ATCC 17978, MG-17978) were obtained from the Belgian Coordinated Collections of Microorganisms (BCCM). *Escherichia coli* BW25113 (**CGSC#:** 7636) and the *Escherichia coli* ΔtolC (**CGSC#:** 11430) were obtained from the Coli Genetic Stock Center (CGSC). *Staphylococcus aureus* (SH1000) was kindly provided by Simon J Foster (University of Sheffield). These bacteria were routinely cultured and tested in Cation-Adjusted Mueller Hinton II Broth (CAMHB).

Identification of novel anti-tuberculosis hit (screening)

A library of 958 natural product like compounds was assembled and screened. Using acoustic liquid technology (Echo® 550 liquid Handler, Labcyte), 50 nL of each library compound (at 10 mM) was transferred to the wells of column 3-22 of a transparent flat bottom 384 well plate (Corning, 3701). As on-plate controls, DMSO (50 nL, negative control) or rifampicin (50 nL of 0.1 mg/mL, positive control) were added in a checkerboard distribution to the wells of column 1,2,23 and 24. In a biosafety 3 facility, frozen stocks of *Mtb* strain H37Rv (at OD_{600} of 1), were thawed and diluted 1 in 2,500 into an appropriate volume of sterile complete Middlebrook 7H9 media. Using a viafill liquid handler, 50 µL of this diluted bacterial suspension was added to the compounds in the wells of the 384-well plates, plates were sealed (Axygen PCR-SP transparent seals) and incubated (7 days, 37°C). Bacterial viability was determined by evaluating the bacterial ability to metabolize resazurin. This was achieved by adding 5 µL of 0.025% (w/v) resazurin to each well of the 384-well plates (using the viaFILL), resealing and incubating the plates (overnight, 37°C) and measuring the appearance of the resazurin metabolite, resorufin, by reading the fluorescence of each well [Ex 530nm, Em 590nm] using a Victor fluorescence plate reader (Perkin Elmer). Bacterial viability was determined as a percentage of resazurin turnover relative to the control wells.

Determination of MICs

The minimum inhibitory concentration (MIC) of compounds against *Mtb* was determined using the resazurin microtiter assay (REMA) in 96-well plates. Briefly, mycobacteria were grown to mid-log phase in complete Middlebrook 7H9 media and diluted to an OD_{600} of 0.001. The bacterial suspension was then added to the wells of a 96-well plate (200 µL to the first column of wells and 100 µL to all other wells). Test compounds were then spiked into the first well, and serially diluted down the plate using a multichannel pipette. Plates were incubated for 8-10 doubling times (37°C, 6 days) and bacterial viability was determined by subsequent addition of resazurin (10 µL of 0.025% (w/v) resazurin), incubation (37°C, overnight) and measuring resorufin production [Ex 530nm, Em 590nm] using a fluorescence microplate

reader. The MIC of TriSLa compounds against *Mtb* was considered to be the lowest compound concentration where resazurin turnover was less than 2% of the background fluorescence.

For the MIC analysis of non- *Mtb* mycobacteria, experiments were performed in a similar manner as for *Mtb*, but incubation times were adjusted according to the bacterial generation time (5 days for *M. avium and M. marinum* and 2 days for *M. abscessus* and *M. smegmatis*). In addition, *M. marinum* was cultured at 30°C, rather than 37°C and their viability was determined by visual inspection of bacterial growth in the microtitre plates. For the other bacteria, MIC was determined as the lowest compound concentration where resazurin turnover was less than 10% of the background fluorescence.

TriSLa compounds MIC determination on *E. coli* BW25113, *E. coli* BW25113: *ΔtolC*, *Acinetobacter baumannii*, *Pseudomonas aeruginosa, Klebsiella pneumoniae, Staphylococcus aureus* and *Bacillus subtilis* were also performed by a similar REMA protocol, but bacteria were cultured in Cation-Adjusted Mueller Hinton II Broth (CAMHB). Here, bacterial viability (for all except *P. aeruginosa*) was determined following 5 h of bacterial incubation in the presence of the antibiotics, by the addition of resazurin (as above) and resazurin oxidation measured by fluorescence reading [Ex 530nm, Em 590nm]. For *P. aeruginosa,* where resazurin does not work as a viability dye (probably does not enter the bacterium), bacterial viability was determined visually, and by OD_{600} reading, following overnight compound exposure (around 18 h).

X-Ray structural determination

A suitable single crystal of BDM44410.HCl was selected, glued at the tip of a Mitegen sample holder and mounted on a Bruker SMART APEX2 area detector diffractometer, equipped by an Incoatec microsource delivering copper Kalpha radiation. The crystal was kept at RT during data collection. Using Olex2 [1], the structure was solved with the Superflip [2–4] structure solution program using Charge Flipping and refined with the XL [5] refinement package using Least Squares minimization. Crystal Data for $C_{20}H_{29}ClN_2O_2$ (M =364.90 g/mol): monoclinic, space group P21 (no. 4), a = 12.219(3) Å, b = 6.7700(14) Å, c = 13.136(3) Å, β = 112.610(13)°, V = 1003.1(4) Å3, Z = 2, T = 298 K, μ(CuKα) = 1.797 mm-1, Dcalc = 1.208 g/cm3, 24497 reflections measured (7.29° ≤ 2Θ ≤ 136.868°), 3550 unique (Rint = 0.0658, Rsigma = 0.0476) which were used in all calculations. The final R1 was 0.0493 (I > 2σ(I)) and wR2 was 0.1337 (all data). The structure is published in the Cambridge Structural Database: CCDC 2143694.

Phys-Chem and *in vitro* ADME

To determine compound solubility, 10 mM of the compound in DMSO was diluted 50-fold either in PBS pH 7.4 or in organic MeOH solvent in PP tubes (n = 3 for PBS and methanol). The tubes were gently shaken for 24 h at room temperature. Then, the three PBS tubes and three of the six methanol tubes were centrifuged for 5 min at 4000 rpm and filtered over 0.45 μm filters (Millex-LH Millipore). Each sample was diluted 50-fold in MeOH before LC-MS/MS analysis. For each compound, the test was performed in triplicate. The solubility was determined by the following ratio: $(AUC_{PBS}/ AUC_{MeOH})*200$.

To determine compound LogD, 10 mM of the compound in DMSO was diluted 50-fold in a mixture of 1:1 octanol:PBS at pH 7.4. The mixture was gently shaken for 2 h at room temperature. Each sample was then diluted 50-fold in MeOH before LC-MS/MS analysis. For each compound, the test was performed in triplicate. LogD was determined as the logarithm of the ratio of concentration of product in octanol and PBS, respectively, determined by mass signals.

To determine compound microsomal stability, liver microsomes from female mice (CD-1) were used (Corning). All incubations were performed in duplicate in a shaking water bath at 37 °C. The incubation mixtures contained 1 μM compound with 1% methanol used as a vehicle, mouse liver microsomes (0.3 mg of microsomal protein per mL), 5 mM MgCl2, 1 mM NADP, 5 mM glucose 6-phosphate, 0.4 U/mL glucose 6- phosphate dehydrogenase, and 50 mM potassium phosphate buffer (pH 7.4) in a final volume of 0.5 mL. Aliquots were removed at 5, 10, 20, 30, and 40 min after microsome addition, and the reaction

was stopped by adding four volumes of ice-cold acetonitrile containing an internal standard. Propranolol, known as a high hepatic clearance drug in rodents, was used as a quality-control compound for the microsomal incubations. The samples were centrifuged for 10 min at 12,000 rpm and the supernatants were transferred in matrix tubes for LC-MS/MS analysis. Each compound was quantified by converting the corresponding analyte/internal standard peak area ratios to percentage drug remaining, using the initial ratio values in control incubations as 100%. *In vitro* intrinsic clearance (CL_{int} expressed as µL/min/mg protein) was calculated according to the following formula: CL_{int} = (dose/AUC_{∞})/[microsome], where 'dose' is the initial amount of compound in the incubation mixture (1 µM), AUC_{∞} the area under the concentration versus time curve extrapolated to infinity and [microsomes] the concentration in microsomes expressed in mg/µL.

Cytotoxicity

The cytotoxicity of compounds **BDM44410 (1)**, **BDM88689 (11)**, **BDM88690 (12)** and **BDM89000 (13)** was determined on BALB/3T3 cells using live imaging following both Hoechst 33342 and NucView 488 Caspase-3 staining. Briefly, BALB/3T3 cells were seeded in 384-well plate, and 24h later, compounds were added (0, 12.5, 25, 50 and 100 µM) to the culture medium, as well as Hoechst 33342 and NucView 488 Caspase-3 substrate. 24h and 48h after compounds addition, live imaging was performed using an In Cell Analyzer 6000 (GE Healthcare). The cytotoxicity was defined based on the ratio of the apoptotic cell population (NucView staining) and the total population (Hoechst staining) using Columbus software. Compounds were tested in triplicate. Carfilzomib (499, 249,142, 61 and 30.6 nM) was used as positive control in this assay.

Time dependent bactericidal activity by cfu

To evaluate the bactericidal activity of TriSLa compounds, the impact of inhibitor exposure was determined by measuring surviving colony forming units (cfu). For these experiments, H37Rv was grown in Middlebrook 7H9-GTy-OADC, to mid log phase. Bacteria were then diluted to OD_{600} 0.02 (~1 x 10^6 cfu/mL, 20 times higher concentrations than for MIC by REMA), and incubated in the presence of different concentrations of various inhibitors in a 96-well plate. To evaluate the impact of time on antibiotic activity, replica plates were generated, one for 1 week exposure, the other for 2 weeks exposure. The bacterial concentration of the starting inoculum, and the number of bacteria remaining after 1 and 2 weeks of compound exposure was determined by plating (50 µL) serial 1 in 10 dilutions of mixed sample wells onto Petri dishes containing 20 mL of Middlebrook 7H11 agar containing 0.5% glycerol and 10% OADC, incubation (6 weeks, 37 °C), and weekly counting of the cfu (week, 3, 4, 5 and 6). To define the compound concentrations that has to be plated for cfu counting, the 3 lowest concentrations where no bacterial growth was visually observed at week 1 and 2 were chosen (as the starting inoculum was high, growth of bacteria at sub MIC concentrations was easily observed). Experiment was performed four independent times and the results are presented as $\log_{10}$ cfu/mL ± SD.

Antibiotic activity against non-replicating ss18b

This work is based on methodology described previously [6,7] where compound activity is tested on a streptomycin-dependent *Mtb* strain 18b that has been shifted into a non-replicating but viable form by removal of streptomycin from the media (streptomycin-starved 18b). Bacterial viability was determined both using an integrated luciferase reporter (18b-lux [6]) and by determining cfu. Briefly, 18b-lux was grown in complete Middlebrook 7H9 media with 50 µg/mL streptomycin and 100 µg/mL hygromycin to an OD_{600} of 0.8. 18b-lux were then washed 3 times in Middlebrook 7H9 base media (3,200 x g, 6 min) and frozen in 1 mL aliquots at an OD_{600} of 10 (in Middlebrook 7H9 base with 15% glycerol). To generate the non-replicating streptomycin starved 18b-lux (ss18b-lux), a frozen aliquot was thawed and placed into 20 mL of Middlebrook 7H9-GTw-AAN (0.2% glycerol, 0.05% tween 80, 0.5% albumin fraction V, 0.1% acetate, 0.95 g/L NaCl: glucose impacts ss18b-lux viability and replaced by acetate), with 50 µg/mL hygromycin and incubated (37°C, 100 rpm). The induction of a fully non-replicating viable state requires 2 weeks of

incubation in the absence of streptomycin, but on day 7 and 13 the OD_{600} of the culture was adjusted to 0.2 with antibiotic free Middlebrook 7H9-GTw-AAN (also helps declumping). On day 14 ss18b-lux is ready for testing.

To determine antibiotic activity on ss18b-lux, the non-replicating culture was diluted to OD_{600} = 0.15, and dispensed using a viafill (Integra Biosciences), into white 96 well plates containing antibiotics of interest added using Echo liquid handling technology. The plates were sealed (Axygen PCR-SP transparent seals) and incubated (37°C). On day 0, 2, 5 bacterial luminescence was determined using a Victor microplate reader (Perkin Elmer). From the luminescence data, the wells that showed antibiotic activity could be determined, and on day 7, serial dilutions of these wells were plated onto Middlebrook 7H11-G-OADC plates supplemented with 50 µg/mL streptomycin, and incubated for up to 8 weeks, for cfu determination.

Antibiotic activity against Intracellular *M. tuberculosis*

Similar to assays already described [8,9], the ability of test compounds to protect infected macrophages from *Mtb* induced death was used as a surrogate read out to evaluate intracellular antibiotic activity. Here, the THP-1 monocyte cell line (ECACC 88081201) was grown and passaged in RPMI Glutamax medium supplemented with 10% heat inactivated foetal bovine serum (FBS) and 1% Zell Shield (Minerva Biolabs GmbH, Berlin, Germany) at 37°C with 5% CO_2. To generate adherent macrophage like- THP-1 cells (A-THP-1), 25 mL of 8 x 10^5/mL THP-1 cells were differentiated in a T75 tissue culture flasks (Sarstedt) using 50 ng/mL (81 nM) Phorbol 12-myristate 13-acetate (PMA) for 72 h to form A-THP-1. A-THP-1 were then washed with pre-warmed RPMI 10% FBS (to remove any Zell Shield) and infected in the T75 flask with log-phase H37Rv at an MOI of 10 (2 x 10^8 H37Rv cells in 25 mL) (2 h, 37°C, 5% CO2). Following infection, the cell culture media was replaced by RPMI 10% FBS with 50 µg/mL amikacin to kill remaining extracellular bacteria (1 h, 37°C, 5% CO_2). Infected A-THP-1 cells were then washed twice with warm RPMI media, detached from flasks using 2 mL trypsin PBS buffer (trypsin-versene solution containing 0.1% trypsin 1:250 (Gibco) with 0.125% EDTA and 17.5 µg/mL gentamycin) and re-suspended in 40 mL of RPMI media with 10% FBS and 50 ng/mL PMA (concentration of 5x10^5 infected cells/mL). 100 µL of infected A-THP1 cells were distributed into 96-well plate pre-loaded (by echo technology) with test compounds, sealed with a breathable film (Air-O-Seal sterile adhesive seal, 044877, Dutscher), and incubated for 96h (37°C, 5% CO_2). A-THP-1 viability was determined by the addition of 10 µL of 0.05% resazurin to the wells, and measuring fluorescence [Ex 530 nm, Em 590 nm] using a fluorescence microplate reader (Victor, Perkin Elmer).

Isolation and characterization of BDM44410 resistant mycobacteria

To select spontaneous resistant H37Rv isolates, log-phase H37Rv was concentrated to an OD_{600} of 50 and 25 µL spread onto Middlebrook 7H11 agar containing **BDM44410** (**1**) (14, 28, 56, 112 µM) or **BDM88689** (**11**) (1 µM) and incubated (37°C, 4-6 weeks). Resistant colonies were re-streaked onto solid media containing the same concentrations of antibiotic. The resistant isolates were then grown in antibiotic free liquid media to mid-log phase for the determination of antibiotic susceptibility by REMA.

To select spontaneous resistant *M. marinum* isolates, 50 mL of *M. marinum* (OD_{600} of 0.2) in 7H9 complete media was inoculated with **BDM88689** (**11**) (final concentration 4 µM) and grown (30 °C, 100 rpm) to an OD_{600} of 1.8. The culture was diluted 1:500 into complete Middlebrook 7H9 media containing 4 µM **BDM88689** (**11**) and allowed to grow to reach log-phase (30 °C, 100 rpm). Serially 10-fold dilutions of the selected culture were then plated on complete Middlebrook 7H11 agar containing 4 µM **BDM88689** (**11**) and incubated (30 °C) until colonies appeared. Single colonies were picked and re-streaked on solid media containing 4 µM **BDM88689** (**11**). Following the culture of selected isolates in antibiotic-free complete Middlebrook 7H9 media, antibiotic susceptibility of isolates was confirmed by REMA.

Identification of genetic variants

Genomic DNA was extracted from the parental H37Rv *Mtb* strain and two **BDM44410** (**1**) resistant isolates (RC 14.2 and 28.1) using bead beating and conventional phenol: chloroform: isoamyl alcohol methodology. Whole genome sequencing of these 5 strains was then performed by Illumina Hiseq 2500 sequencing of paired-end reads (Genoscreen, France) and fastq files deposited at NCBI (project number, PRJNA808942). For the identification of the genetic variants, the sequence files were initially processed with the PRINSEQ-lite PERL script (PRINSEQ-lite 0.20.4; http://prinseq.sourceforge.net/) to remove low-quality data with the following parameters (-min_len 50 -min_qual_mean 30 -trim_qual_right 30 -ns_max_n 0 -noniupac). Reads were aligned to the *Mtb* reference genome (Genbank accession number AL123456.3) with BWA-MEM (https://github.com/lh3/bwa). The output SAM alignment files were converted to BAM files and sorted using SAMtools view with default parameters (http://www.htslib.org/). Duplicated reads were removed using Picard MarkDuplicates with the REMOVE_DUPLICATES option (http://broadinstitute.github.io/picard/). SNPs and indels were called using GATK HaplotypeCaller (https://gatk.broadinstitute.org/hc/en-us/articles/360037225632-HaplotypeCaller). Identified variants were annotated using snpEff (http://pcingola.github.io/SnpEff/). Variants with a low read depth (PD ≤ 5) or those located in the repetitive PE/PPE/PE_PGRS genes were removed.

Sanger sequencing was used to confirm the genetic variants found in selected **BDM44410** (**1**) resistant H37Rv isolates (primers 746 and 749, **Table S7**). Sanger sequencing was also used to sequence *ndh* (*Rv1854c* and *Mmar_2728* respectively) and *ndhA* with promoter (*Rv0392*) for the selected **BDM88689** (**11**) resistant *Mtb* and *M. marinum* isolates (primers indicated in **Table S7**)

QPCR for *ndh* and *ndhA* expression levels

The *ndh* and *ndhA* mRNA expression level of the parental and **BDM44410** (**1**) resistant H37Rv isolates was determined by quantitative PCR (QPCR). Briefly, 3 independent cultures of each isolate were grown in complete Middlebrook 7H9 media to mid-log phase, synchronized to OD_{600} = 0.05, and grown to OD_{600} of 0.4-0.6 (37 °C, 100 rpm). For each culture, 5 mL of bacterial culture was pelleted (5 min, 3,200 x g), and resuspended in 1 mL TRIzol reagent (Fisher Scientific), transferred to 2 mL Lysing Matrix B tubes (MP Bio) and stored for later processing (-80 °C). For RNA extraction, the samples were thawed and the bacteria were disrupted by bead beating (3 cycles of 30s of 6.5 m/s, with 5 min on ice in-between) using a FastPrep bead beater (MP Bio). RNA was then extracted from the samples according to the TRIzol manufacturing instructions and remaining genomic DNA depleted with two rounds of amplification grade DNase I treatment (ThermoFisher) with nucleic acid purification between (using Agencourt AMPure XP beads, Beckman Coulter Genomics). RNA was quantified using Quant-iT PicoGreen dsDNA kit (Life Technologies).

cDNA was synthesized with the Verso cDNA synthesis kit (Thermo Scientific, Waltham, MA) using the random hexamer primers and 100ng of purified RNA per reaction as per manufacturer's instructions. 20 µL real time PCR reactions were setup using 10 µL of 2X KAPA SYBR FAST qPCR Universal Master Mix (Sigma Aldrich), 2 µL of cDNA product and 0.4 µL of each 10 µM of each primer pair. Primer pairs are shown for the amplification of *ndh*, *ndhA* and housekeeping *sigA* are shown in **Table S7**. The real time PCR was followed on a LightCycler® 480 Instrument II (Roche) over 40 cycles (3 s at 98 °C and 40 s at 60 °C) followed by a melting curve analysis. The relative quantities of the genes of interest were analyzed using the ΔΔ-c(t) quantification method. QPCR experiments were performed 3 independent times for the three independent biological replicate samples.

Biochemical validation - Cloning and site directed mutagenesis

For the biochemical evaluation of the inhibition of the *Mtb* type II NADH dehydrogenase by the identified compound, recombinant Ndh (Rv1854c) with an N-terminal maltose binding protein (MBP) was produced and purified from *E. coli* using a similar method to that described previously [10]. Briefly, Rv1854c (*ndh*) was PCR amplified from H37Rv gDNA using primers 760-761 (**Table S7**) and cloned in frame with MBP into the XbaI and HindIII sites of pMALc2x (New England Biolabs) forming pMALc2x::*ndh*, which was validated by

Sanger sequencing. For the generation of the Y403C, Y403F and Q334P variants of Ndh, site directed mutagenesis of pMALc2x::*ndh* was performed using the DpnI based approach. Here, using specific mutation introducing primers designed using QuikChange® Primer Design tool (Agilent) (**Table S7**) in conjunction with DNA amplification using Q5 High Fidelity DNA Polymerase (NEB), and dpnI, pMALc2x::*ndh*(Y403C), pMALc2x::*ndh*(Y403F) and pMALc2x::*ndh*(Q334P) were generated, with mutations confirmed by Sanger sequencing of plasmids.

For MBP-*ndh* production and purification, pMALc2x::ndh (or mutants) were transformed into chemically competent *E. coli* Rosetta (DE3) (novagen), and selected on 100 µg/mL ampicillin and 25 µg/mL chloramphenicol. Freshly transformed bacteria were grown in 1 L of LB media (supplemented with 0.2% glucose, 25 µg/mL chloramphenicol and 100 µg/mL ampicillin) to an OD_{600} = 0.1-0.2 (37°C, 200 rpm) after which the temperature was decreased to 16°C. At an OD_{600} = 0.4, protein production was induced with 0.3 mM IPTG (overnight, 16°C, 200 rpm), and bacterial pellet harvested (7000 x g, 20 min, 4°C) and stored at -20°C until purification. For MBP-Ndh purification the bacterial pellet was thawed and suspended in 30 mL of buffer A (50 mM HEPES adjusted to pH 7.1 with 1M K_2HPO_4 and 5% (w/v) glycerol) with 10 µg/mL DNase, cOmplete EDTA-free Protease Inhibitor Cocktail, 5 µM FAD, 10 mM MgCl2, and 0.25% CHAPS (all purchased from Sigma-Aldrich). Cells were lysed using a French pressure cell (Sim-Aminco) (2 rounds at 1100 psi) and cell debris was removed by centrifugation (25,000 x g for 30 min at 4°C). 5 mL of pre-equilibrated amylose resin (New England Biolabs) was added to the supernatant and mixed (1 h, 4 °C, rotating mixer) before being transferred to a gravity flow column. Following the flow through of the unbound supernatant, the resin was washed with 20 mL buffer A with 0.25% CHAPS, followed by 40 mL buffer A without CHAPS (4 °C). Resin bound proteins were then eluted with 10 mL of buffer A containing 5 mM maltose (4 °C) and concentrated using Vivaspin turbo 4 PES 30 kDa concentrator columns (Sartorius). An equal volume of glycerol was then added to the protein, and aliquots flash frozen in liquid nitrogen and stored at −80 °C. Protein concentration was determined using Pierce BCA protein assay kit (Thermo scientific)

Purification of recombinant codon optimized *Mtb* MBP-Ndh using *M. smegmatis*

A codon optimized MBP-*ndh* sequence (59.8 % GC) with specific homologous flanks for recombination was purchased from Genscript. These homologous flanks allowed for the cloning of the codon optimized MBP-*ndh* sequence downstream of the acetamidase promoter of *M. smegmatis* expression vector pSD26 [11] by recombination (using NEBuilder® HiFi DNA Assembly), according to the manufacturer's instructions. The correct assembly of the resulting pSD26-MBP-*ndh* vector was confirmed by restriction mapping with XbaI, SmaI and EcoRI. To generate an equivalent pSD26-MBP-*ndhA* construct, the *Mtb ndhA* was PCR-amplified (primers 1267 and 1268 (**Table S7**)) and cloned into pSD26-MBP-*ndh* between SpeI and EcoRV sites (introduced in the custom design), replacing the *ndh* and yielding pSD26-MBP-*ndhA*. This insert sequence was validated by Sanger sequencing (primers 751, 1267 and 1268 (**Table S7**)).

For the production of recombinant MBP-Ndh and MBP-NdhA in *M. smegmatis*, pSD26-MBP-*ndh* and pSD26-MBP-*ndhA* constructs were transformed into *M. smegmatis* mc^2155 by electroporation, and clones selected on Middlebrook 7H11 agar containing 100 µg/mL hygromycin. Protein induction was performed as described previously[11], where briefly, *M. smegmatis* clones were grown in 1 L of expression media (Middlebrook 7H9 containing 0.05% tween-80, 0.2% glycerol and 0.2% glucose) with 50 µg/mL hygromycin at 37°C (shaking, 200 rpm). At an OD_{600} of 0.4-0.6 protein production was induced by the addition of 0.2% acetamide (overnight, 16°C, 200 rpm). Bacterial cells were then pelleted (7,000 x g, 20 min) and Ndh-2 protein purification was performed as described for the purification from *E. coli*.

Biochemical evaluation of MBP-Ndh inhibition

To define the activity of test compounds on purified MBP-Ndh, a biochemical assay was setup to monitor MBP-Ndh dependent oxidation of NADH in the presence of an electron acceptor menadione, similar to methods described previously [10]. Briefly, to evaluate the IC_{50} of TriSLas, the compounds were transferred

to a black 384-well plate with transparent bottom using Echo liquid handling acoustic technology (Labcyte) and backfilled to 500 nL with DMSO. Using a Viafill liquid dispenser (INTEGRA Biosciences) a 45 µL mixture was added to these wells containing a *Mtb* recombinant MBP tagged Ndh-2 enzyme (either 70 nM recombinant MBP-Ndh produced in *E. coli* -; 0.66 nM recombinant MBP-Ndh produced in *M. smegmatis,* or 30 nM recombinant MBP-NdhA produced in *M. smegmatis,* concentration adjusted to have similar rate of NADH oxidation) and NADH (500 µM) in 50 mM HEPES buffer (pH 7.1 with K_2HPO_4). Following a pre-incubated (25°C, 15 min), enzyme activity was initiated by the addition of menadione (5 µL, 100 µM final concentration (dispensed into wells using ENVISION, Perkin Elmer), and the kinetics of NADH oxidation monitoring at 340 nm (measured every 60 sec, ENVISION plate reader, Perkin Elmer). The rate of NADH oxidation was calculated as the slope of the linear decrease in 340 nm signal using Microsoft Excel, and enzyme inhibition parameters determined using Graphpad Prism v.9. IC_{50} are reported as mean and standard deviation of at least 3 independent experiments.

Biochemical competition assays

To determine if the TriSLa Ndh inhibitors act through competition with either the menadione or NADH substrate, competition assays were performed. Here, TriSLa inhibition of MBP-Ndh mediated NADH oxidation was determined as above, with either a range of menadione concentrations (25 - 200 µM), or a range of NADH concentrations (25 - 200 µM). Kinetic oxidation of NADH was measured and processed as above. Competition experiments were performed a least 3 independent times, and Lineweaver-burk plots were generated using Graphpad prism (v. 9).

Impact of TriSLa exposure on *Mtb* NADH and NAD^+ levels

Mtb H37Rv was cultured in complete Middlebrook 7H9 media to mid-log phase (OD600 0.4-0.8). Bacterial cultures were diluted to an OD_{600} of 0.3 (50 mL), spiked with compounds of interest and incubated (37°C). Following 2 h and 24 h exposure, 12 mL aliquots of treated bacterial suspension (one for NAD^+ detection and another for NADH detection) were pelleted (3,200 x g for 10 min). After centrifugation and removing media, the bacterial pellets were resuspended in 300 µL of 0.2 M HCl extraction buffer (for NAD+ extraction) or in 0.2 M NaOH extraction buffer (for NADH extraction). Cells were transferred to 2 mL Lysing Matrix B tubes (MP Bio) tubes and disrupted using a MM 400 mixer mill (Retsch GmbH, Haan, Germany), (5 min, 30 Hz). Samples were then heated (55 °C for 10 min) followed by cooling on ice. NAD^+ and NADH samples were neutralized using (300 µL) 0.1M NaOH and 0.1M HCl respectively, and cell debris was separated by centrifugation. The NAD/NADH-Glo™ assay kit was used to measure the amount of NAD^+ and NADH from H37Rv cells, according to the manufacturer's directions. 20 µL of sample was incubated with 20 µL of detection reagent for 30 minutes in a 384 well white flat bottom plate (Corning, NY). Luminescence were measured using EnSight™ multimode plate reader at t=0 and t=30 min. Experiment was performed three independent times with two technical replicates for each sample. Average net luminescence was calculated after subtracting average background luminescence at t=0 and the average luminescence of the blank reactions. Each experiment had NADH standard curve to perform linear regression analysis and interpolate NADH and NAD^+ concentration. These values are OD_{600} corrected and are presented in a kinetics graph.

Impact of TriSLa exposure on *Mtb* ATP levels

The wells of a sterile white polystyrene 96-well plates (Corning Inc) were prepared to contain 0.5 µL of concentrated (100 x) compound of interest dissolved in DMSO. Log phase *Mtb* H37Rv culture (OD_{600} of 0.3-0.4) was then diluted to OD_{600} of 0.01 in complete Middlebrook 7H9 media and 50 µL added to each well and incubated (37°C). After 4 and 24 h, bacterial ATP levels were measures using the BacTiter-Glo reagent (Promega) as per manufacturer's instructions, and luminescence measured using an EnSight reader (Perkin Elmer). Experiments were repeated 3 times independently.

Impact of media components on inhibitor MIC

To address the impact of media carbon source, L-serine and detergents on TriSLA antibiotic activity, the MIC of the inhibitors was re-evaluated in a series of select media. To determine the impact of fatty acids on TriSLa activity two different base media were used supplemented with and without fatty acids. The first media was a Middlebrook-7H9 based medium with 5 g/L fatty acid free bovine serum albumin (fraction V, Roche), 0.85 g/L NaCl, 0.2 % glycerol, 4 mg/L catalase, 0.05 % tyloxapol with and without 200 µM (56 mg/L) oleic acid. The second media used was a "minimal modified Sauton's medium" as described previously [12] containing 0.05% KH_2PO_4, 0.05 % $MgSO_4.7H_2O$, 0.2% citric acid, 0.005% ferric ammonium citrate, 0.0001 % $ZnSO_4$, 0.2 % glycerol, 0.4 % dextrose, 5 g/L fatty acid free bovine serum albumin (fraction V, Roche), 0.085% NaCl, 4 mg/L catalase, (pH 7.2) with and without 200 µM (56 mg/L) oleic acid. To evaluate the impact of L-serine media supplementation on TriSLa MIC, complete Middlebrook 7H9 media (supplemented with 10% OADC, 0.2 % glycerol and 0.05% tyloxapol) was spiked with no, 0.1mM or 1mM L-serine (Acros organics). To evaluate the impact of detergents in the growth media on TriSLa MIC, complete Middlebrook 7H9 media (supplemented with 10% OADC, 0.2 % glycerol) was spiked with no detergents, 0.05 % tween 80 or 0.05% tyloxapol.

For evaluating the impact of detergents and L-serine supplementation, MICs were evaluated as described above by the resazurin reduction assay. For evaluating the impact of fatty acids, removal of all fatty acids from the media resulted in a significantly slower growth of the bacteria. For this reason, and in line with Beites and colleagues, [12], MICs experiments were performed with small modifications, where bacteria were tested at an OD600 of 0.01 (instead of 0.001), and bacterial growth was determined after 12 days (*Mtb*) or 5 days (*M. marinum*) incubation either visually (photo) or by OD600 reading. This protocol was performed for both

Bacterial strains and culture conditions for *in vitro* POC in zebrafish

M. marinum M strain is a human isolate that has been extensively characterized [13]. Bacterial cultures were grown on Middlebrook 7H10 agar enriched with 10% oleic acid, albumin, dextrose and catalase (OADC; BD Difco) at 30°C or grown in Middlebrook 7H9 broth supplemented with 10% OADC and 0.025% Tyloxapol (Sigma-Aldrich). Green fluorescent *M. marinum* expressing Wasabi was obtained after transformation with pTEC15 [14] and selection in the presence of 50 µg/mL hygromycin. For infection in zebrafish, *M. marinum* M strain harboring pTEC15 was grown in Middlebrook 7H9 liquid broth and processed to generate homogenous bacterial preparations, as reported earlier [15]. Aliquots were frozen and kept at -80°C until further use.

Zebrafish care, maintenance and ethic statements

Zebrafish experiments were completed under European Union guidelines for the handling of laboratory animals (http://ec.europa.eu/environment/chemicals/lab_animals/home_en.htm). Housing and husbandry was approved by the Direction Sanitaire et Vétérinaire de l'Hérault for the CRBM zebrafish facility (Montpellier) (registration number C-34-172-39). Handling and experiments were approved by "le ministère de l'enseignement supérieur, de la recherche et de l'innovation" under the reference APAFIS#24406-2020022815234677 V3. Experiments were done using the *golden* mutant [16] and the macrophage reporter Tg(*mpeg1:mCherry)* line [17]. Embryos were obtained from adult zebrafish pairs by natural spawning and were raised at 28.5 °C in zebrafish tank water. Ages of embryos are expressed as hours post-fertilization (hpf).

Assessment of TriSLa efficacy in *M. marinum* infected zebrafish

Bacterial aliquots were thawed and diluted with PBS and phenol red dye (0.5%, w/v) to OD_{600} ≈ 1 *M. marinum* expressing Wasabi were microinjected into the caudal vein (2-3 nL containing ≈ 200-250 cfu) of embryos anesthetized with 0.016% Tricaine at 30 hours post-fertilization (hpf) previously dechorionated. The bacterial inoculum was checked *a posteriori* by plating 2-3 nL of the bacterial suspension on Middlebrook 7H10 and cfu determination. Following infection, embryos were transferred into E3 media

at 28.5°C. Infected embryos were transferred into 6-well plates (12 embryos/well) and kept at 28.5°C to follow the kinetics of infection and embryo survival. Survival curves were generated by counting the dead larvae at a daily basis for up to 10 days post-infection (dpi), with the experiment concluded when uninfected embryos (PBS injected) started to die. TriSLa treatment of infected and uninfected larvae was started at 24 hpi (hours post-infection) for 4 days period. The drug-containing solution was renewed daily. Bacterial burdens in live embryos were determined by anesthetizing embryos in tricaine as reported earlier, mounting on 3% (w/v) methylcellulose solution and taking fluorescent images using a Zeiss Axio Zoom.V16 coupled with an Axiocam 503 mono (Zeiss). Fluorescence measurements were determined using the 'Analyze particles' function in ImageJ [15].

Supplementary Figures

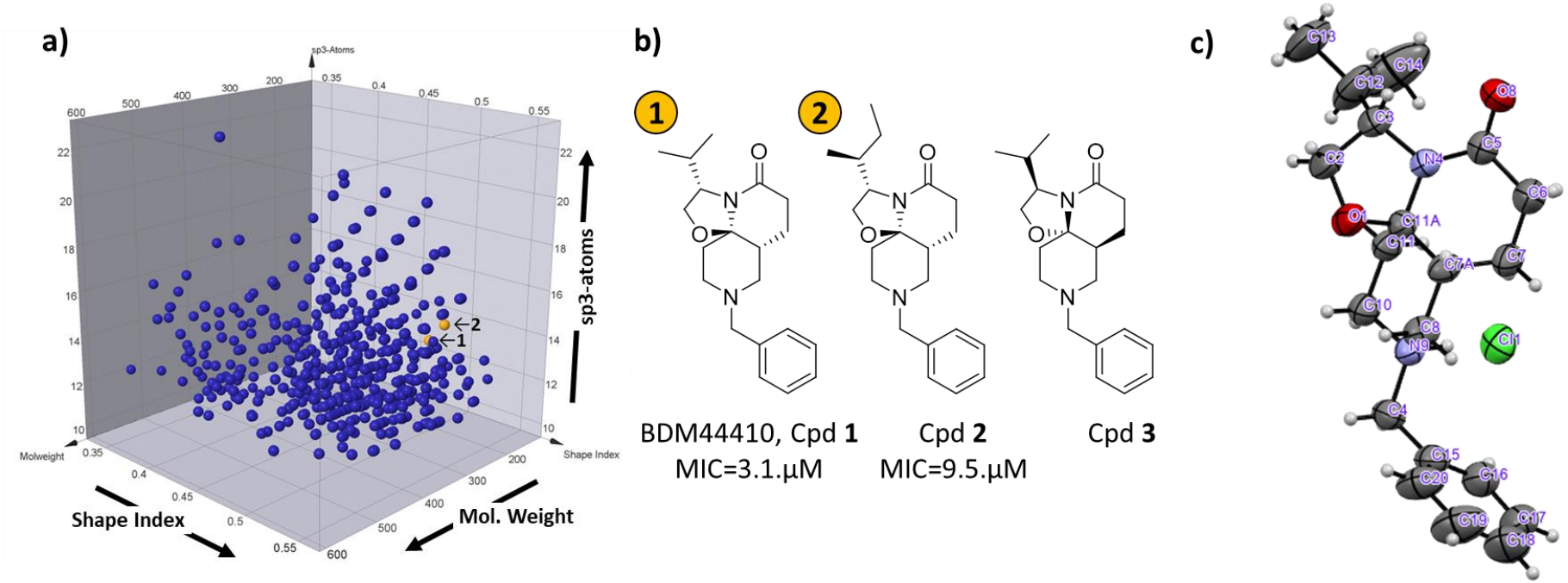

Figure S1: **a**) Molecular diversity of compounds screened against H37Rv in this study. A 3D-graph depiction of the molecular weight, the molecular shape index (calculated using datawarrior [18]) and the number of sp3 carbon atoms of the 958 screened compounds. **b**) The chemical structures of the two TriSLas hits that emerged from the screening (BDM44410, **1** and BDM44434, **2**: highlighted in orange in figure S1a), and the structure of BDM44410 enantiomer (compound **3**). **c**) X-ray crystal structure of BDM44410.HCl confirming the expected configuration of the tricyclic core of TriSLas, exemplifying the enhanced 3-D (non-flat) structure of the molecule.

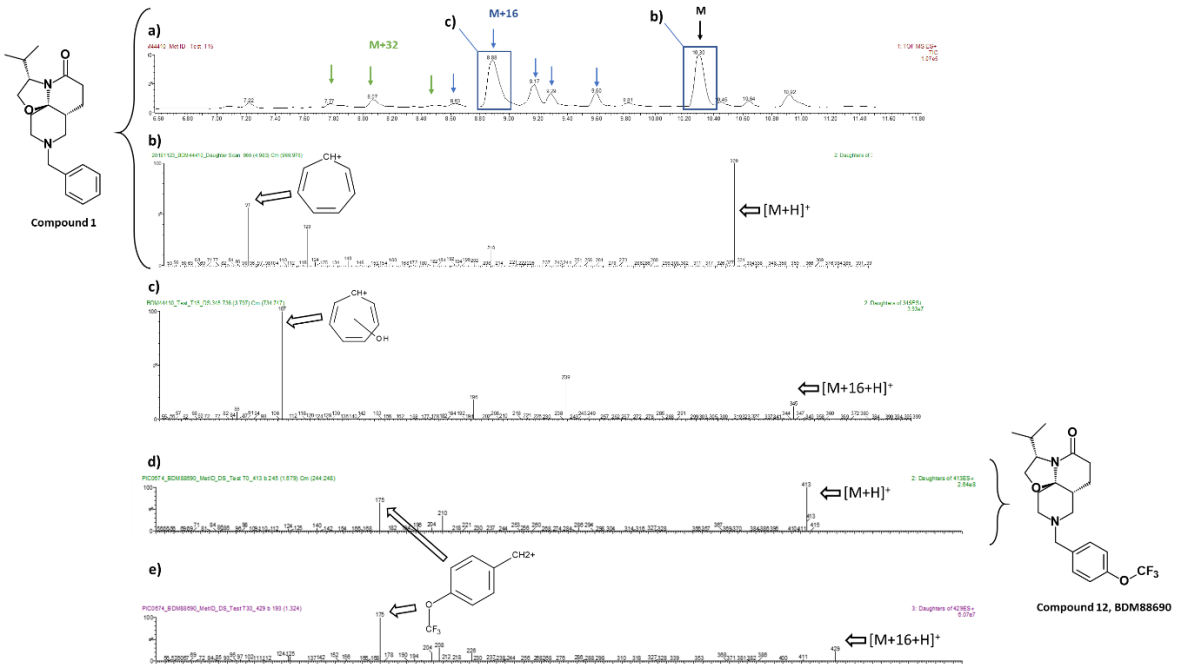

Figure S2: ***In vitro*** **metabolism of compounds 1 and 12 a)** HPLC-MS total ion count (TIC) chromatogram of compound 1 following 15 min incubation with mice female liver microsomes. Black arrow points at the parent compound (parent mass M); blue arrows point at likely mono-hydroxylated metabolites (with parent mass +16); and green arrows point at likely double-hydroxylated metabolites (parent mass +32). **b)** HPLC-MS/MS daughter scan of compound **1**. The detected fragment ion with a mass of 91 is predicted to corresponds to the tropylium ion, originating from the fragmented benzyl group of compound **1**. **c)** HPLC-MS/MS daughter scan of the major M+16 metabolite of compound **1**. Fragments analysis shows no detection of the tropylium ion, but instead a fragment ion with a mass of 107, which corresponds to the mass of a hydroxylated tropylium ion, likely originating from an original hydroxylated benzyl group. This major metabolite with a retention time of 8.88 min is the only such +16 metabolites to fragment into this hydroxylated tropylium ion (the others have fragment into the tropylium ion) and hence likely the only metabolite hydroxylated on the benzyl of compound **1**. d**)** HPLC-MS/MS daughter scan of compound **12**. The detected fragment ion with a mass of 175 is predicted to correspond to the 4-trifluoromethoxybenzyl cation, originating from the fragmented 4-trifluorometheoxybenzyl group of compound **12**. **e)** HPLC-MS/MS daughter scan of the major M+16 metabolite of compound **12**. The detected fragment ion with a mass of 175 is predicted to correspond to the 4-trifluoromethoxybenzyl cation, originating from the fragmented 4-trifluorometheoxybenzyl group. This data suggests that hydroxylation is not occurring on the 4-trifluoromethoxylbenzyl moiety. Similar fragmentation was observed for all M+16 metabolites, suggesting that substitution in position 4 of the phenyl ring blocked the main metabolism observed in compound **1**. However, further analysis is required to identify metabolism of compound **12** and design more metabolically stable analogs.

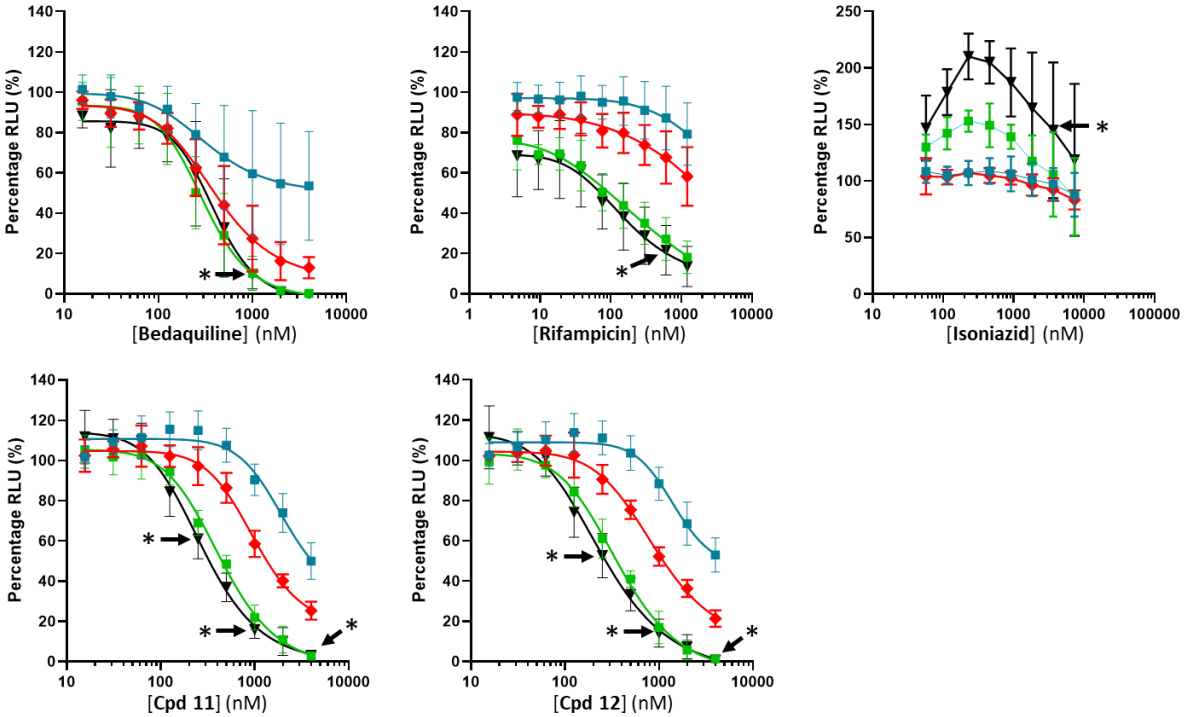

Figure S3: Time-dependent decrease in luminescence of ss18b-lux following exposure to a concentration range of bedaquiline, rifampicin, isoniazid, **11** (**BDM88689)** and **12** (**BMD88690)**. Luminescence was measure following 1 (blue), 2 (red), 5 (green) and 7 (black) days of antibiotic exposure. Data are presented as the mean ± SD of the relative luminescence measured compared to no antibiotic controls (n≥3). Asterisks indicate the conditions where cfu were determined.

a)

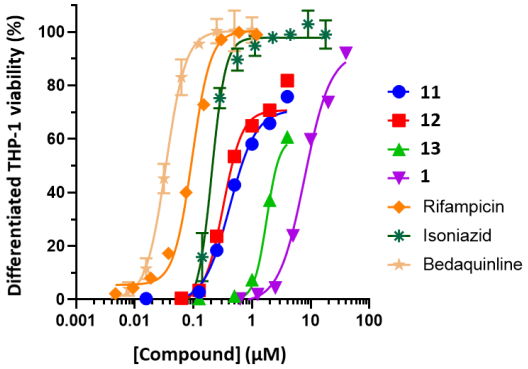

b)

Compound	IC50s for Macrophage survival after H37Rv infection Mean IC50 ± SD (µM)
1	8.180 ± 1.566
11	0.461 ± 0.106
12	0.359 ± 0.026
13	2.387 ± 1.312
Rifampicin	0.091 ± 0.032
Isoniazid	0.204 ± 0.020
Bedaquiline	0.034 ± 0.003

Figure S4: **TriSLa protection of H37Rv infected macrophages. a**) Graph shows the percentage viability of H37Rv infected pma-differentiated macrophages (A-THP1) in the presence of a concentration range of TriSLa compounds and other anti-tuberculosis molecules. **b**) Table showing the calculated IC_{50} ± SD derived from 5 independent biological replicates.

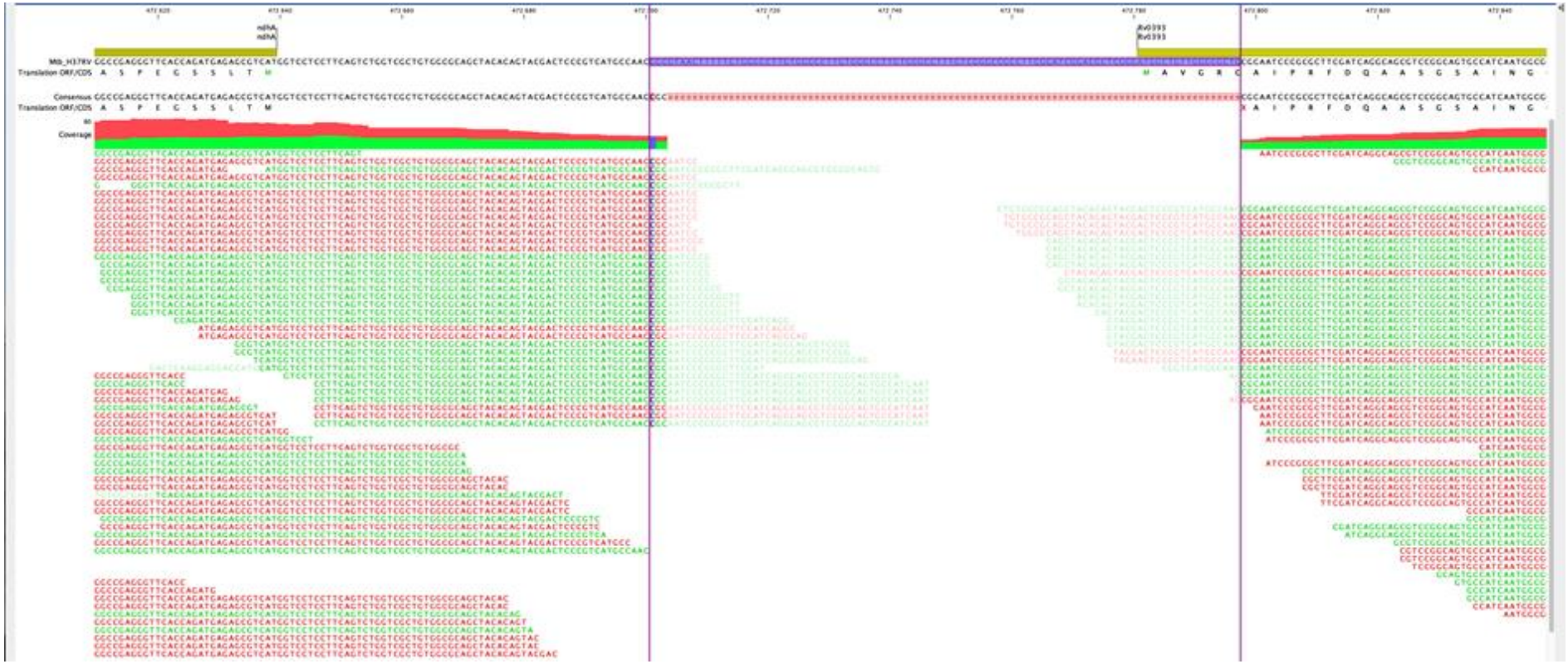

Figure S5: Screen shot from CLC genomics viewer showing the sequencing reads for H37Rv compound **1** RC14.2 mapped onto the *ndhA* promoter region of the reference genome of H37Rv. In this region, there is a clear 97-bp deletion with reads spanning across the deletion.

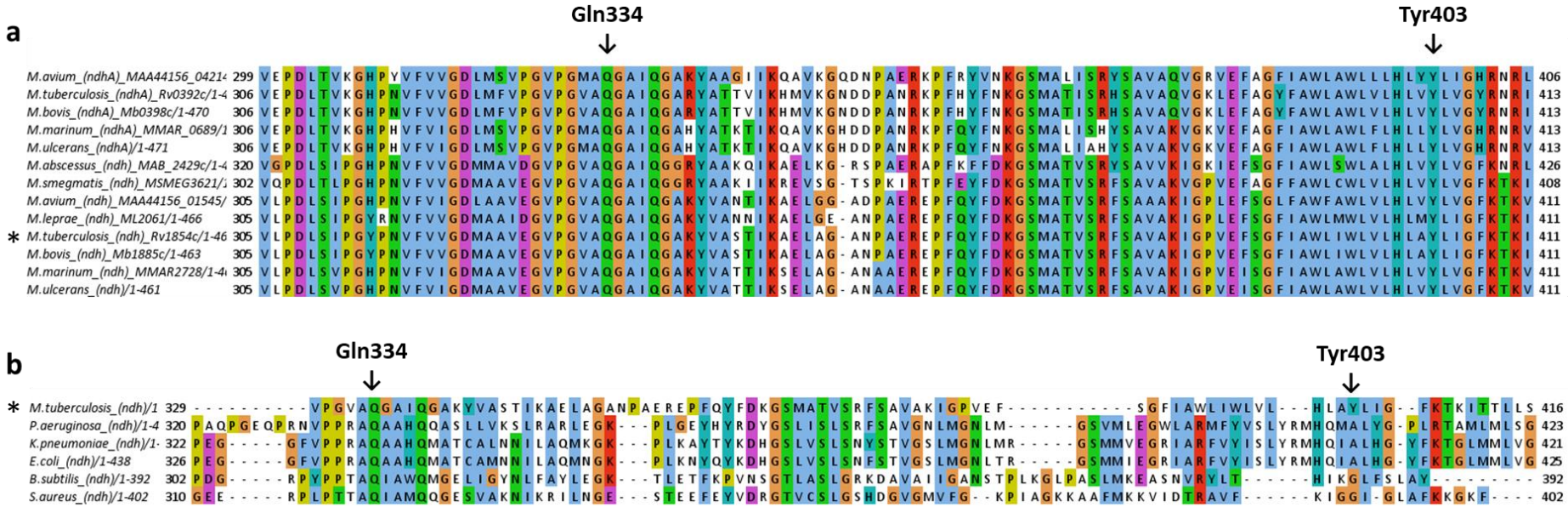

Figure S6: Protein sequence alignment of type II NADH dehydrogenases from **a)** different *Mycobacterium species* and **b)** additional Gram-negative and -positive bacteria. Indicated are the three potential interacting residues at the menaquinone access pocket (Gln334, Lys367 and Tyr403 : *Mtb* Ndh numbering), which are highly conserved between mycobacterial Ndh-2 proteins, but not in selected other bacteria, with the exception of Gln334. Mutations in Gln334 and Tyr403 were found to confer resistance to TriSLa inhibitors. Alignment was performed with Clustal Omega [19], and image generated using Jalview [20].

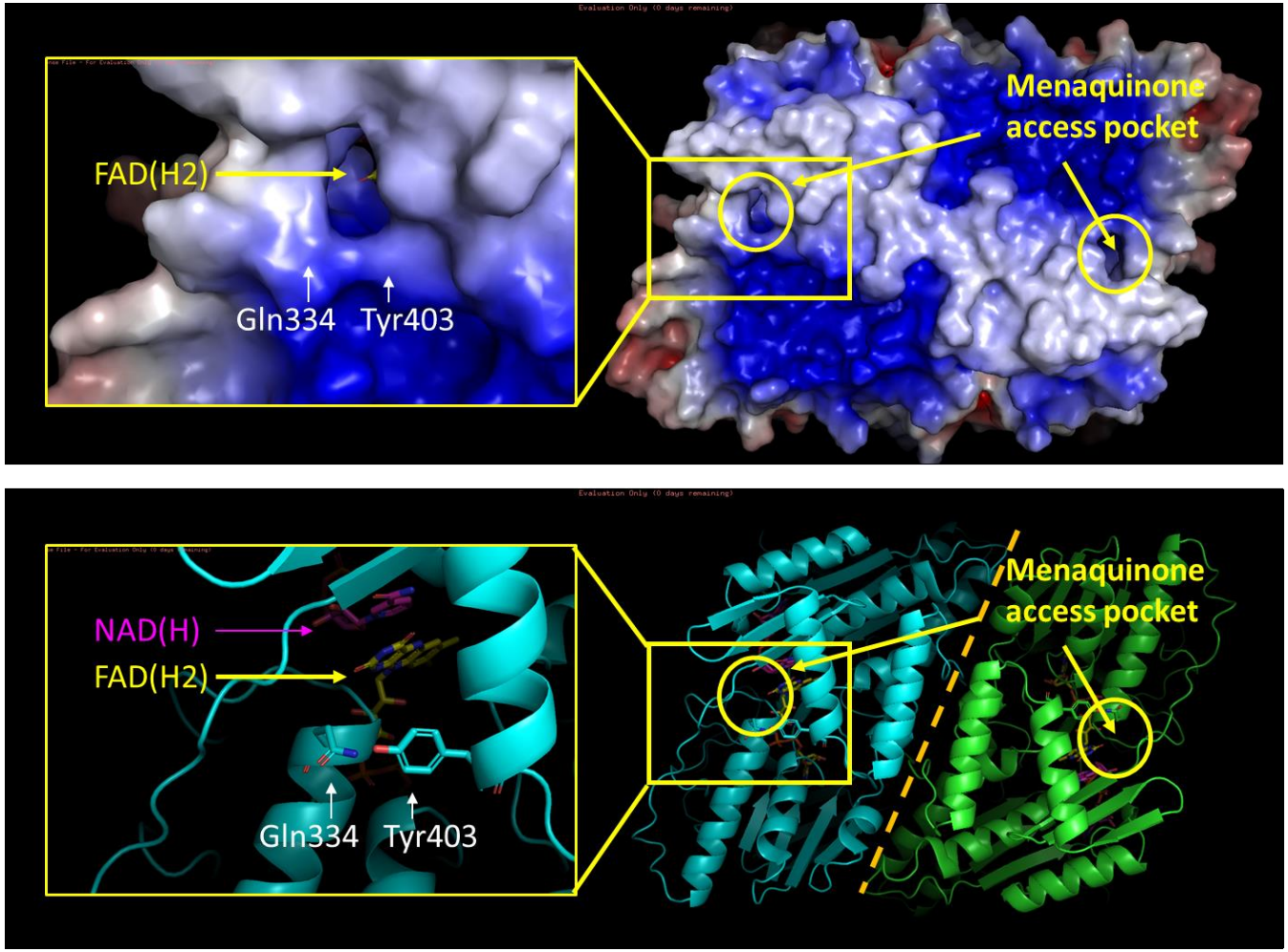

Figure S7: Structural model of the *Mtb* Ndh-dimer showing the position of Gln334 and Tyr403. The structural model of the Ndh dimer was generated using Alphafold [21,22], and superimposed on pdb 4G73 to locate cofactor binding pockets. The orientation of the structural image is as from the within the membrane, with the near side imbedded in the membrane, and the far side in the cytosol. The **top image** shows the electrostatic surface of the Ndh dimer clearly showing the modelled obstruction of the menaquinone access pocket. The **bottom image** is as above, but in cartoon form, showing Gln334 and Tyr403, that interact and seem to act as a gate to the menaquinone pocket, and that confer resistance to TriSLa when mutated. Image generated using PyMol.

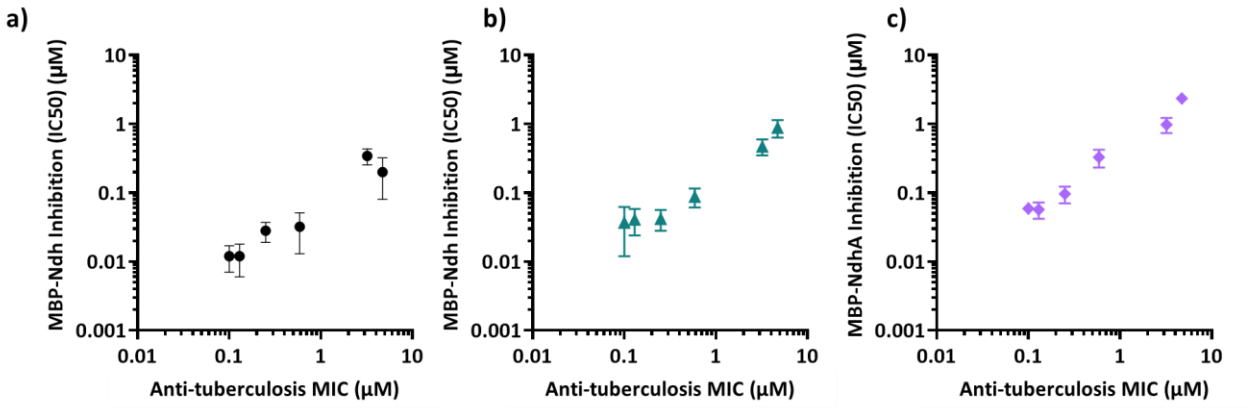

Figure S8: Correlation between the anti-*Mtb* MIC_{98} of TriSLa compounds (as measured using REMA), and their biochemical inhibition of NADH oxidation (IC_{50}) by recombinant MBP-Ndh purified from **a**) *E. coli* Rosetta cells, **b**) *M. smegmatis*, and **c**) recombinant MBP-NdhA purified from *M. smegmatis*.

Supplementary Tables

Table S1: Intrinsic clearance of TriSLa compounds as measured using mouse liver microsomes.

Compound	Mouse Liver Microsome Intrinsic clearance Clint (µL/min/mg protein)
1	640
12	275
11	375
13	110
Propranolol	121

Table S2: Genotype of selected TriSLa resistant mycobacterial mutants

Isolated strain	Genotyping technique	Genotype identified
H37Rv BDM44410, **1** RC14.2	WGS	97 bp del in *ndhA* promoter region
H37Rv BDM44410, **1** RC28.2	WGS	*ndh* (*a1208g* : Tyr403Cys)
H37Rv BDM88689, **11** RC1.1	Sanger Sequencing	*ndh* (*t1207c* : Tyr403His)
H37Rv BDM88689, **11** RC1.2	Sanger Sequencing	ndh (*t1207a* : Tyr403Asn)
Mmar BDM88689, **11** RC1	Sanger Sequencing	*MMAR_2728 [ndh]* (*a1001c :* Gln334Pro)
Mmar BDM88689, **11** RC2	Sanger Sequencing	*MMAR_2728 [ndh]* (*a1001c :* Gln334Pro)
Mmar BDM88689, **11** RC3	Sanger Sequencing	*MMAR_2728 [ndh]* (*a1001g :* Gln334Arg)
Mmar BDM88689, **11** RC6	Sanger Sequencing	*MMAR_2728 [ndh]* (*a1001g :* Gln334Arg)
Mmar BDM88689, **11** RC8	Sanger Sequencing	*MMAR_2728 [ndh]* (*a1001g :* Gln334Arg)

Table S3: *ndh-2* mRNA expression levels in TriSLa resistant strain. Quantitative PCR results showing the expression levels of *ndh* and *ndhA* relative to housekeeping gene *sigA* and parental H37Rv (2^ΔΔct), in parental H37Rv, TriSLa resistant isolate RC14.2 and RC28.1

gene	Parental H37Rv	TriSLa RC 14.2 With 97bp- deletion in ndhA promoter	TriSLa RC 28.2 With point mutation in ndh (Y403C)
ndh	1.00 ± 0.07	0.91 ± 0.14	0.88 ± 0.02
ndhA	1.01 ± 0.13	21.1 ± 3.6	1.03 ± 0.17

Table S4: Biochemical inhibition of recombinant *Mtb* MBP-Ndh, MBP-Ndh(Tyr403Cys) and MBP-Ndh(Gln334Pro) by compounds **1** (**BDM44410**), **11** (**BDM88689**) and **12** (**BDM88690**) as presented by the mean IC_{50} and standard deviation of at least 3 independent replicates.

TriSLa	MBP-Ndh(WT) Inhibition IC_{50} (nM)	MBP-Ndh(Y403C) Inhibition IC_{50} (nM)	MBP-Ndh(Q334P) Inhibition IC_{50} (nM)
1	318 ± 90	20426 ± 8865	23178 ± 7264
11	8.5 ± 0.9	271.2 ± 91.7	1720 ± 214
12	8.1 ± 1.4	283.8 ± 45.4	1553 ± 174

Table S5: The MIC of TriSLa against *M. tuberculosis* H37Rv *M. marinum* M strain grown in media with and without fatty acids. Experiments were performed in two different fatty acid-free media with and without supplementation of 200 µM (56 mg/L) oleic acid. Base media 7H9-GANDCTy was composed of Middlebrook 7H9 base medium (7H9), 0.2 % glycerol (G), 0.05% Tyloxapol (Ty), 5 g/L fatty acid-free bovine serum albumin (A), 0.85 g/L NaCl (N), 2 g/L glucose/dextrose (D) and 4 mg/L catalase (C). Sauton's minimal modified medium (SMMM) was as in [12], composed of 0.05% KH_2PO_4, 0.05% $MgSO_4.7H_2O$, 0.2% citric acid, 0.005% ferric ammonium citrate and 0.0001% $ZnSO_4$ with 0.2% glycerol, 0.4% dextrose, 5 g/L fatty acid-free bovine serum albumin, 0.085% NaCl and 4mg/L catalase. Because of the slow growth of H37Rv in fatty acid-free medium, MIC assays were performed with a starting OD_{600} of 0.01, were exposed to antibiotics for 2 weeks (1 week for *M. marinum*), and viability evaluated visually and by OD_{600}. MIC values are the mean MIC (MIC range) of 2 independent biological replicates.

	Growth Medium	Cpd 1 MIC_{98} (µM)	Cpd 11 MIC_{98} (µM)	Cpd 12 MIC_{98} (µM)	BDQ MIC_{98} (µM)	RIF MIC_{98} (nM)	CBR5992 MIC_{98} (µM)
Activity against *Mycobacterium tuberculosis* H37Rv	**Variable fatty acid content (2-week exposure, viability by REMA)**						
	7H9-GTy-ANDC (**fatty acid free**)	16.7 (12.5-25)	6.7 (5-10)	3.3 (2.5-5)	0.51 (0.31-0.63)	75	8.3 (5-10)
	7H9-GTy-ANDC with **200 µM oleic acid**	3.1	0.26 (0.16-0.31)	0.31	0.63	66 (38-75)	2.5
	Variable fatty acid content (2-week exposure, viability by OD600)						
	7H9-GTy-ANDC (**fatty acid free**)	/	12.5-50	12.5-50	0.63	75-300	12.5-50
	7H9-GTy-ANDC with **200 µM oleic acid**	/	0.3-0.4	0.3-0.4	0.63	75	3.1-6.3
	SMMM (**fatty acid free**)	/	25-50	25-50	0.63	150-600	>50
	SMMM with **200 µM oleic acid**	/	0.3-0.4	0.3-0.8	0.63	150-300	6.3
Activity against *Mycobacterium marinum M strain*	**Variable fatty acid content (2-week exposure, viability by OD600)**						
	7H9-GTy-ANDC (**fatty acid free**)	n/a	25	25	0.16	500->500	>50
	7H9-GTy-ANDC with **200 µM oleic acid**	n/a	0.39-0.78	0.39-0.78	0.16	>500	>50
	SMMM (**fatty acid free**)	n/a	25	25	0.16	>500	>50
	SMMM with **200 µM oleic acid**	n/a	0.20-0.39	0.39	0.16	>500	>50

Table S6: The MIC of TriSLa against H37Rv grown in media without and with 0.1 or 1 mM L-serine or in in media without detergents or with 0.05% Tween80 or 0.05% Tyloxapol. Experiments for L-serine were performed in Middlebrook 7H9 base medium (7H9), supplemented with 0.2 % glycerol (G), 0.05% tween 80 (T) and 10% OADC (commercial). MIC assays were performed with a starting OD_{600} of 0.001, with bacterial viability evaluated by REMA following 1-week compound exposure. MICs are minimal concentrations that prevent less than 2% resazurin turnover MIC values are the mean MIC (MIC range) of 3 independent biological replicates.

Mtb **Growth Medium**	**Cpd 1** **MIC_{98} (µM)**	**Cpd 11** **MIC_{98} (µM)**	**Cpd 12** **MIC_{98} (µM)**	**BDQ** **MIC_{98} (µM)**	**RIF** **MIC_{98} (nM)**	**CBR5992** **MIC_{98} (µM)**
7H9-GT-OADC (**No L-serine**)	6.25	0.16	0.219 (0.16-0.31)	0.36 (0.16-0.5)	5 (3.1-6.3)	0.63
7H9-GT-OADC (**0.1 mM L-serine**)	14.6 (6.25-25)	0.69 (0.31-1.25)	0.75 (0.63-1.25)	0.36 (0.16-0.5)	3.13	2.5 (1.25-5)
7H9-GT-OADC (**1 mM L-serine**)	50	1.25	1.25	0.42 (0.31-0.5)	5.63 (3.13-6.25)	4.0 (2.5-5)
7H9-G-OADC (**detergent free**)	5.73 (3.13-6.25)	0.13	0.17 (3.13-6.25)	0.17 (0.125-0.25)	61	n/a
7H9-GT-OADC (**0.05% Tween80**)	7.30 (6.25-12.5)	0.19 (0.125-0.25)	0.19 (0.125-0.25)	0.33 (0.25-0.5)	3.0 (1.8-3.6)	n/a
7H9-GTy-OADC (**0.05% Tyloxapol**)	6.25	0.13	0.13	0.33 (0.25-0.5)	30	n/a

Table S7: Primers used in this work.

Oligonucleotides		
760	5’-ATAATCTAGAATGAGTCCCCAGCAAGAACC	Mtb *ndh* amplification for cloning
761	5’-ACATAAGCTTCTAGCTGGCCACCTTAGCG	Mtb *ndh* amplification for cloning
762	5’-ATAATCTAGAATGACGCTCTCATCTGGTGAC	Mtb *ndhA* amplification for cloning
763	5’-ACATAAGCTTCTAACCCGCTGCCTCTTGC	Mtb *ndhA* amplification for cloning
802	5’-TGCTGCACCTGGCGTGCCTGATCGGGTTCAA	*ndh* site directed mutagenesis Y403C
803	5’-TTGAACCCGATCAGGCACGCCAGGTGCAGCA	*ndh* site directed mutagenesis Y403C
1106	5’-GGATGGCGCCCGGCGCCACACCC	*ndh* site directed mutagenesis Q334P
1107	5’-GGGTGTGGCGCCGGGCGCCATCC	*ndh* site directed mutagenesis Q334P
746	5’-CACATCGACTCGACCAAGG	qPCR primer *ndh* (forward)
747	5’-GTCGACGTCGGTGACCAT	qPCR primer *ndh* (reverse)
750	5’-AGACAACGACCCACCTGTTC	qPCR primer *ndhA* (forward)
751	5’-TCCATCAATTTCGACGTGAC	qPCR primer *ndhA* (reverse)
57	5’-AAACAGATCGGCAAGGTAGC	qPCR primer *sigA* (forward)
58	5’-CTGGATCAGGTCGAGAAACG	qPCR primer *sigA* (reverse)
1036	5’-TACACATGCTCACGAGTTGG	Sequencing primer for Mmar *ndh* (*MMAR_2728*)
1037	5’-TTAGTACGTGGCAAGCGGAA	Sequencing primer for Mmar *ndh* (*MMAR_2728*)
749	5’-GAACAGGTGGGTCGTTGTCT	Sequencing of *ndhA* promoter in H37Rv
1267	5’-TACTACTAGTACGCTCTCATCTGGTGAACCC	Cloning of *ndhA* into pSD26:MBPndh
1268	5’-TACTGATATCCTAACCCGCTGCCTCTTGC	Cloning of *ndhA* into pSD26:MBPndh

^{1}H, ^{13}C NMR, 2D-NMR, HRMS and LCMS data

Compound 1, ^{1}H NMR (300 MHz, $CDCl_3$)

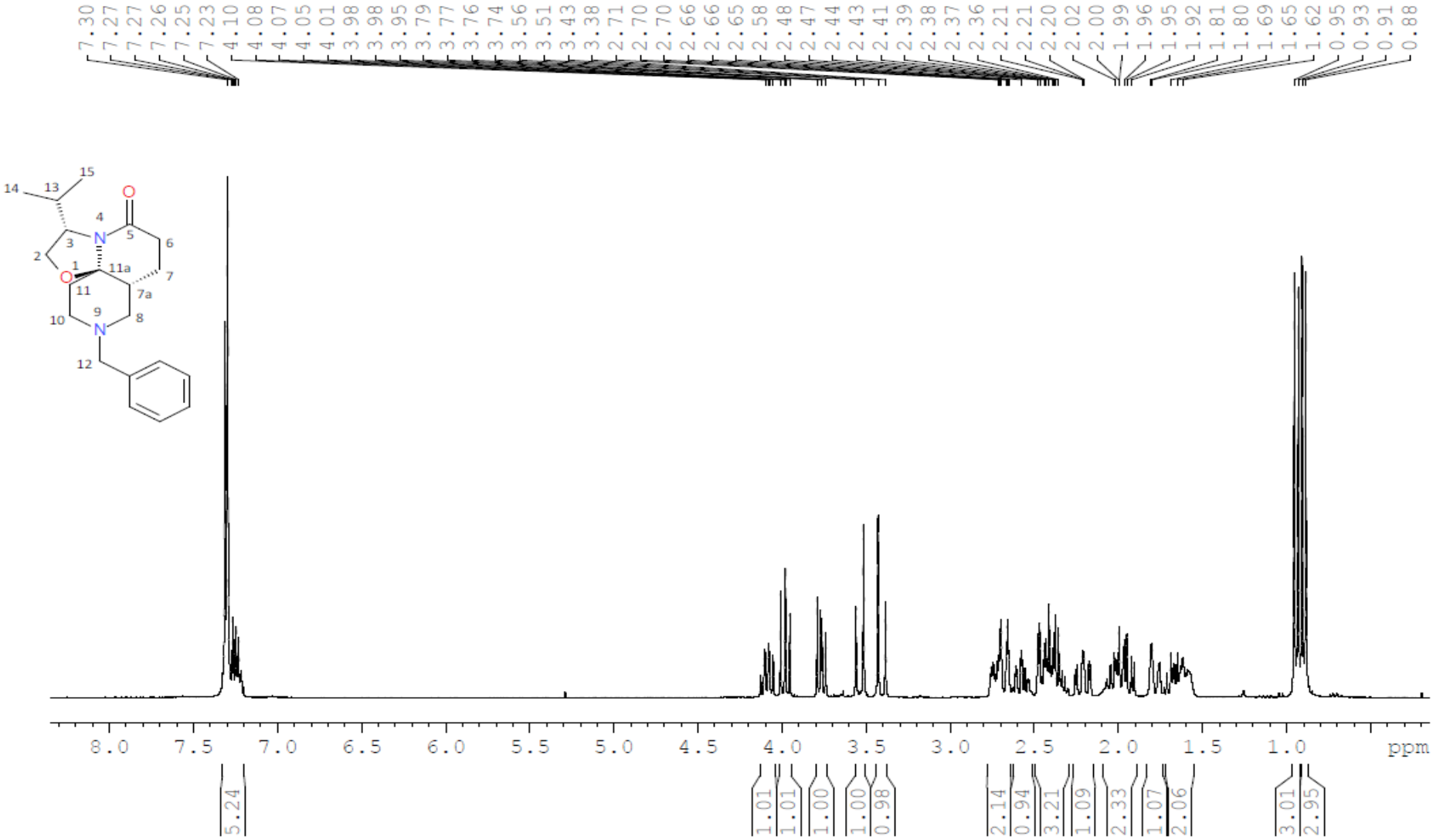

Compound 1,^{13}C NMR (75 MHz, $CDCl_3$)

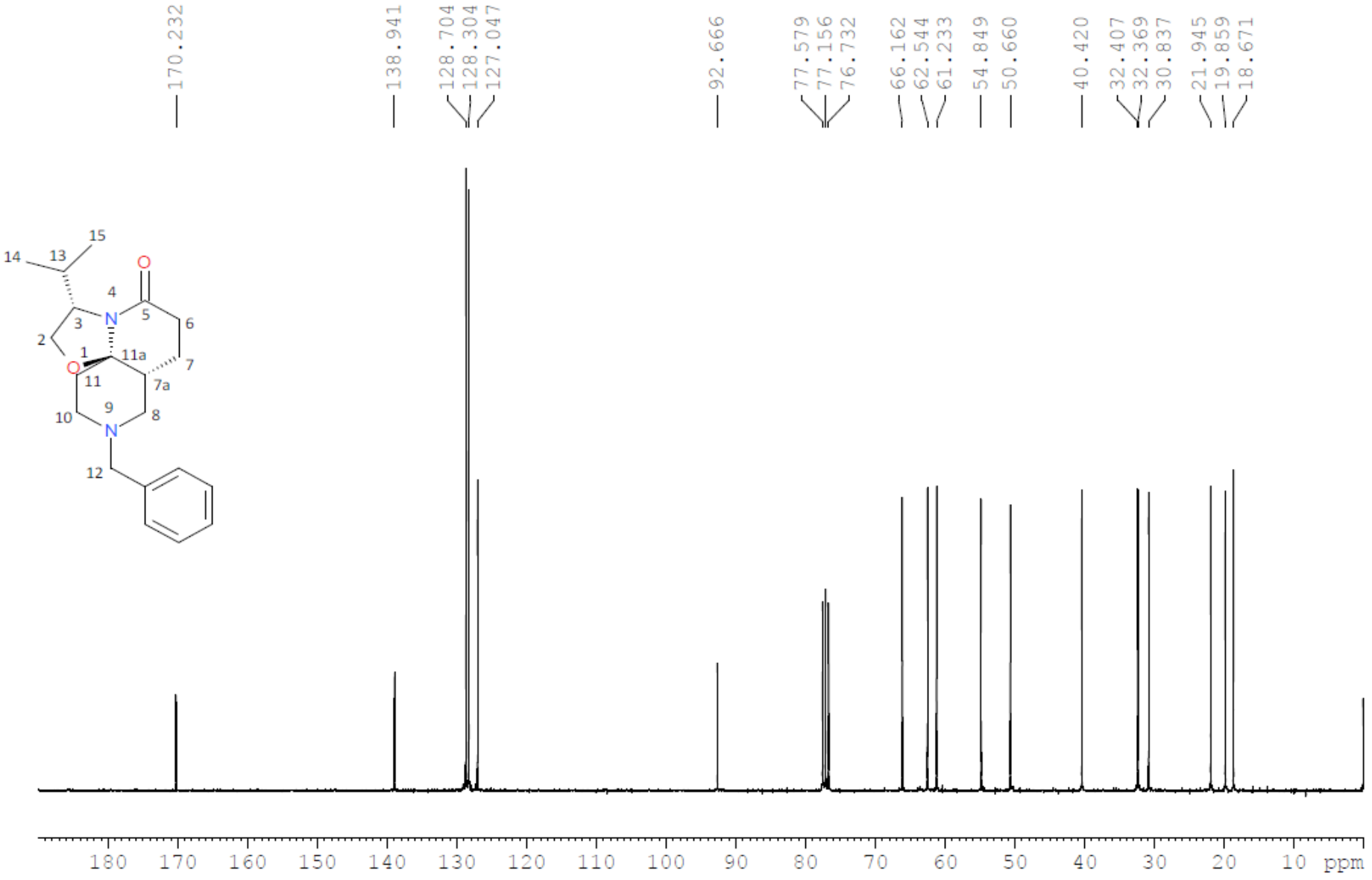

Compound 1, HRMS

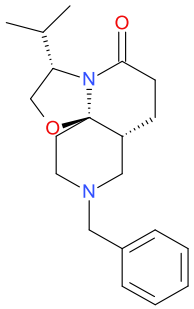

Formula Weight: 328,44851
Exact Mass: 328,215078156
Molecular Formula: $C_{20}H_{28}N_2O_2$

Elemental Composition Report

Single Mass Analysis

Tolerance = 10.0 PPM / DBE: min = -1.5, max = 500.0
Element prediction: Off
Number of isotope peaks used for i-FIT = 3

Monoisotopic Mass, Even Electron Ions
126 formula(e) evaluated with 1 results within limits (up to 10 best isotopic matches for each mass)
Elements Used:
C: 0-40 H: 0-50 N: 0-4 O: 0-5

BDM44410 111 (2.142)

1: TOF MS ES+
4.22e+004

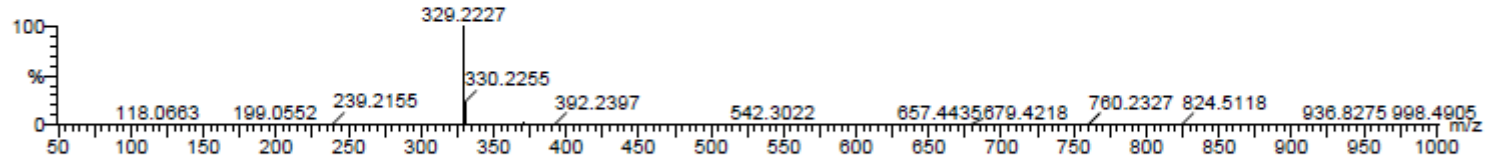

Minimum:				-1.5		
Maximum:		100.0	10.0	500.0		
Mass	Calc. Mass	mDa	PPM	DBE	i-FIT	Formula
329.2227	329.2229	-0.2	-0.6	7.5	11.8	C20 H29 N2 O2

Compound 2, ^{1}H NMR (500 MHz, $CDCl_3$)

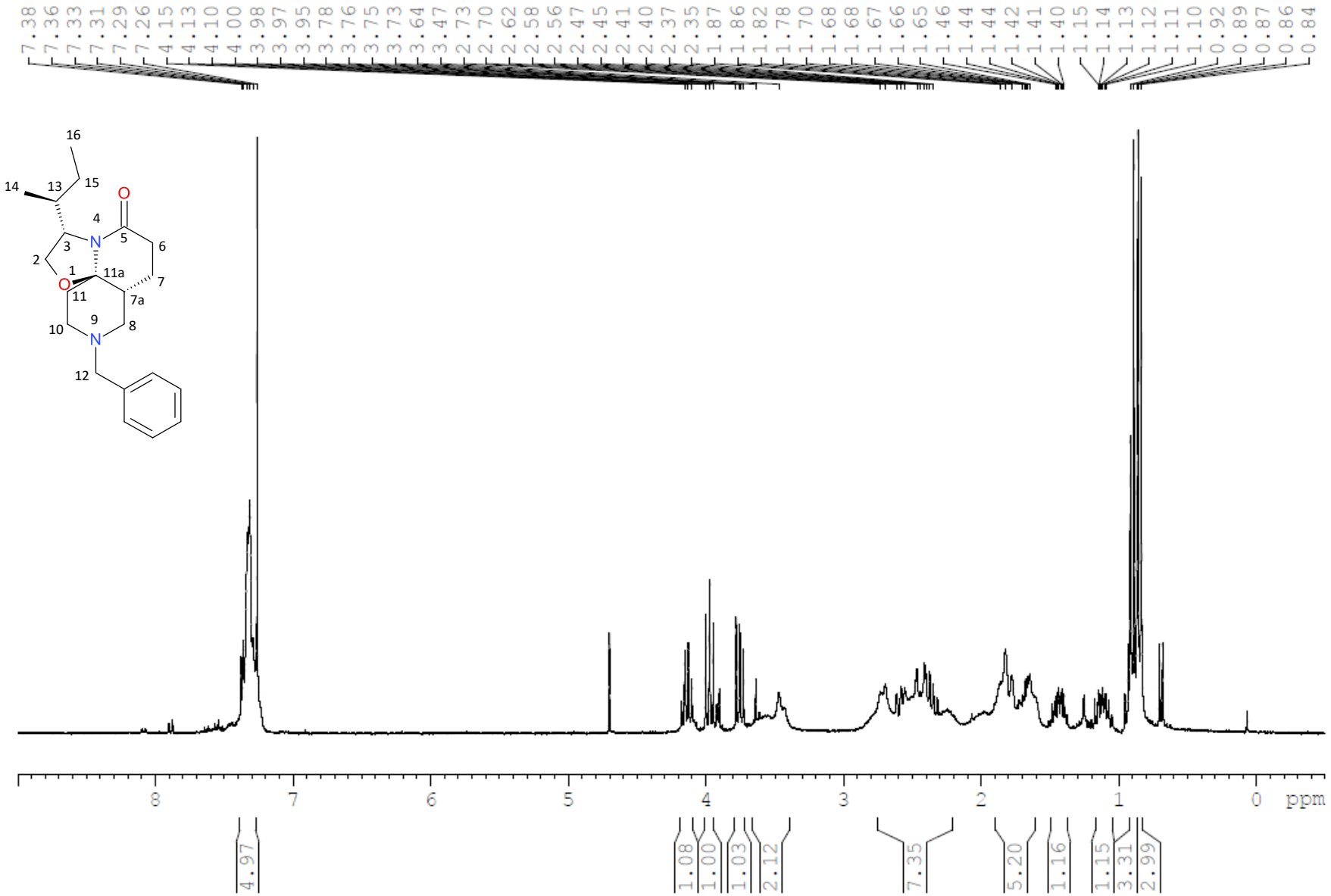

Compound 2, ^{13}C NMR (125 MHz, $CDCl_3$)

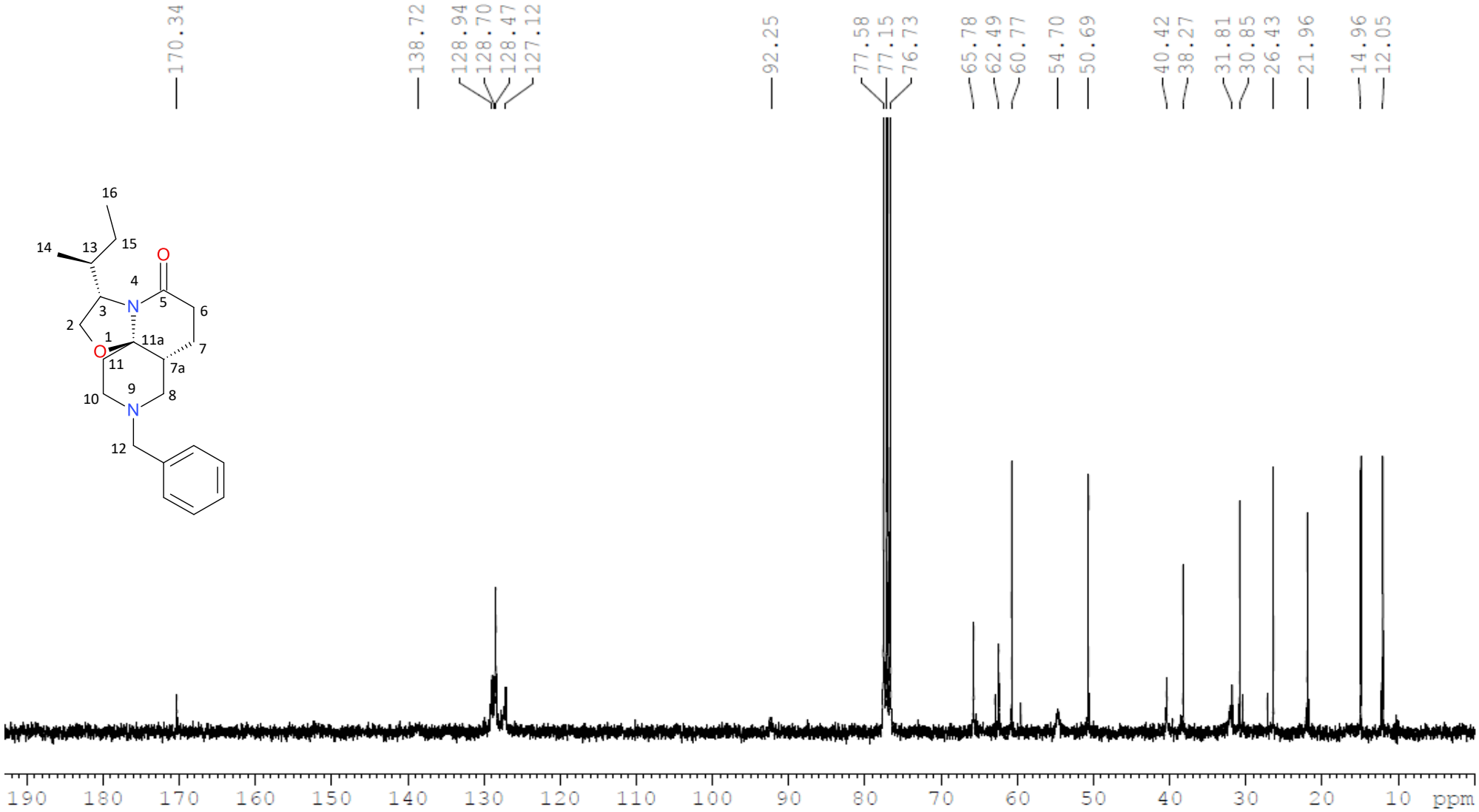

Compound 2, HRMS

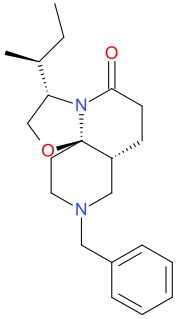

Formula Weight: 342,4751
Exact Mass: 342,23072822
Molecular Formula: $C_{21}H_{30}N_2O_2$

Elemental Composition Report

Single Mass Analysis

Tolerance = 5.0 mDa / DBE: min = -1.5, max = 500.0
Element prediction: Off
Number of isotope peaks used for i-FIT = 2

Monoisotopic Mass, Even Electron Ions
194 formula(e) evaluated with 3 results within limits (up to 5 closest results for each mass)
Elements Used:
C: 0-30 H: 0-48 N: 0-5 O: 0-7

NL4TB-G3 210 (2.112) Cm (210:213-(229:238+192:201))

1: TOF MS ES+
1.64e+005

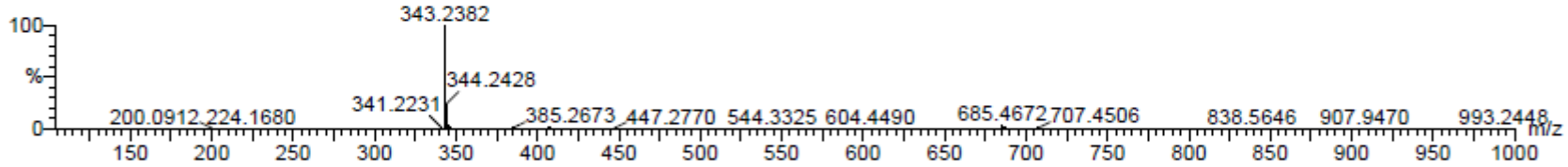

Minimum:				-1.5		
Maximum:		5.0	10.0	500.0		
Mass	Calc. Mass	mDa	PPM	DBE	i-FIT	Formula
343.2382	343.2386	-0.4	-1.2	7.5	25.5	C21 H31 N2 O2
	343.2345	3.7	10.8	3.5	511.8	C16 H31 N4 O4
	343.2426	-4.4	-12.8	11.5	906.0	C26 H31

Compounds 4a and 4b, ^{1}H NMR (300 MHz, CD_2Cl_2)

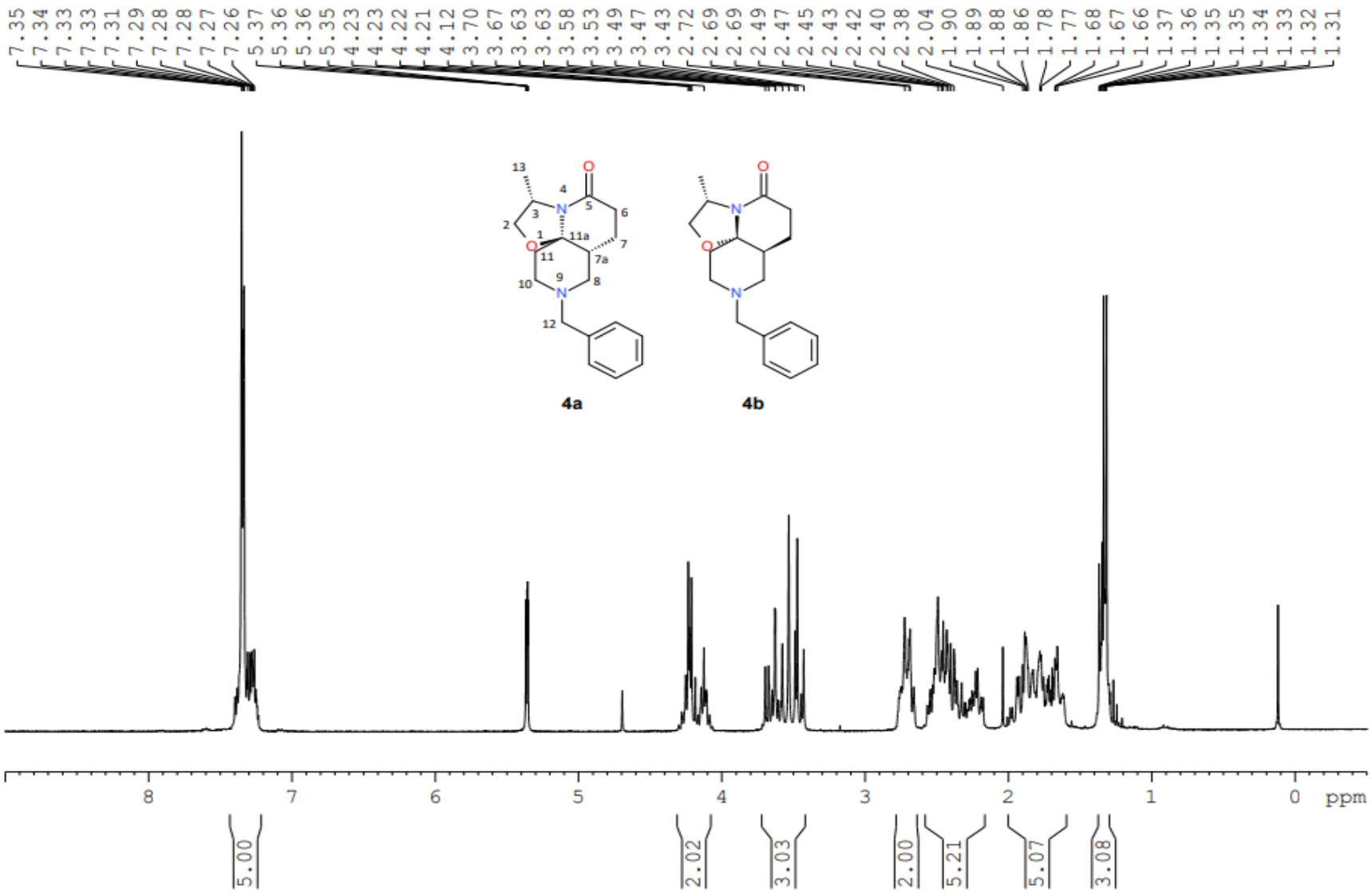

Compounds 4a and 4b, ^{13}C NMR (75 MHz, CD_2Cl_2)

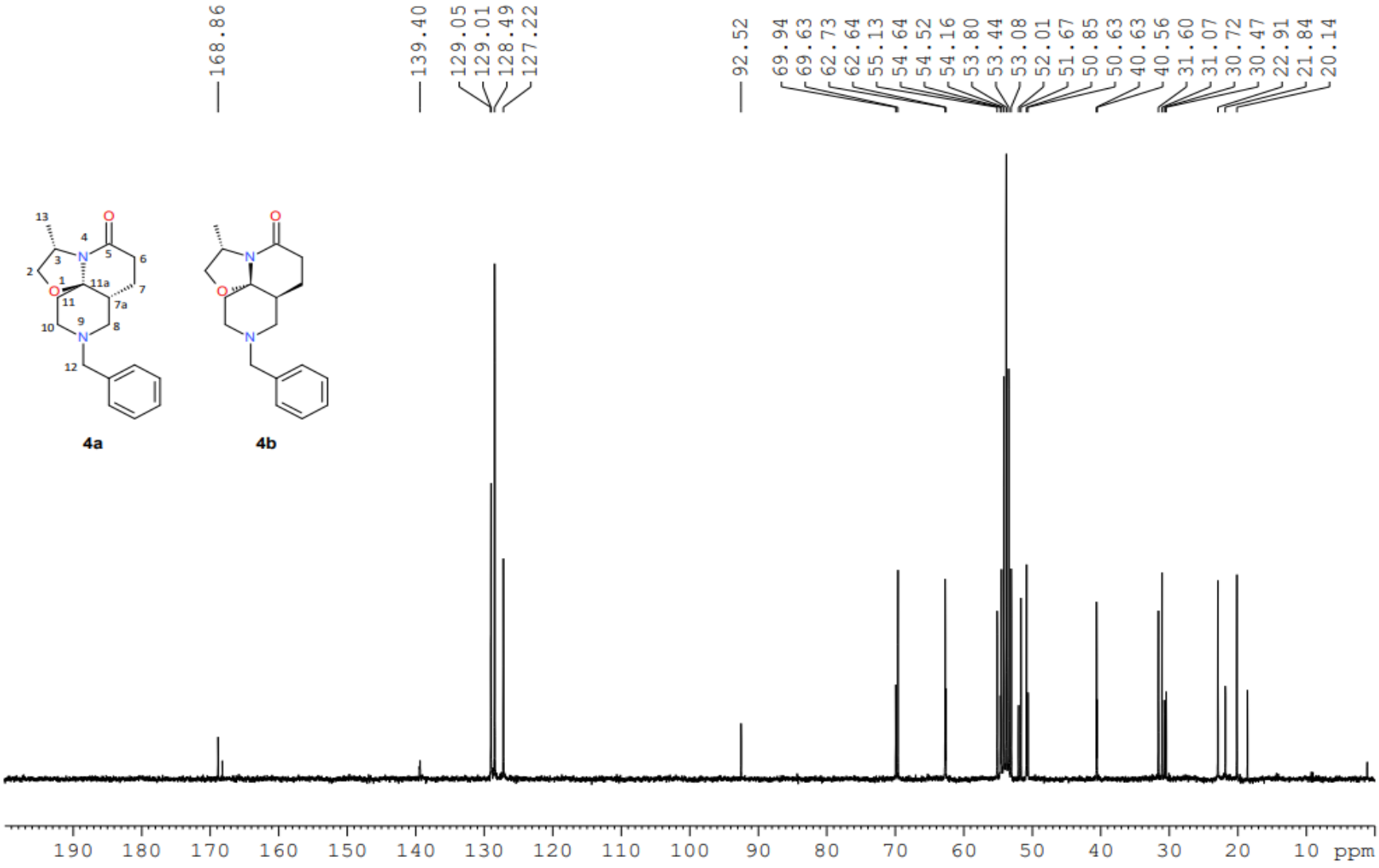

Compounds 4a and 4b, HRMS

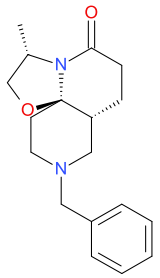

Formula Weight: 300,3953
Exact Mass: 300,1837
Molecular Formula: $C_{18}H_{24}N_2O_2$

Elemental Composition Report

Single Mass Analysis

Tolerance = 100.0 mDa / DBE: min = -1.5, max = 500.0
Element prediction: Off
Number of isotope peaks used for i-FIT = 3

Monoisotopic Mass, Even Electron Ions
2 formula(e) evaluated with 2 results within limits (up to 10 best isotopic matches for each mass)
Elements Used:
C: 10-25 H: 17-40 N: 2-2 O: 2-2

NL4TB2-D1 181 (1.829) Cm (179:182-(190:219+136:171))

1: TOF MS ES+
3.08e+005

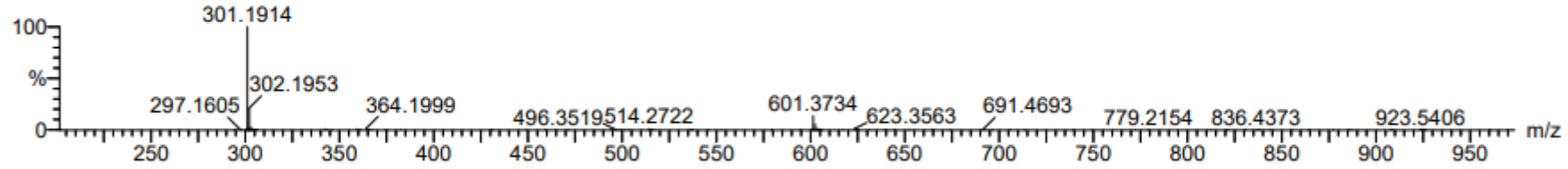

Minimum:				-1.5		
Maximum:		100.0	5.0	500.0		
Mass	Calc. Mass	mDa	PPM	DBE	i-FIT	Formula
301.1914	301.1916	-0.2	-0.7	7.5	9.2	C18 H25 N2 O2
	301.2855	-94.1	-312.4	0.5	102233.1	C17 H37 N2 O2

Compounds 5a and 5b, ^{1}H NMR (300 MHz, CD_2Cl_2)

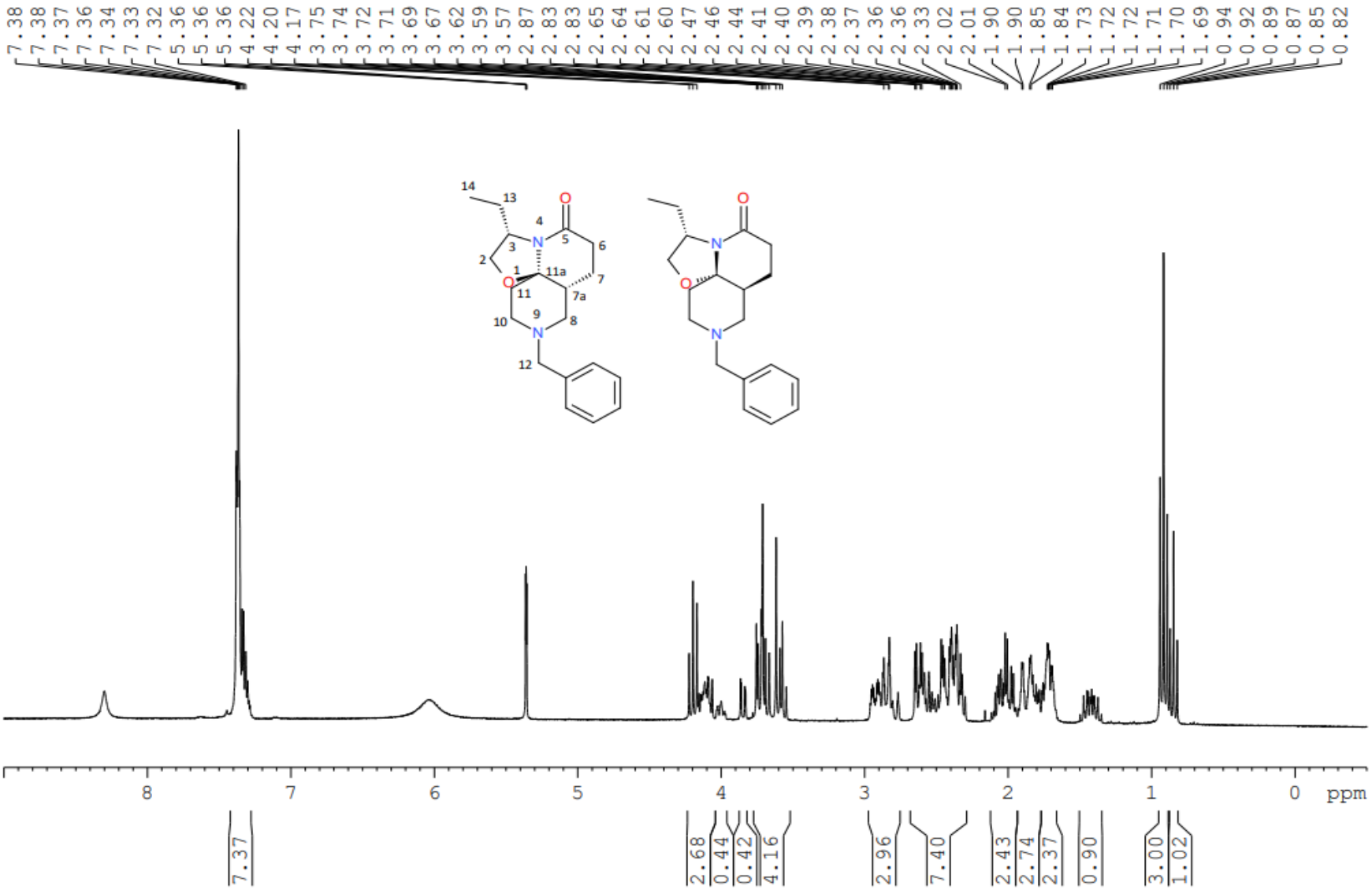

Compounds 5a and 5b, ^{13}C NMR (75 MHz, CD_2Cl_2)

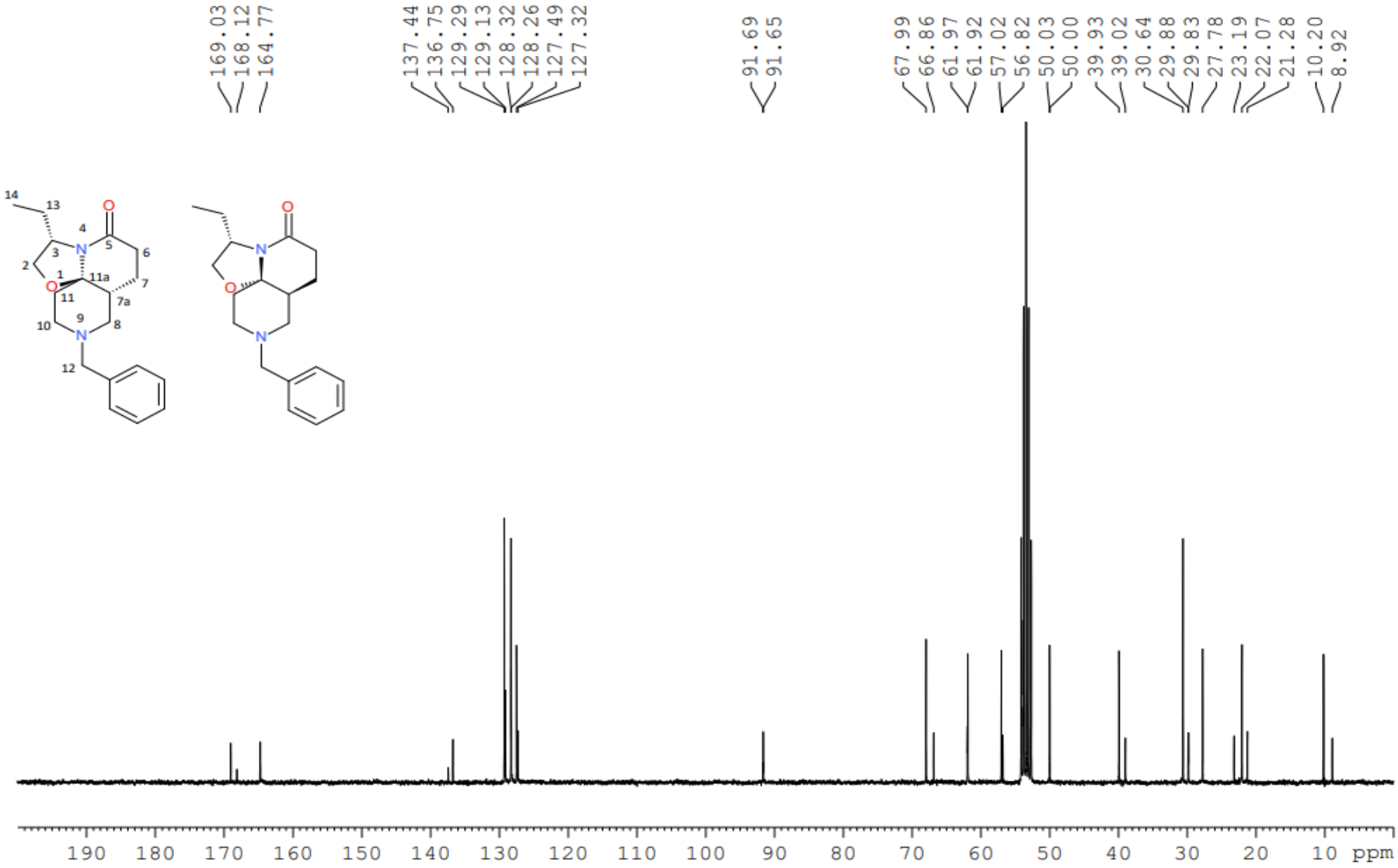

Compounds 5a and 5b, HRMS

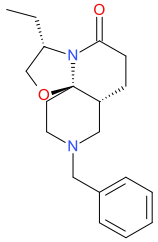

Formula Weight: 314,4219
Exact Mass: 314,1994
Molecular Formula: $C_{19}H_{26}N_2O_2$

Elemental Composition Report

Single Mass Analysis

Tolerance = 10.0 PPM / DBE: min = -1.5, max = 500.0
Element prediction: Off
Number of isotope peaks used for i-FIT = 3

Monoisotopic Mass, Even Electron Ions
10568 formula(e) evaluated with 24 results within limits (up to 5 best isotopic matches for each mass)
Elements Used:
C: 0-30 H: 0-50 N: 0-10 O: 0-10 F: 0-6 S: 0-2 Cl: 0-2

NL4TB-F2 191 (1.931) Cm (189:195-(169:184+200:226))

1: TOF MS ES+
5.97e+005

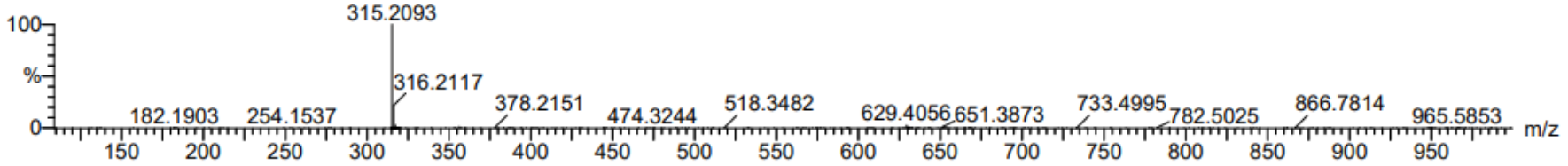

Mass	Calc. Mass	mDa	PPM	DBE	i-FIT	Formula
Minimum:				-1.5		
Maximum:		100.0	10.0	500.0		
315.2093	315.2073	2.0	6.3	7.5	181.3	C19 H27 N2 O2
	315.2124	-3.1	-9.8	7.5	858.3	C21 H28 O F
	315.2084	0.9	2.9	3.5	885.2	C16 H28 N2 O3 F
	315.2111	-1.8	-5.7	0.5	2872.7	C16 H28 F5
	315.2109	-1.6	-5.1	4.5	2910.1	C14 H25 N6 F2

Compound 6, ^{1}H NMR (300 MHz, $CDCl_3$)

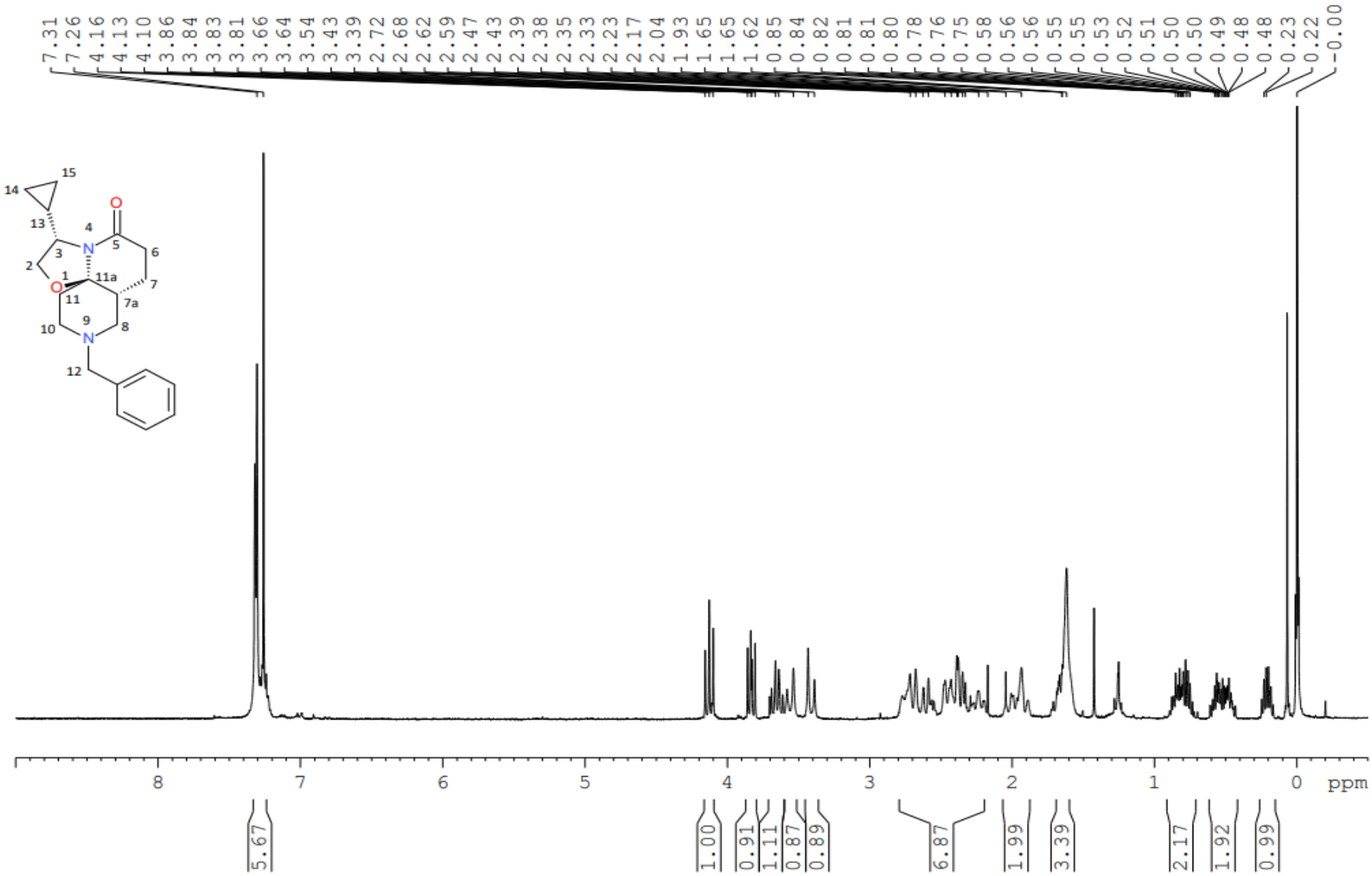

Compound 6, ^{13}C NMR (75 MHz, $CDCl_3$)

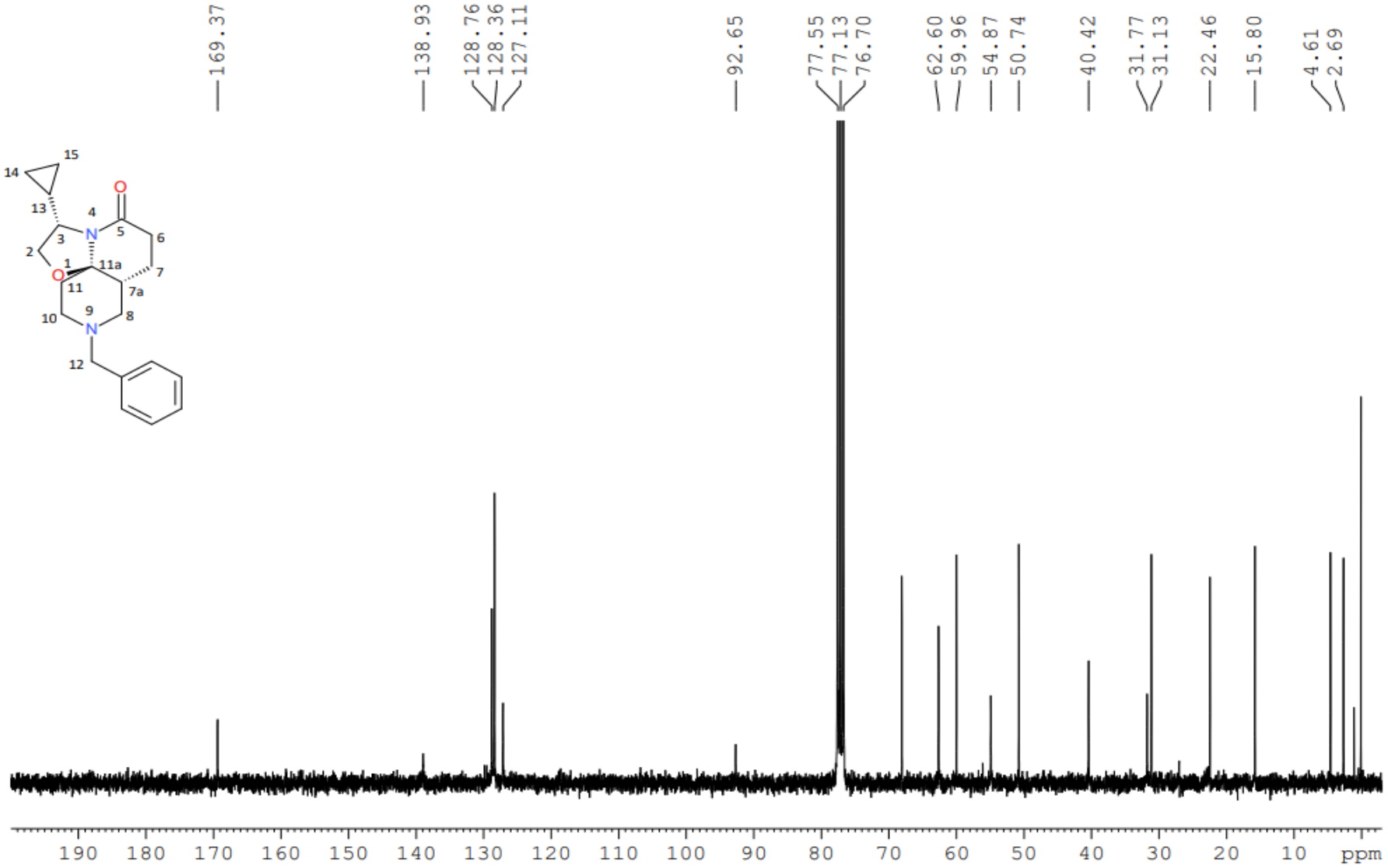

Compound 6, HRMS

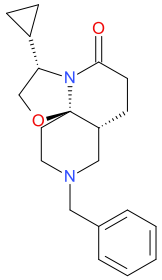

Formula Weight: 326,4326
Exact Mass: 326,1994
Molecular Formula: $C_{20}H_{26}N_2O_2$

Elemental Composition Report

Single Mass Analysis

Tolerance = 10.0 PPM / DBE: min = -1.5, max = 50.0
Element prediction: Off
Number of isotope peaks used for i-FIT = 3

Monoisotopic Mass, Even Electron Ions
146 formula(e) evaluated with 1 results within limits (all results (up to 1000) for each mass)
Elements Used:
C: 10-60 H: 10-70 N: 0-4 O: 0-8

NL4TB2-G5 199 (2.001) Cm (198:205-(160:192+211:244))

1: TOF MS ES+
5.96e+004

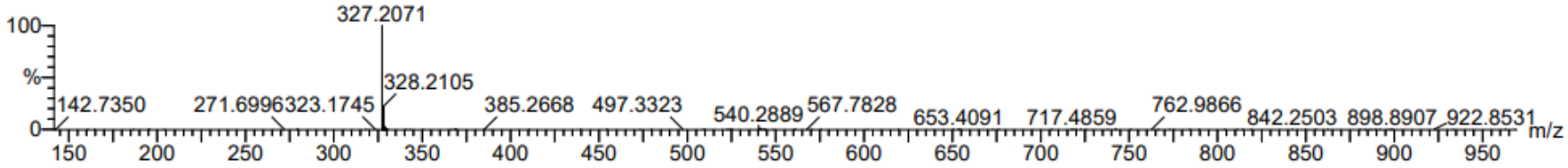

Minimum:				-1.5		
Maximum:		5.0	10.0	50.0		
Mass	Calc. Mass	mDa	PPM	DBE	i-FIT	Formula
327.2071	327.2073	-0.2	-0.6	8.5	34.1	C20 H27 N2 O2

Compound 7, ^{1}H NMR (300 MHz, CD_2Cl_2)

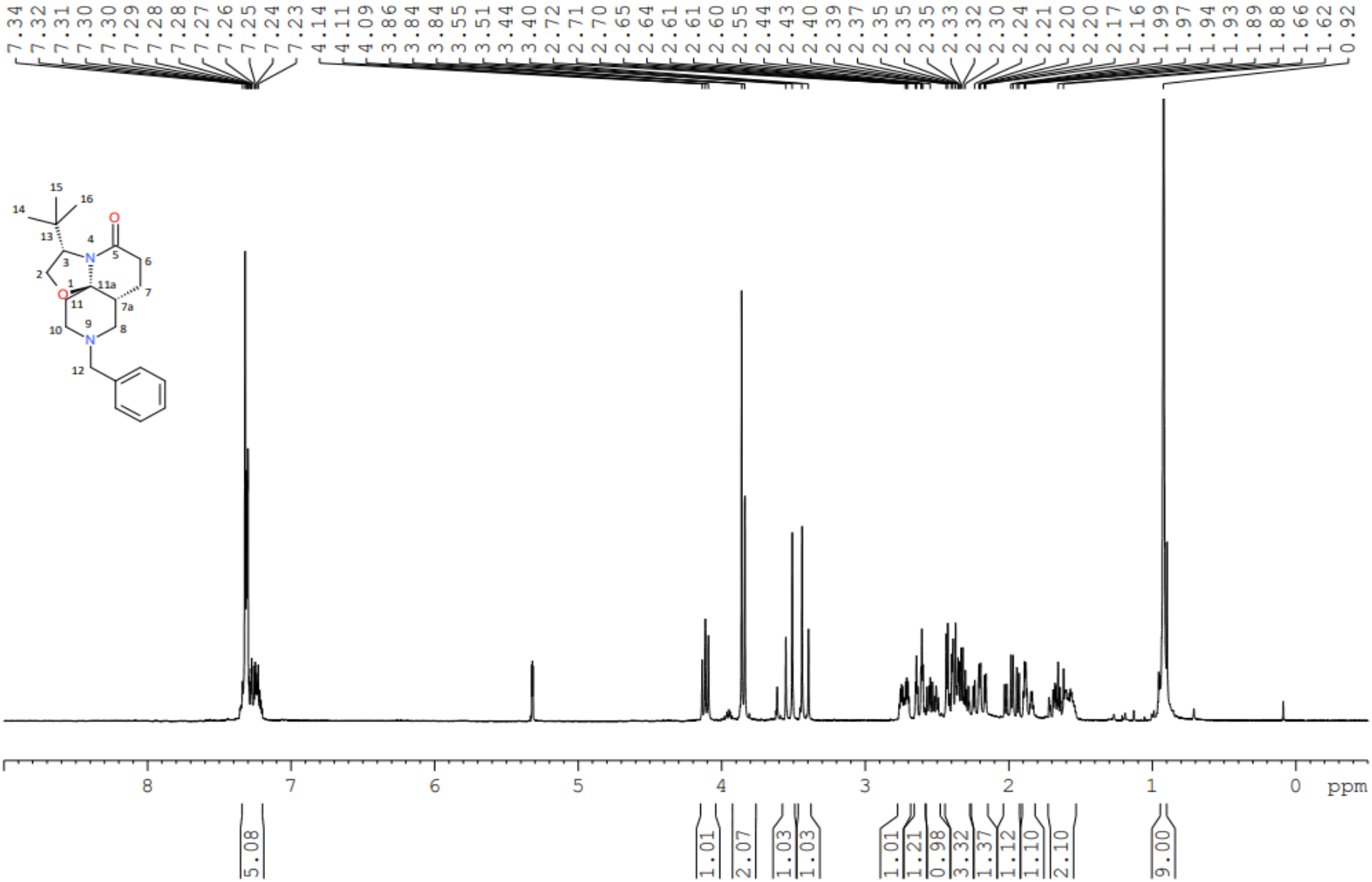

Compound 7, ^{13}C NMR (75 MHz, CD_2Cl_2)

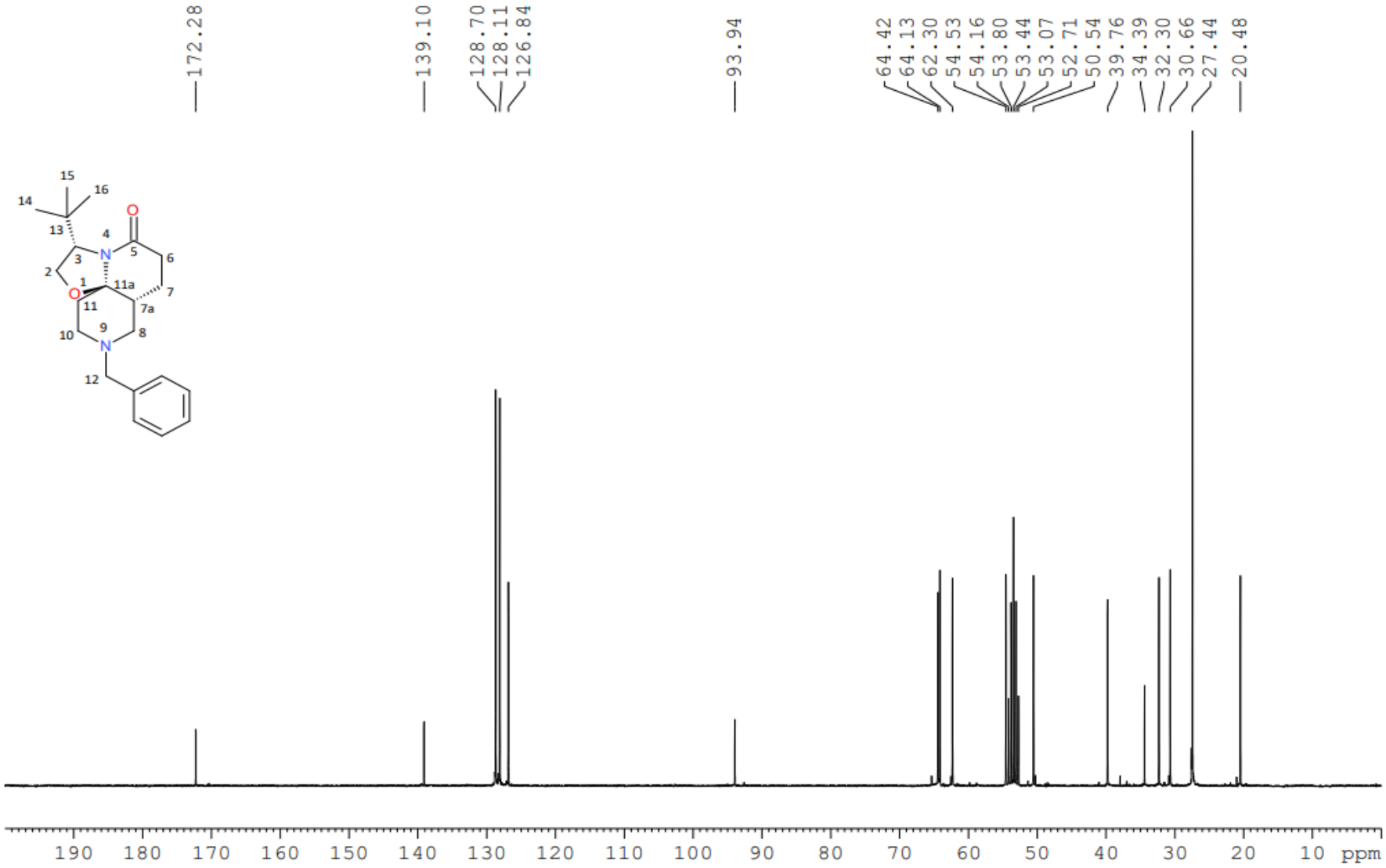

Compound 7, HRMS

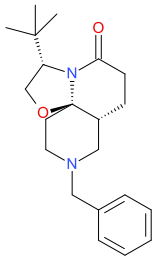

Formula Weight: 342,4751
Exact Mass: 342,2307
Molecular Formula: $C_{21}H_{30}N_2O_2$

Elemental Composition Report

Single Mass Analysis

Tolerance = 5.0 mDa / DBE: min = -1.5, max = 500.0
Element prediction: Off
Number of isotope peaks used for i-FIT = 2

Monoisotopic Mass, Even Electron Ions
194 formula(e) evaluated with 3 results within limits (up to 5 closest results for each mass)
Elements Used:
C: 0-30 H: 0-48 N: 0-5 O: 0-7

NL4TB-A3 216 (2.166) Cm (216:218-(227:236+193:205))

1: TOF MS ES+
2.46e+004

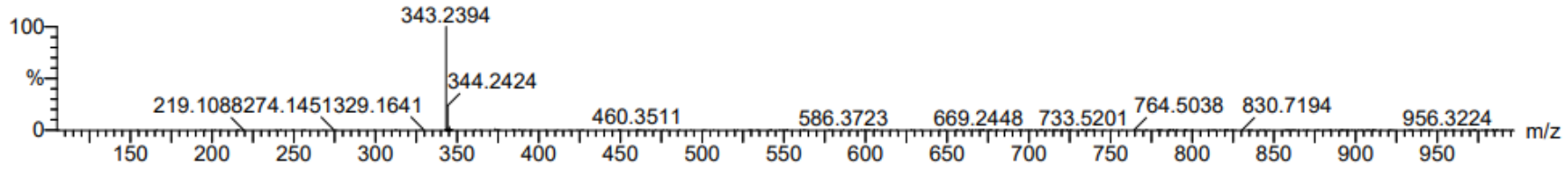

Minimum:				-1.5		
Maximum:		5.0	10.0	500.0		
Mass	Calc. Mass	mDa	PPM	DBE	i-FIT	Formula
343.2394	343.2386	0.8	2.3	7.5	6.4	C21 H31 N2 O2
	343.2426	-3.2	-9.3	11.5	143.7	C26 H31
	343.2345	4.9	14.3	3.5	74.2	C16 H31 N4 O4

Compound 14, ^{1}H NMR (300 MHz, CD_2Cl_2)

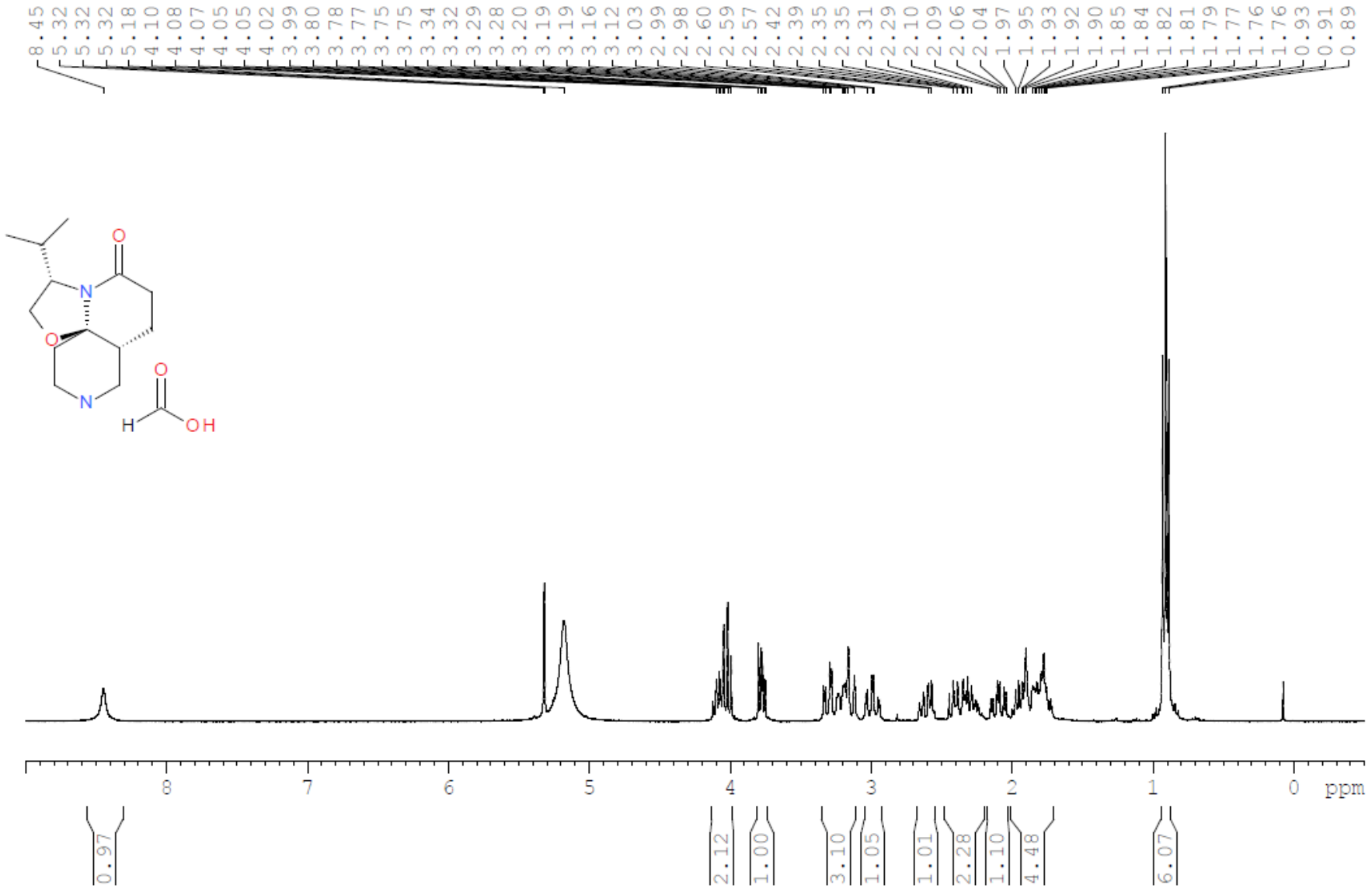

Compound 14, HRMS

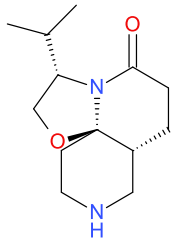

Formula Weight: 238,32598
Exact Mass: 238,168127964
Molecular Formula: $C_{13}H_{22}N_2O_2$

Elemental Composition Report

Single Mass Analysis

Tolerance = 5.0 mDa / DBE: min = -1.5, max = 500.0
Element prediction: Off
Number of isotope peaks used for i-FIT = 2

Monoisotopic Mass, Even Electron Ions
142 formula(e) evaluated with 3 results within limits (up to 5 closest results for each mass)
Elements Used:
C: 0-30 H: 0-48 N: 0-5 O: 0-7

NL4TB-A2 191 (1.932) Cm (190:193-(180:187+199:209))

1: TOF MS ES+
7.51e+004

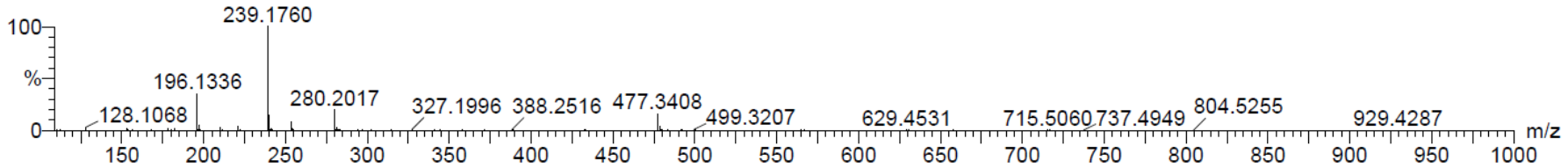

Minimum:				-1.5		
Maximum:		5.0	10.0	500.0		
Mass	Calc. Mass	mDa	PPM	DBE	i-FIT	Formula
239.1760	239.1760	0.0	0.0	3.5	16.3	C13 H23 N2 O2
	239.1800	-4.0	-16.7	7.5	696.5	C18 H23
	239.1719	4.1	17.1	-0.5	425.8	C8 H23 N4 O4

Compound 8, ^{1}H NMR (300 MHz, $CDCl_3$)

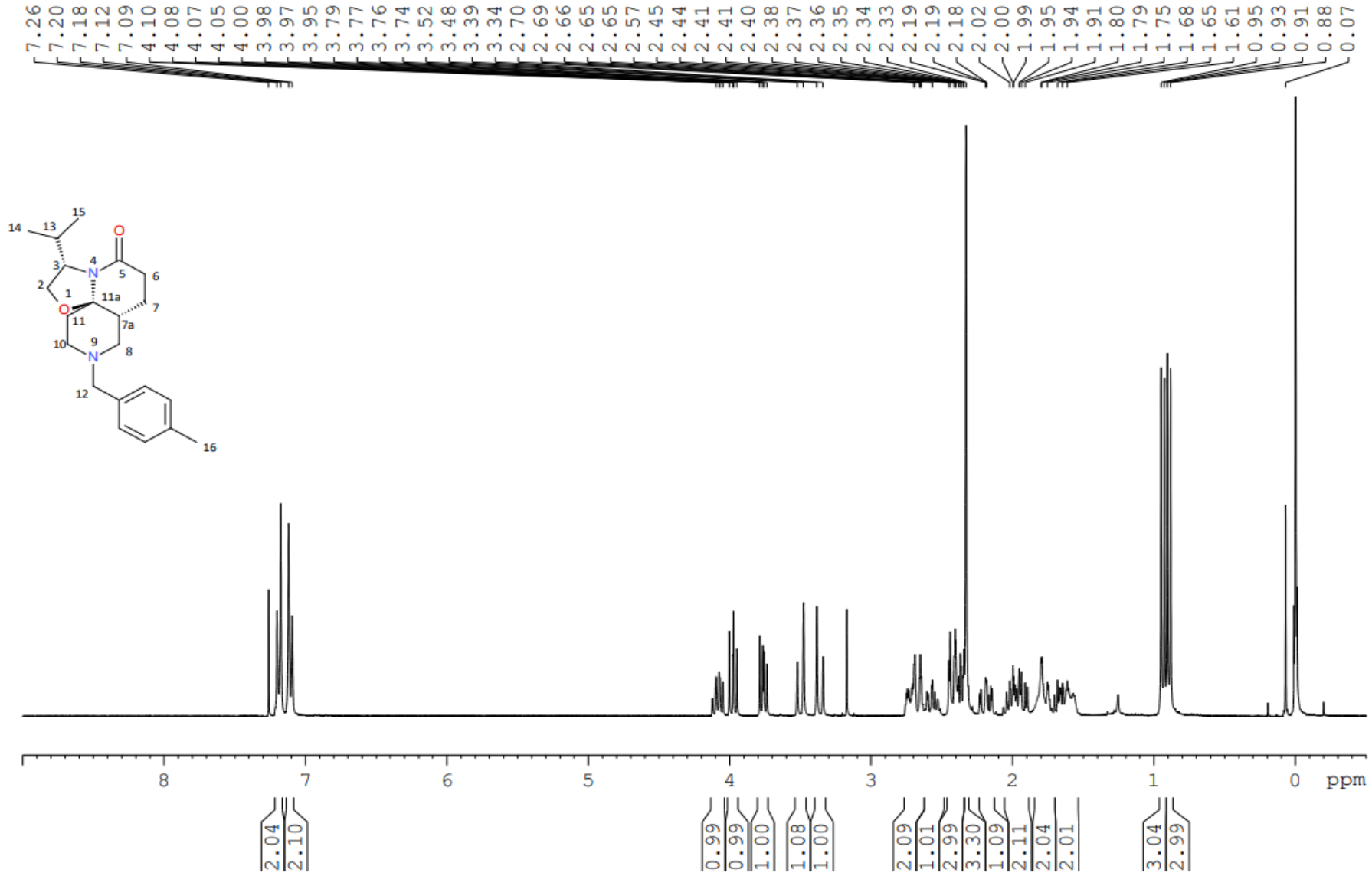

Compound 8, ^{13}C NMR (75 MHz, $CDCl_3$)

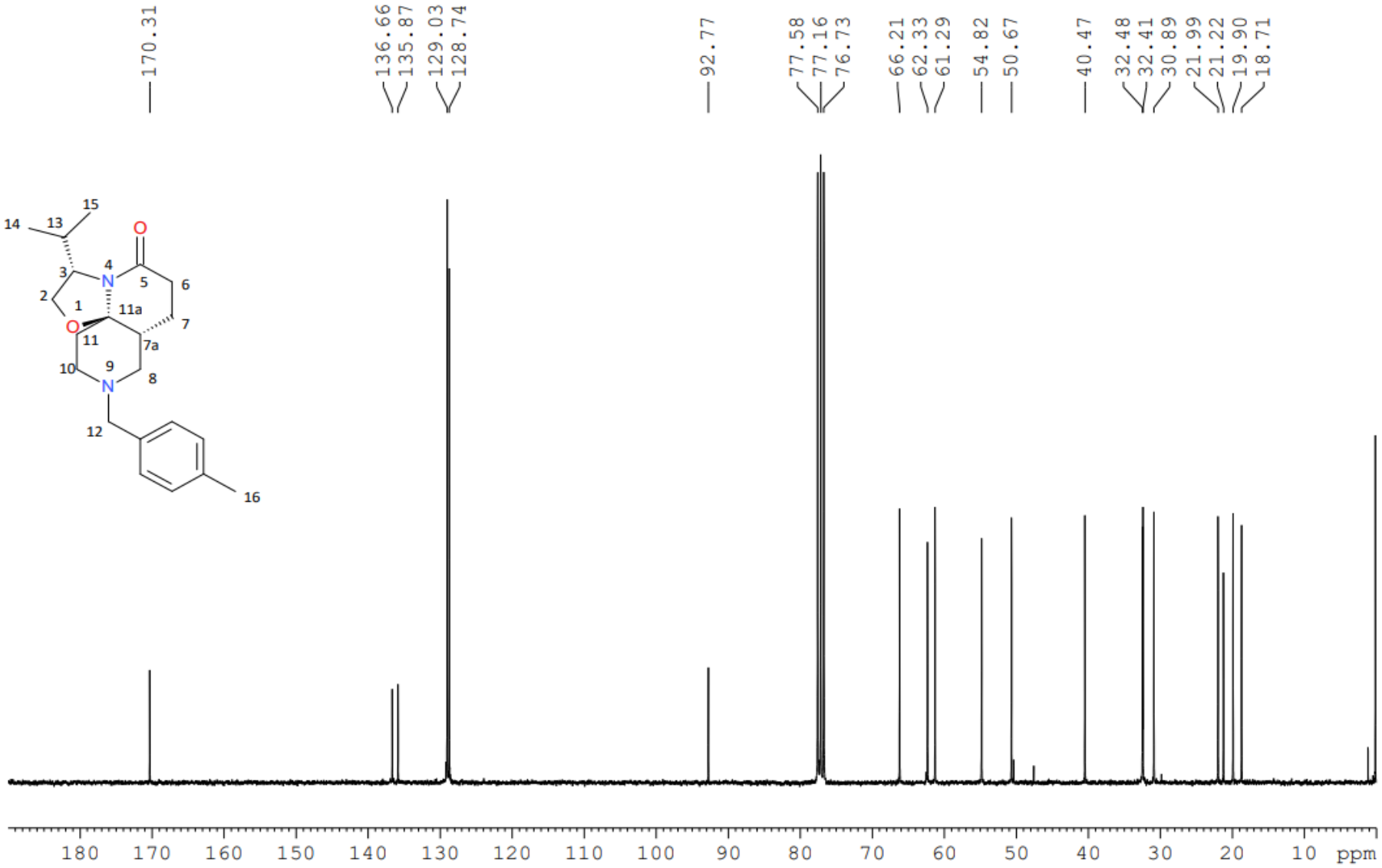

Compound 8, HRMS

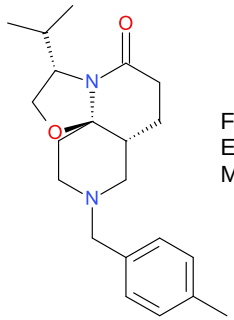

Formula Weight: 342,47509
Exact Mass: 342,23072822
Molecular Formula: $C_{21}H_{30}N_2O_2$

Elemental Composition Report

Single Mass Analysis

Tolerance = 10.0 PPM / DBE: min = -1.5, max = 500.0
Element prediction: Off
Number of isotope peaks used for i-FIT = 3

Monoisotopic Mass, Even Electron Ions
87 formula(e) evaluated with 2 results within limits (up to 10 best isotopic matches for each mass)
Elements Used:
C: 0-40 H: 0-50 N: 0-4 O: 0-3

NL4TB2-B1 210 (2.112) Cm (210:213-(164:200+219:247))

1: TOF MS ES+
2.52e+005

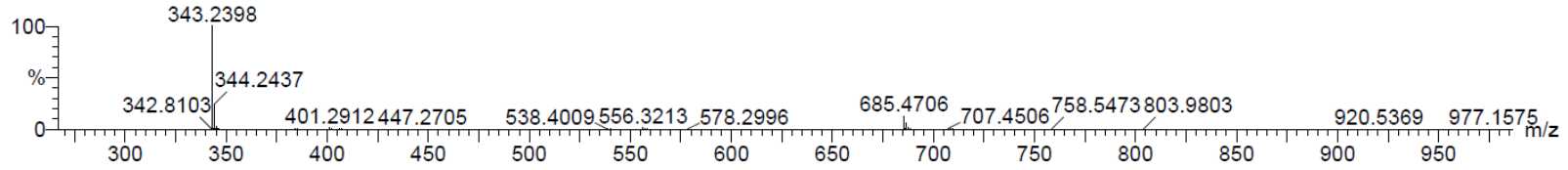

Minimum:				-1.5		
Maximum:		100.0	10.0	500.0		
Mass	Calc. Mass	mDa	PPM	DBE	i-FIT	Formula
343.2398	343.2386	1.2	3.5	7.5	33.4	C21 H31 N2 O2
	343.2426	-2.8	-8.2	11.5	1297.1	C26 H31

Compound 9, ^{1}H NMR (300 MHz, $CDCl_3$)

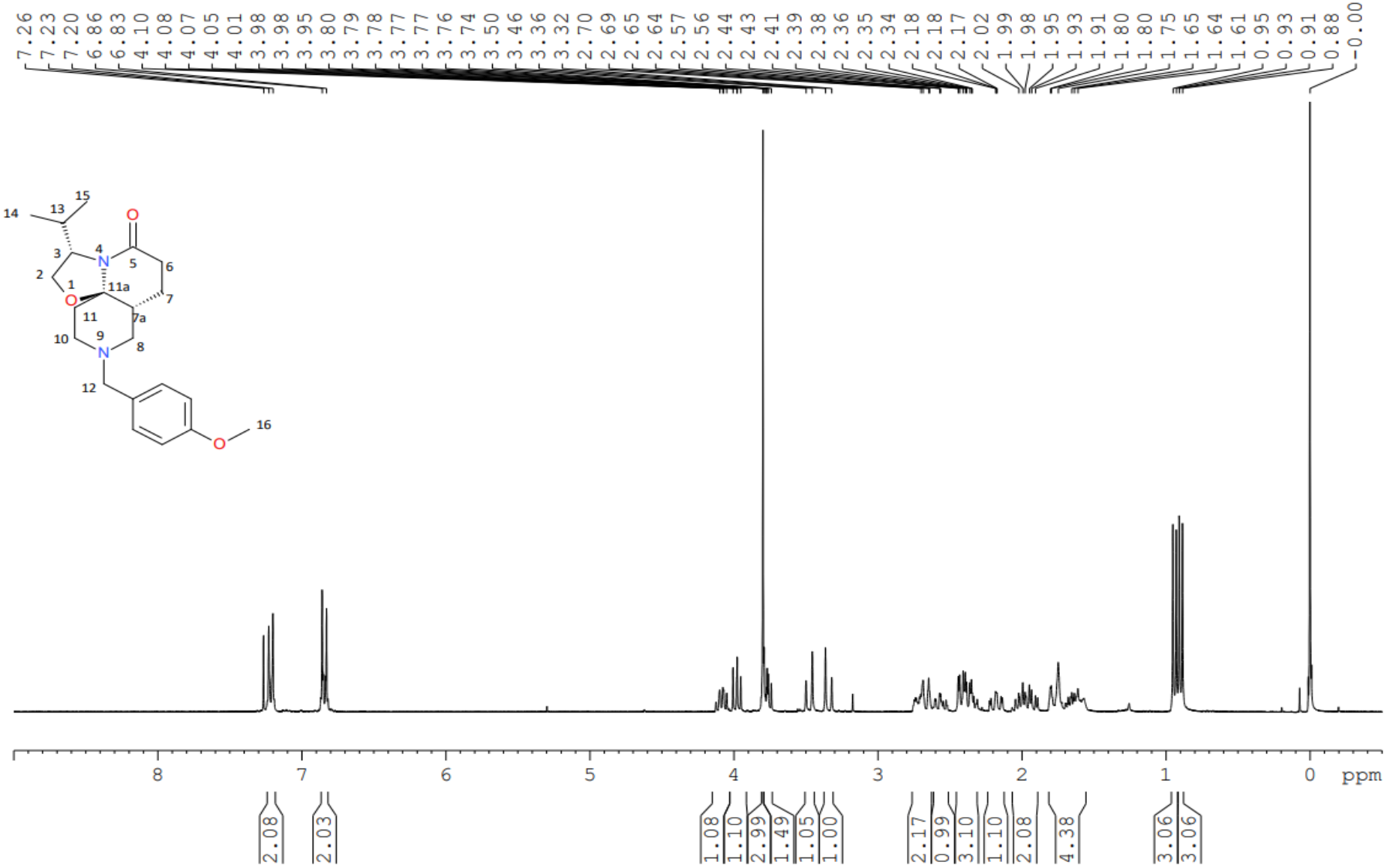

Compound 9, ^{13}C NMR (75 MHz, $CDCl_3$)

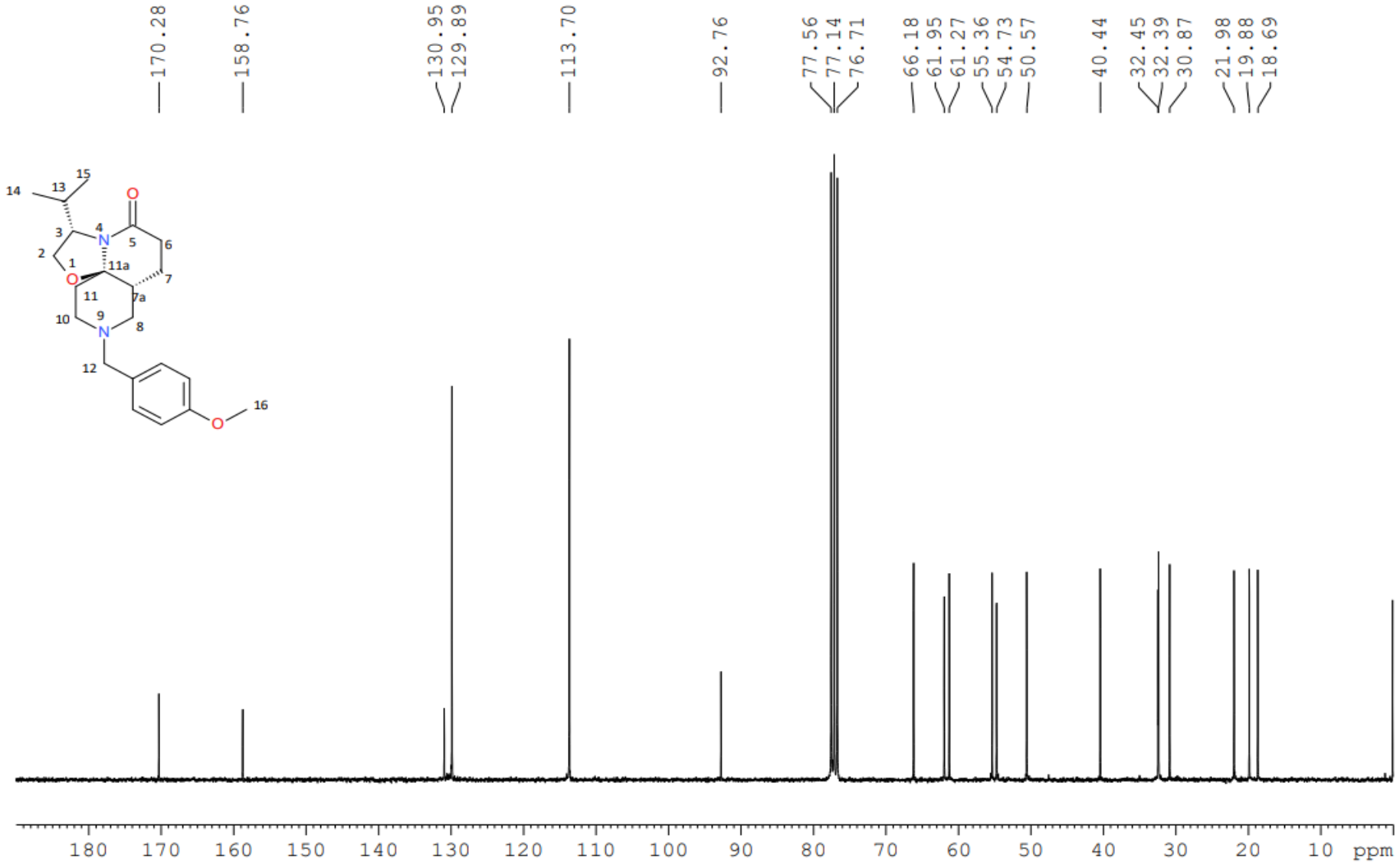

Compound 9, HRMS

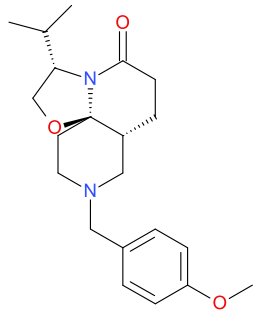

Formula Weight: 358,47449
Exact Mass: 358,22564284
Molecular Formula: $C_{21}H_{30}N_2O_3$

Elemental Composition Report

Single Mass Analysis

Tolerance = 10.0 PPM / DBE: min = -1.5, max = 500.0
Element prediction: Off
Number of isotope peaks used for i-FIT = 3

Monoisotopic Mass, Even Electron Ions
130 formula(e) evaluated with 2 results within limits (up to 10 best isotopic matches for each mass)
Elements Used:
C: 0-40 H: 0-50 N: 0-4 O: 0-5

BDM91151 102 (1.987)

1: TOF MS ES+
1.15e+005

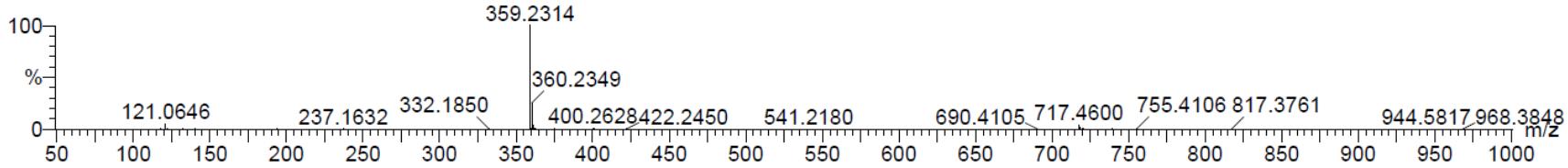

Minimum:				-1.5		
Maximum:		100.0	10.0	500.0		
Mass	Calc. Mass	mDa	PPM	DBE	i-FIT	Formula
359.2314	359.2335	-2.1	-5.8	7.5	16.4	C21 H31 N2 O3
	359.2294	2.0	5.6	3.5	587.1	C16 H31 N4 O5

Compound 10, ^{1}H NMR (300 MHz, $CDCl_3$)

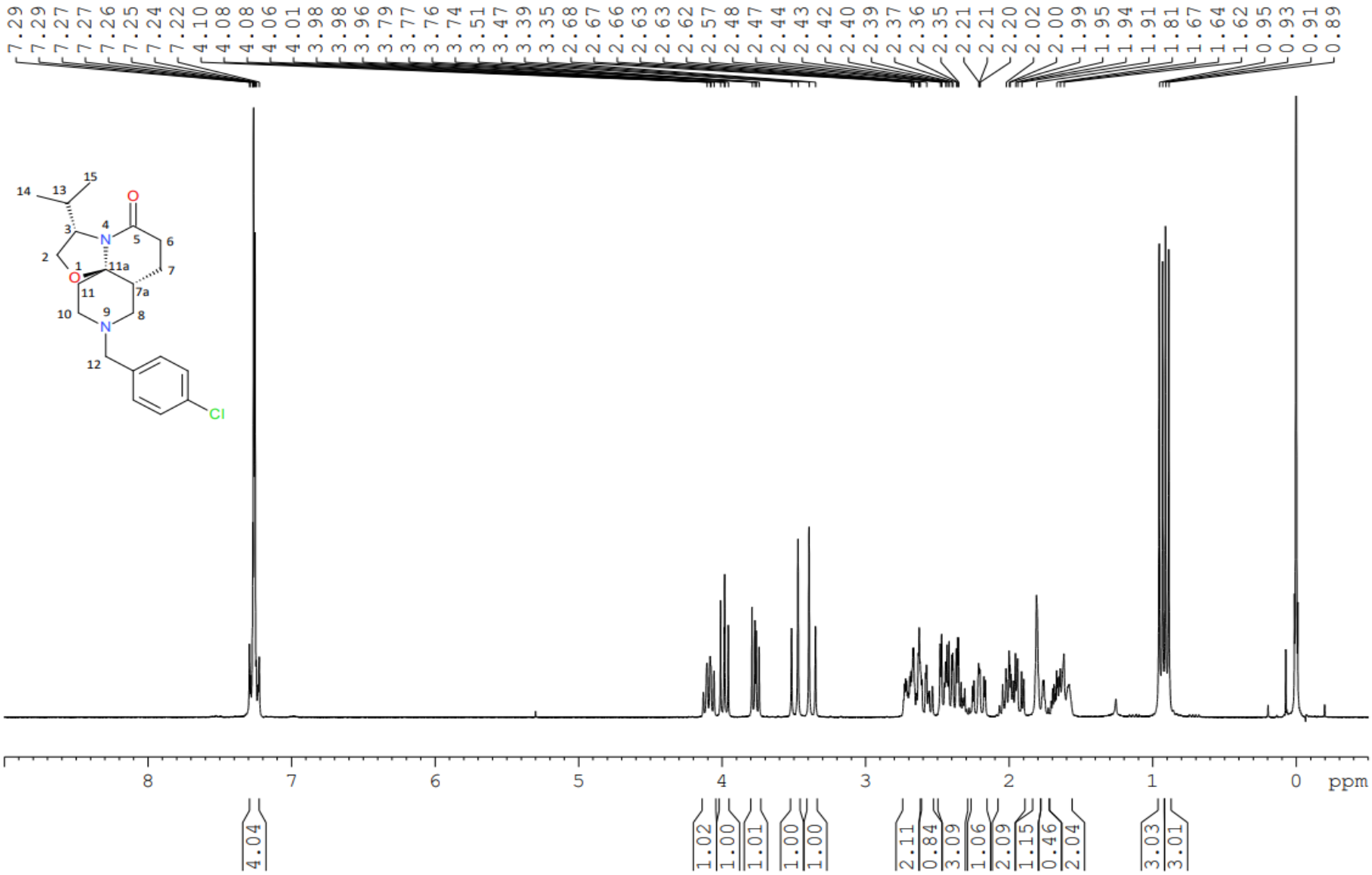

Compound 10, ^{13}C NMR (75 MHz, $CDCl_3$)

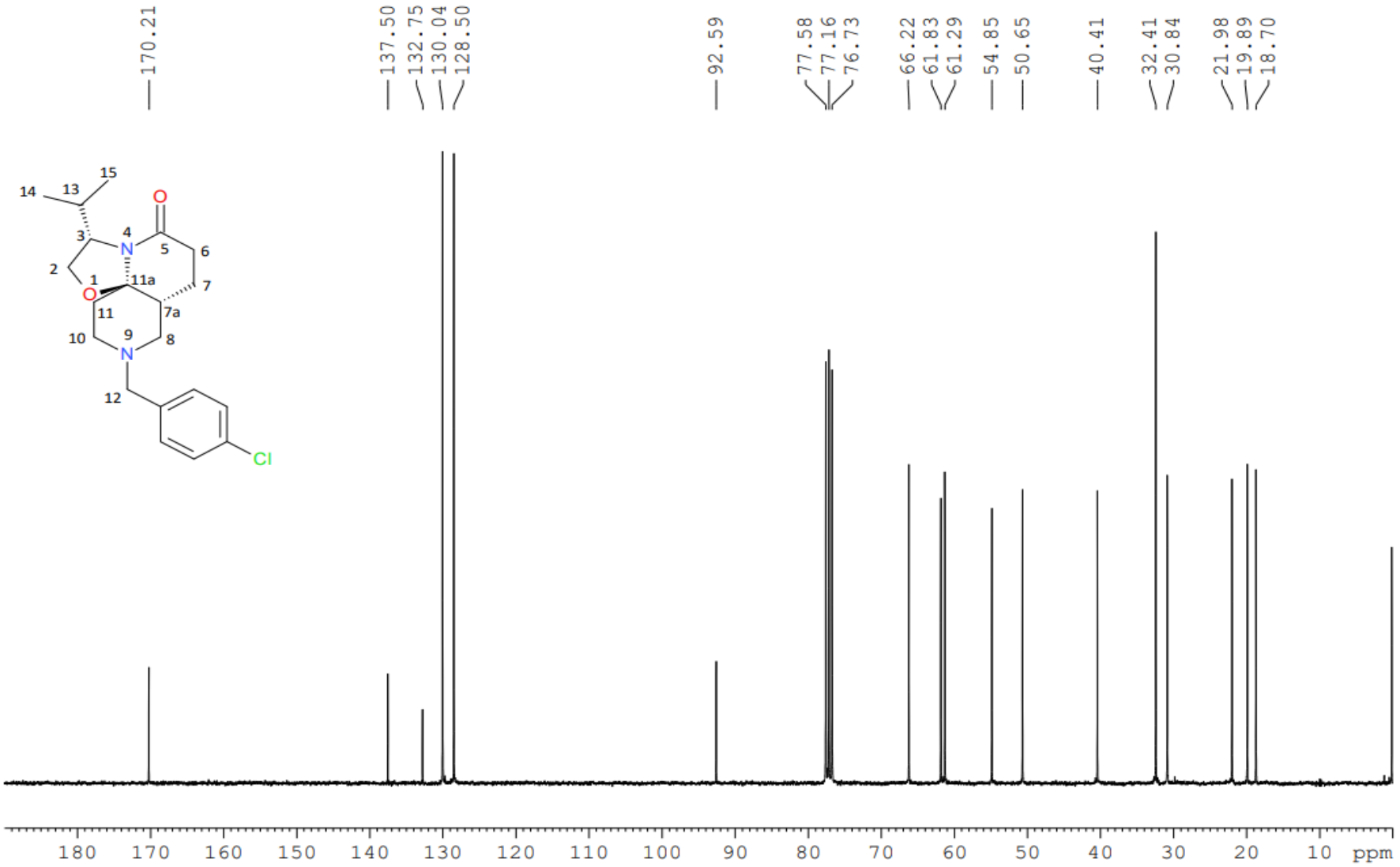

Compound 10, HRMS

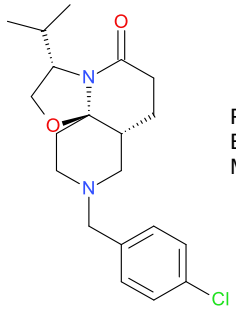

Formula Weight: 362,89357
Exact Mass: 362,176105834
Molecular Formula: $C_{20}H_{27}ClN_2O_2$

Elemental Composition Report

Single Mass Analysis

Tolerance = 10.0 PPM / DBE: min = -1.5, max = 500.0
Element prediction: Off
Number of isotope peaks used for i-FIT = 3

Monoisotopic Mass, Even Electron Ions
251 formula(e) evaluated with 3 results within limits (up to 10 best isotopic matches for each mass)
Elements Used:
C: 0-40 H: 0-50 N: 0-4 O: 0-5 Cl: 0-1

BDM91123 115 (2.233)

1: TOF MS ES+
3.59e+004

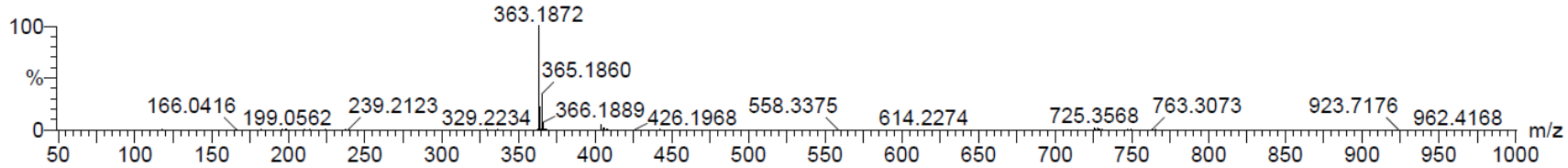

Minimum:				-1.5		
Maximum:		100.0	10.0	500.0		
Mass	Calc. Mass	mDa	PPM	DBE	i-FIT	Formula
363.1872	363.1839	3.3	9.1	7.5	27.1	C20 H28 N2 O2 Cl
	363.1880	-0.8	-2.2	11.5	225.5	C25 H28 Cl
	363.1861	1.1	3.0	16.5	5150.8	C26 H23 N2

BDM88689 (Compound 11), ^{1}H NMR (300 MHz, CD_2Cl_2)

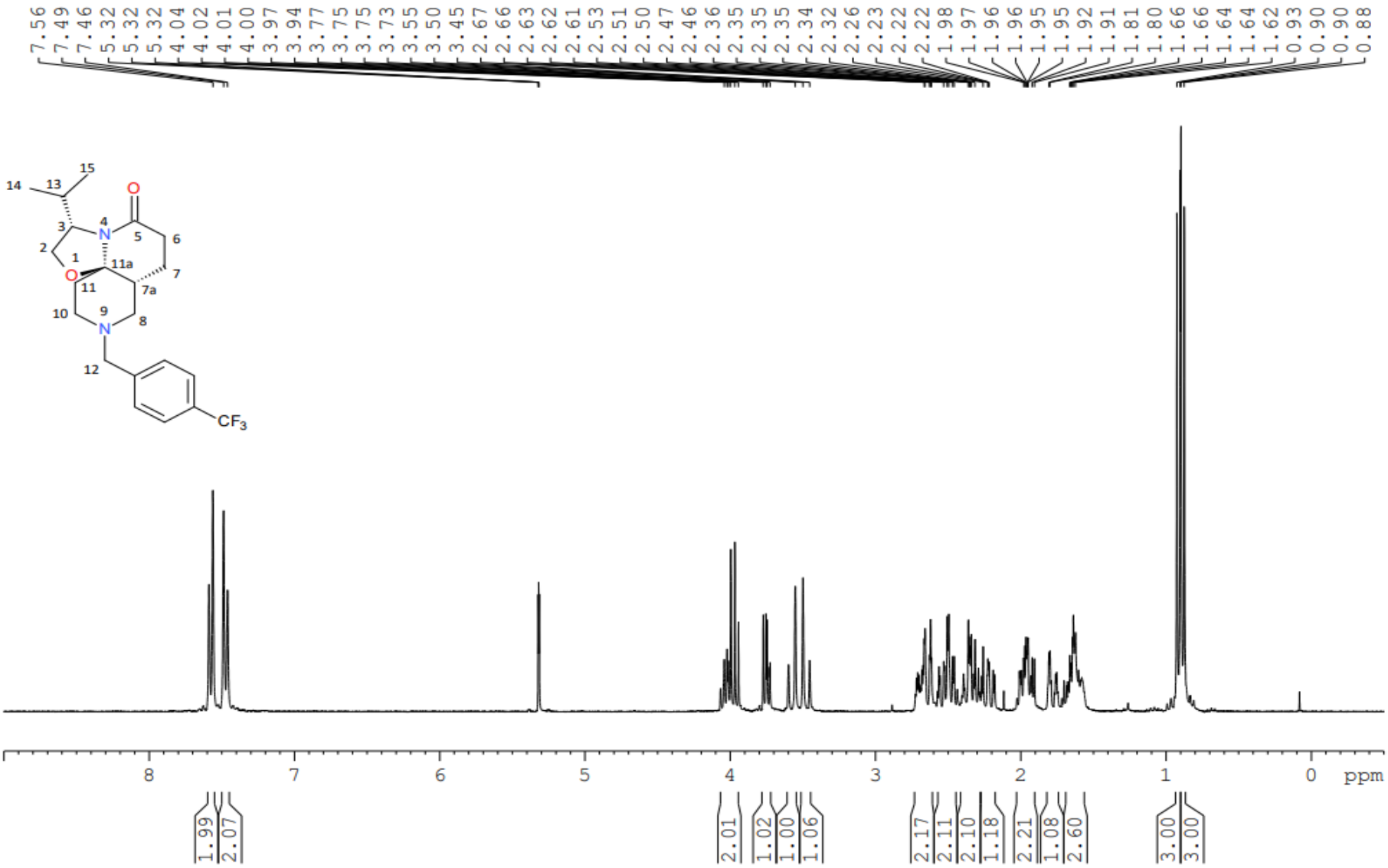

BDM88689 (Compound 11), ^{13}C NMR (75 MHz, CD_2Cl_2)

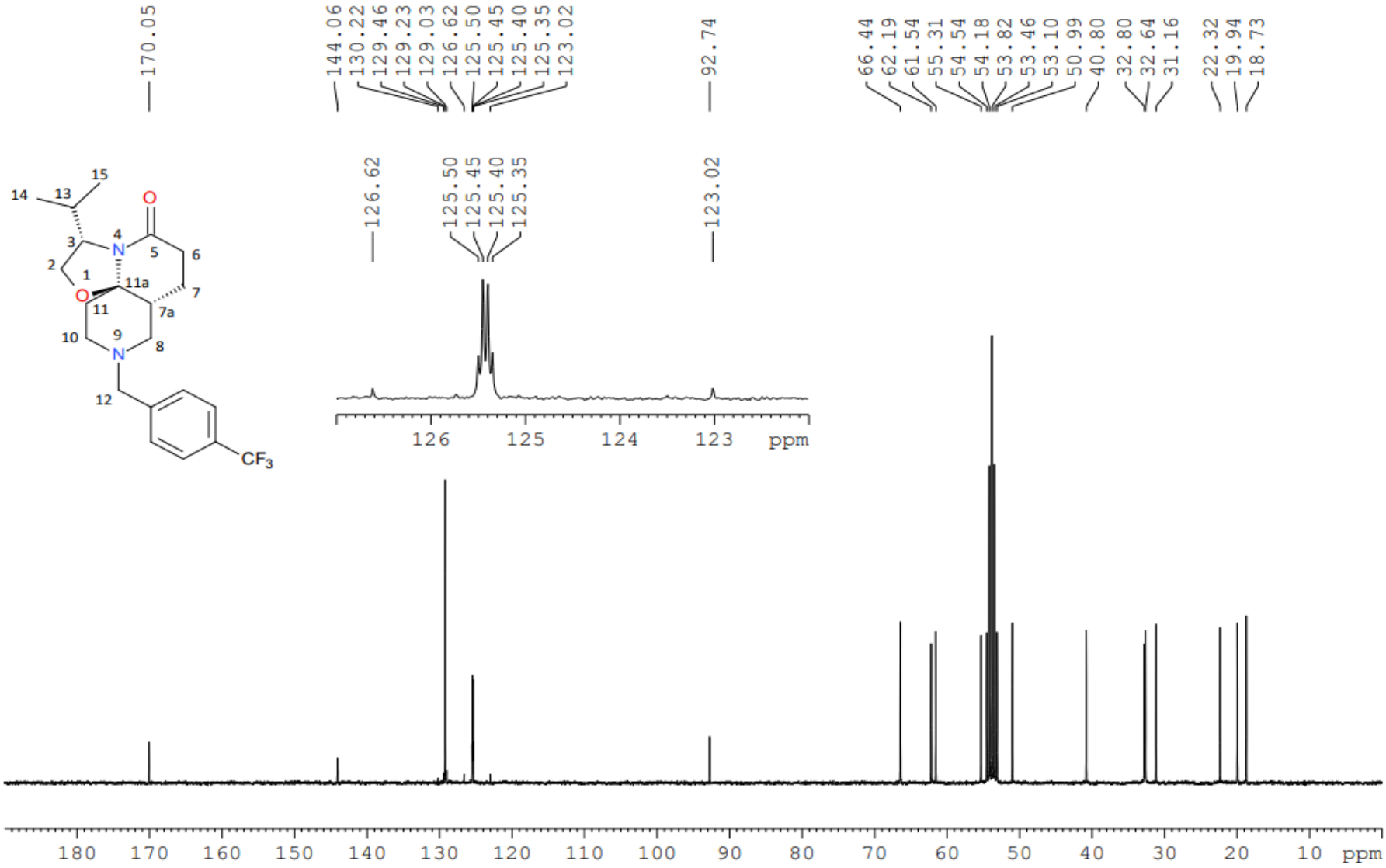

BDM88689 (Compound 11), COSY

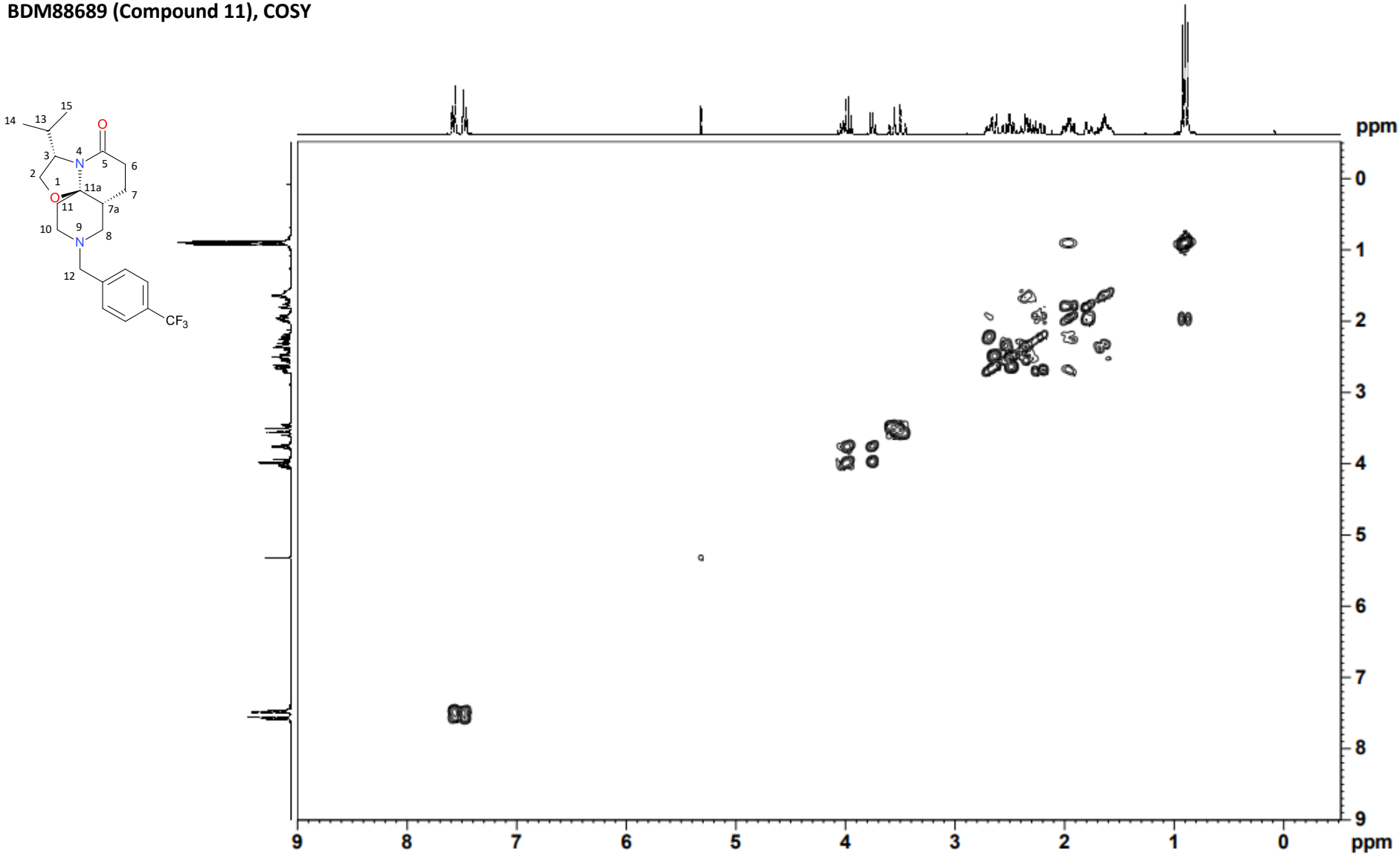

BDM88689 (Compound 11), HSQC

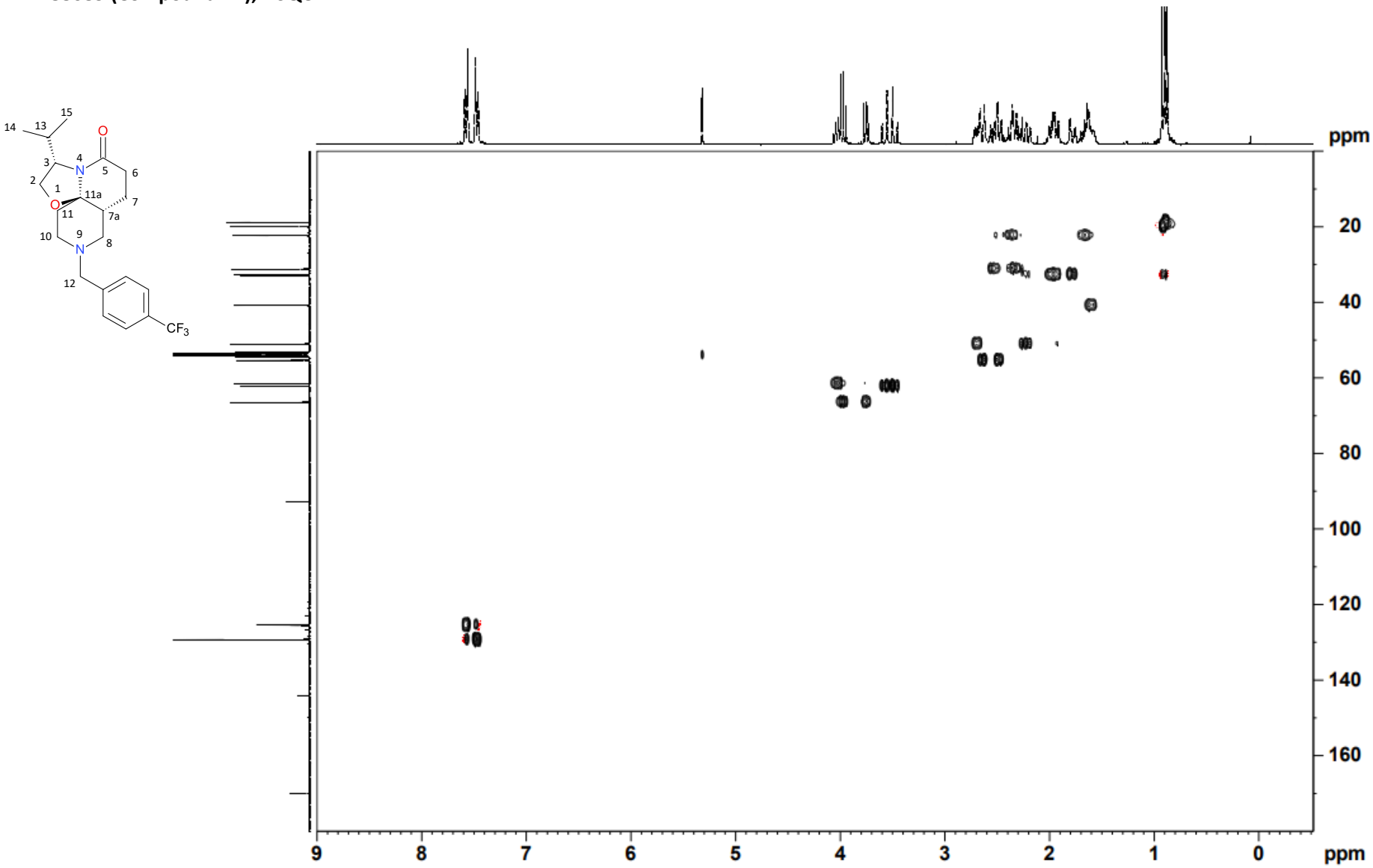

BDM88689 (Compound 11), HRMS

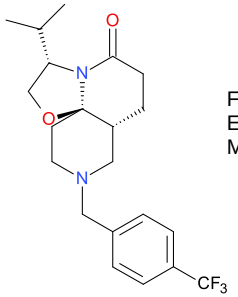

Formula Weight: 396,44648
Exact Mass: 396,202462724
Molecular Formula: $C_{21}H_{27}F_3N_2O_2$

Elemental Composition Report

Single Mass Analysis

Tolerance = 10.0 PPM / DBE: min = -1.5, max = 500.0
Element prediction: Off
Number of isotope peaks used for i-FIT = 3

Monoisotopic Mass, Even Electron Ions
18558 formula(e) evaluated with 76 results within limits (up to 5 best isotopic matches for each mass)
Elements Used:
C: 0-30 H: 0-50 N: 0-10 O: 0-10 F: 0-6 S: 0-2 Cl: 0-2

NL4TB-D2 252 (2.511) Cm (251:255)

1: TOF MS ES+
3.32e+005

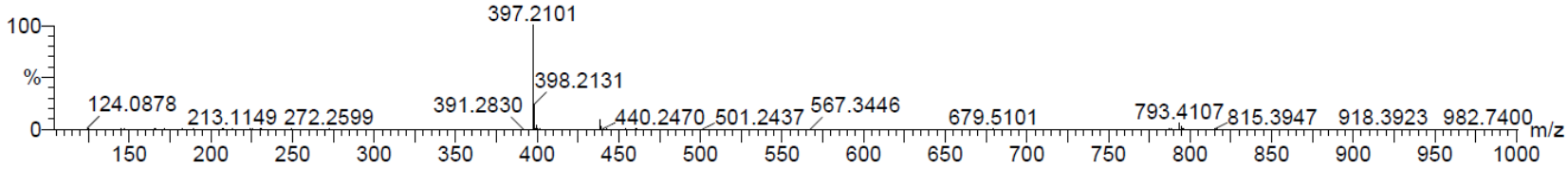

Mass	Calc. Mass	mDa	PPM	DBE	i-FIT	Formula
Minimum:				-1.5		
Maximum:		100.0	10.0	500.0		
397.2101	397.2100	0.1	0.3	11.5	60.4	C19 H25 N8 O2
	397.2103	-0.2	-0.5	7.5	62.4	C21 H28 N2 O2 F3
	397.2139	-3.8	-9.6	6.5	120.7	C20 H30 N2 O5 F
	397.2087	1.4	3.5	6.5	214.6	C18 H29 N4 O6
	397.2127	-2.6	-6.5	10.5	642.3	C23 H29 N2 O4

BDM88689 (Compound 11), LCMS

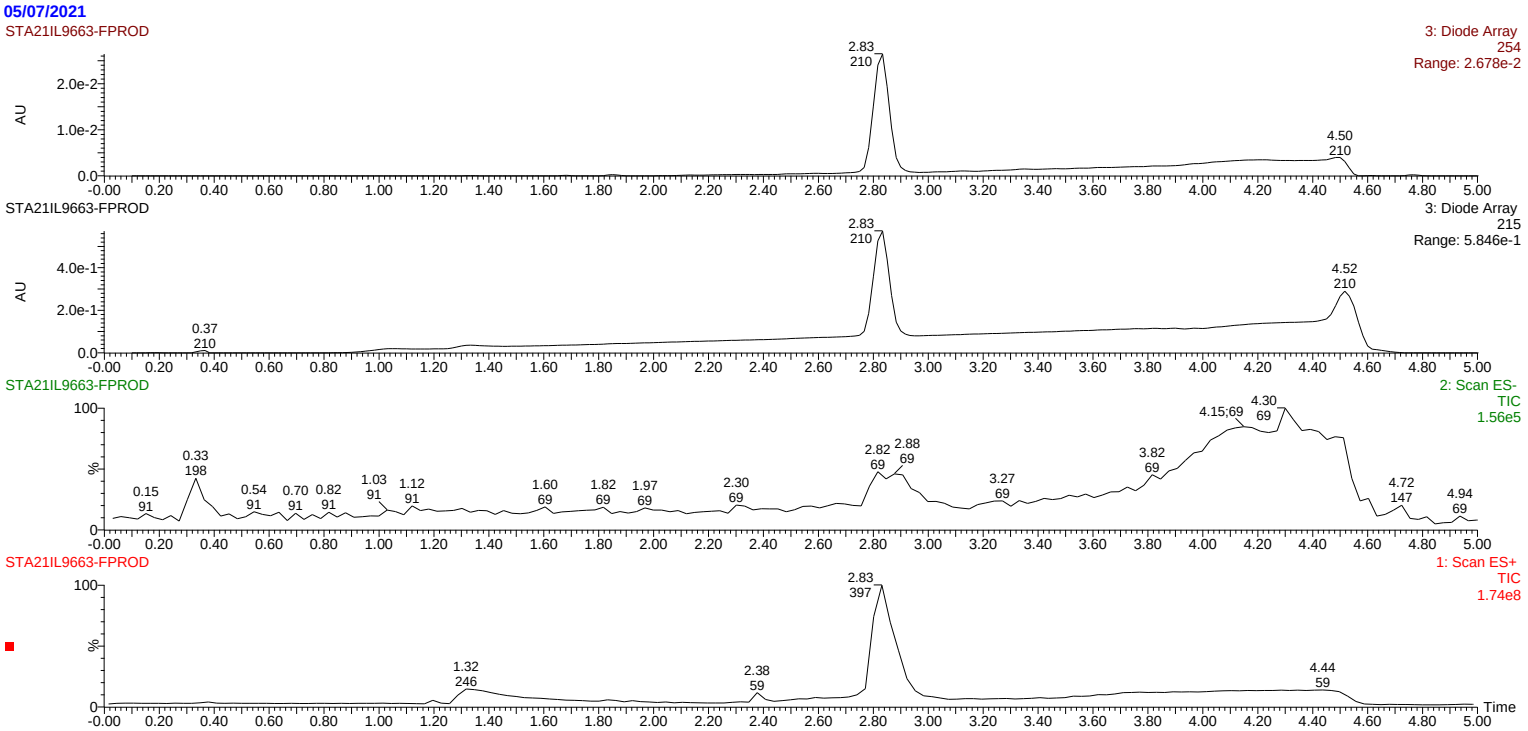

05/07/2021

STA21IL9663-FPROD 94 (2.831)

1: Scan ES+
9.79e7

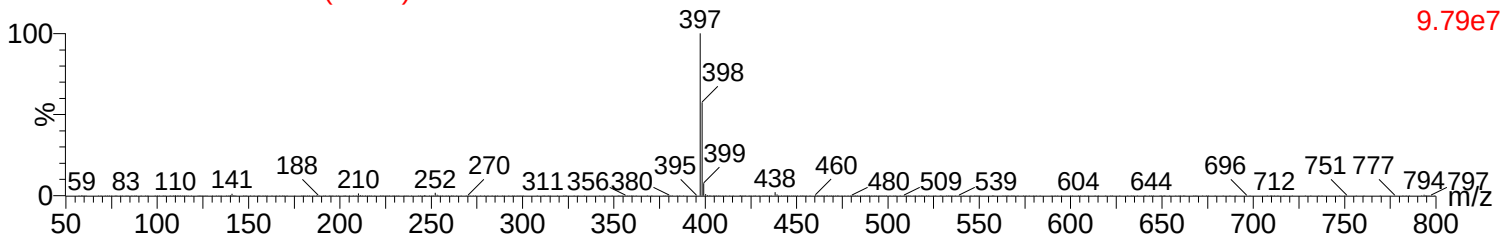

BDM88690 (Compound 12), ^{1}H NMR (300 MHz, CD_2Cl_2)

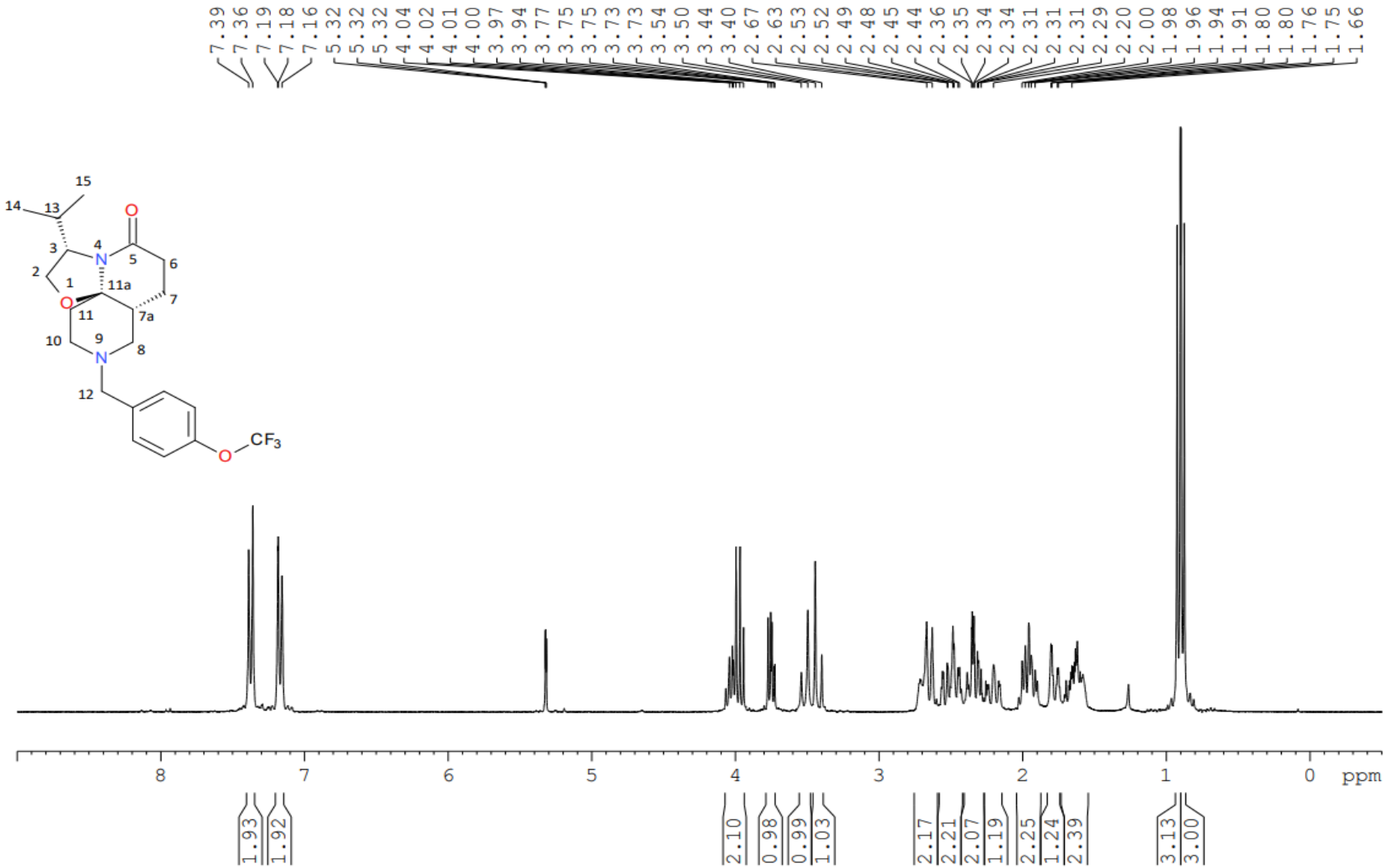

BDM88690 (Compound 12), ^{13}C NMR (75 MHz, CD_2Cl_2)

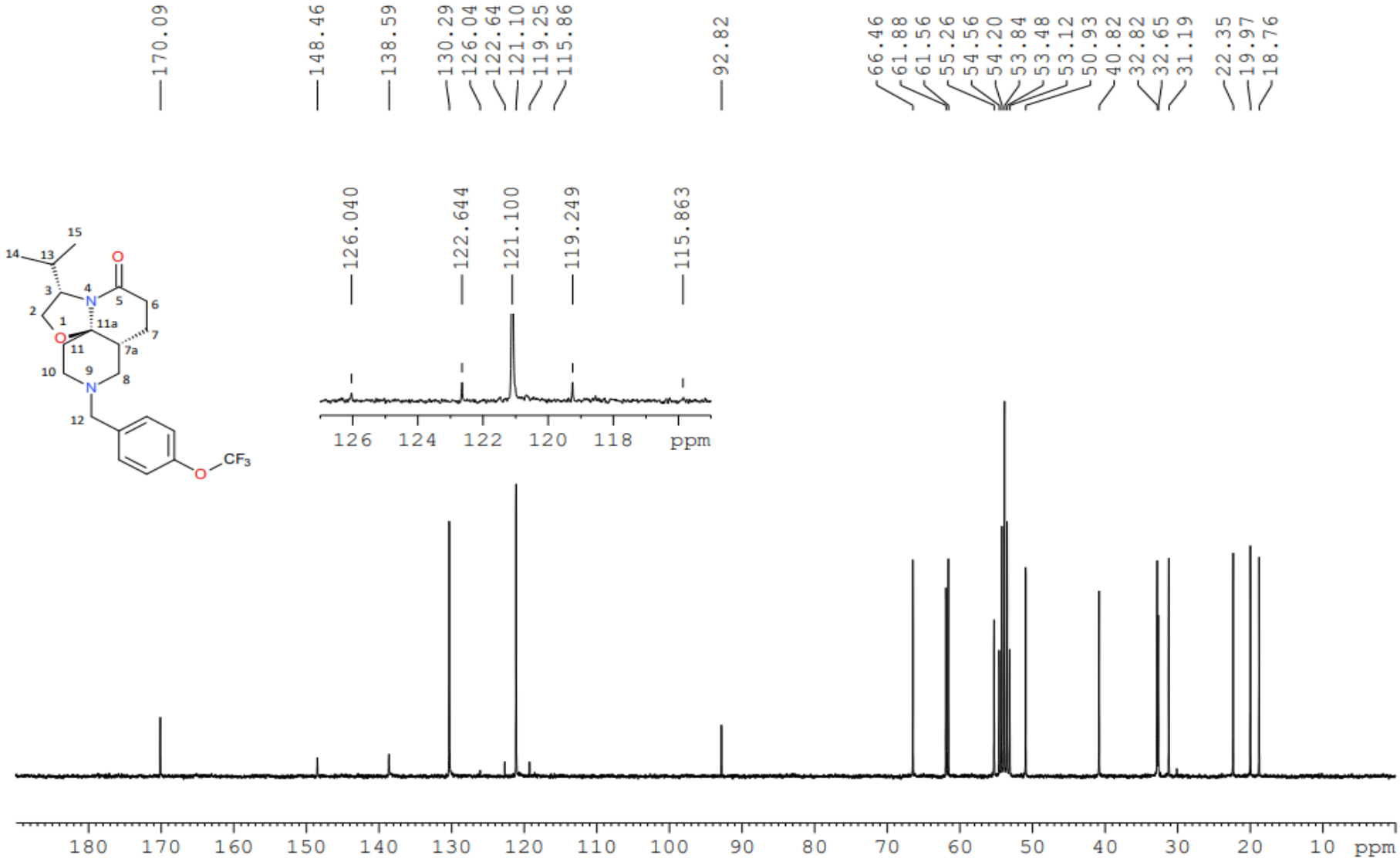

BDM88690 (Compound 12), COSY

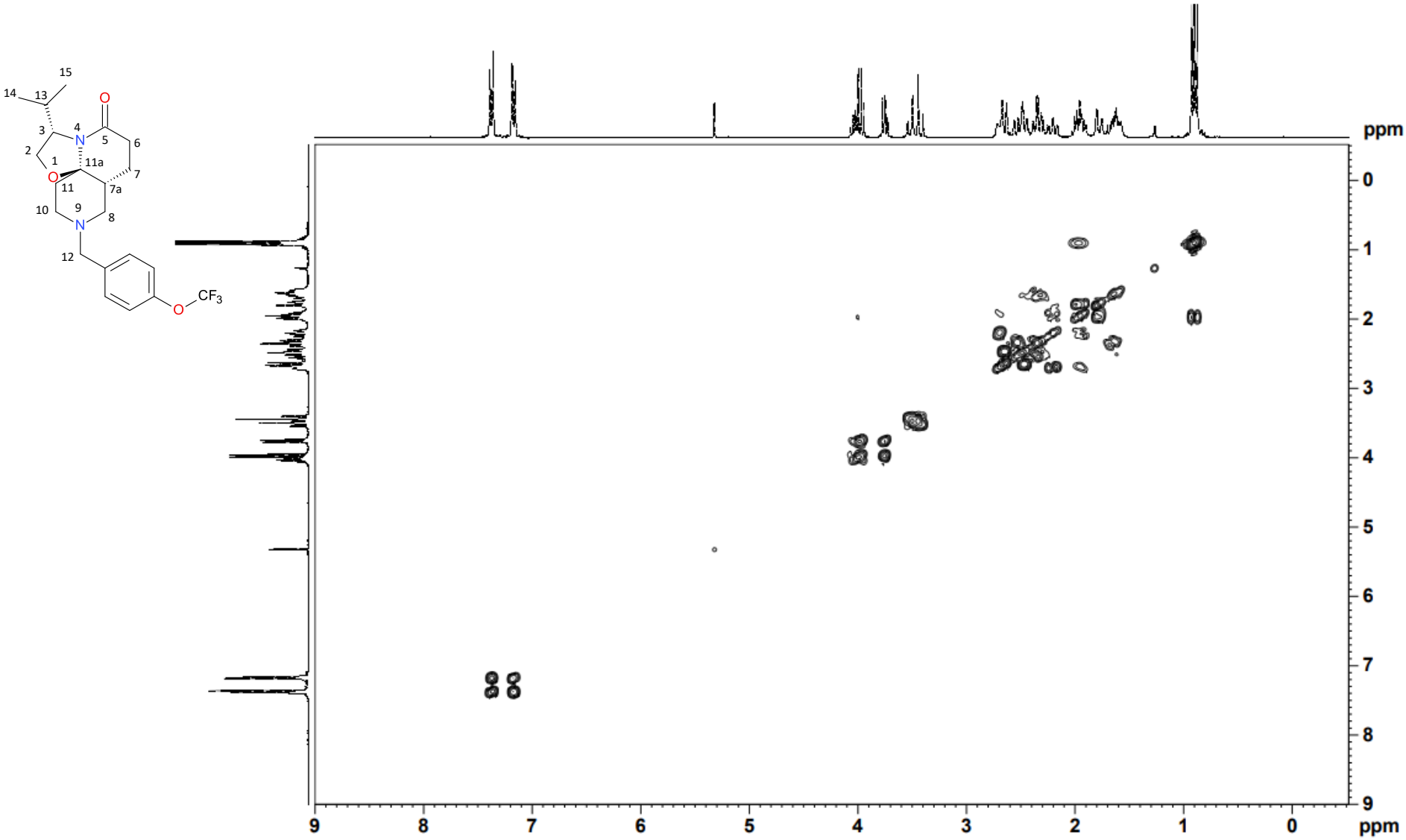

BDM88690 (Compound 12), HSQC

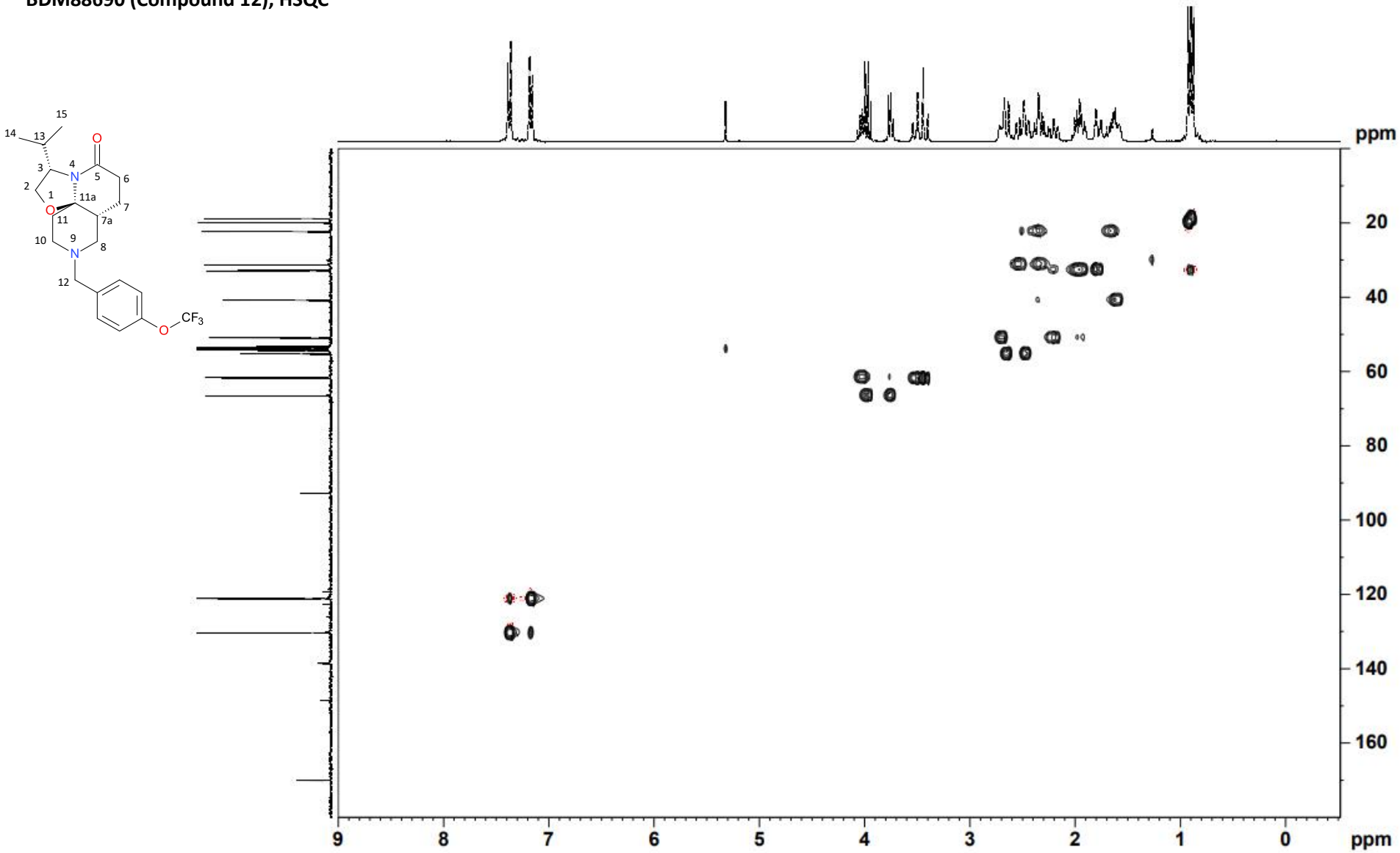

BDM88690 (Compound 12), HRMS

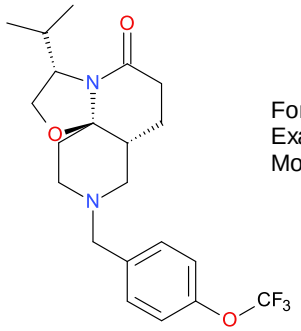

Formula Weight: 412,44588
Exact Mass: 412,197377344
Molecular Formula: $C_{21}H_{27}F_3N_2O_3$

Elemental Composition Report

Single Mass Analysis

Tolerance = 10.0 PPM / DBE: min = -1.5, max = 500.0
Element prediction: Off
Number of isotope peaks used for i-FIT = 3

Monoisotopic Mass, Even Electron Ions
20060 formula(e) evaluated with 102 results within limits (up to 5 best isotopic matches for each mass)
Elements Used:
C: 0-30 H: 0-50 N: 0-10 O: 0-10 F: 0-6 S: 0-2 Cl: 0-2

NL4TB-E2 243 (2.417) Cm (240:247-(255:279+230:234))

1: TOF MS ES+
7.29e+005

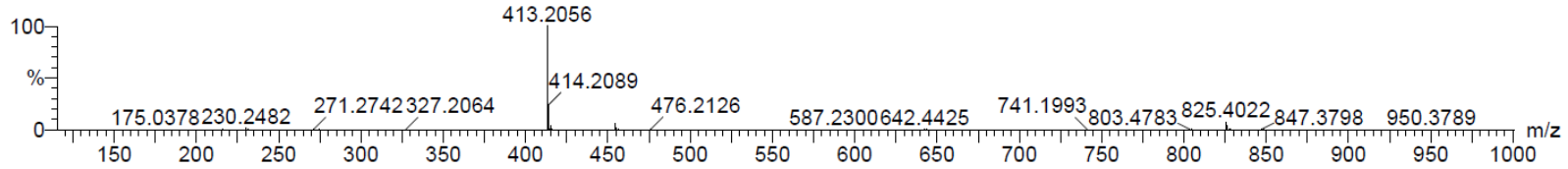

Minimum:				-1.5		
Maximum:		100.0	10.0	500.0		
Mass	Calc. Mass	mDa	PPM	DBE	i-FIT	Formula
413.2056	413.2052	0.4	1.0	7.5	162.1	C21 H28 N2 O3 F3
	413.2050	0.6	1.5	11.5	165.4	C19 H25 N8 O3
	413.2088	-3.2	-7.7	6.5	183.7	C20 H30 N2 O6 F
	413.2036	2.0	4.8	6.5	536.8	C18 H29 N4 O7
	413.2016	4.0	9.7	8.5	1034.8	C22 H26 N2 F5

BDM88690 (Compound 12), LCMS

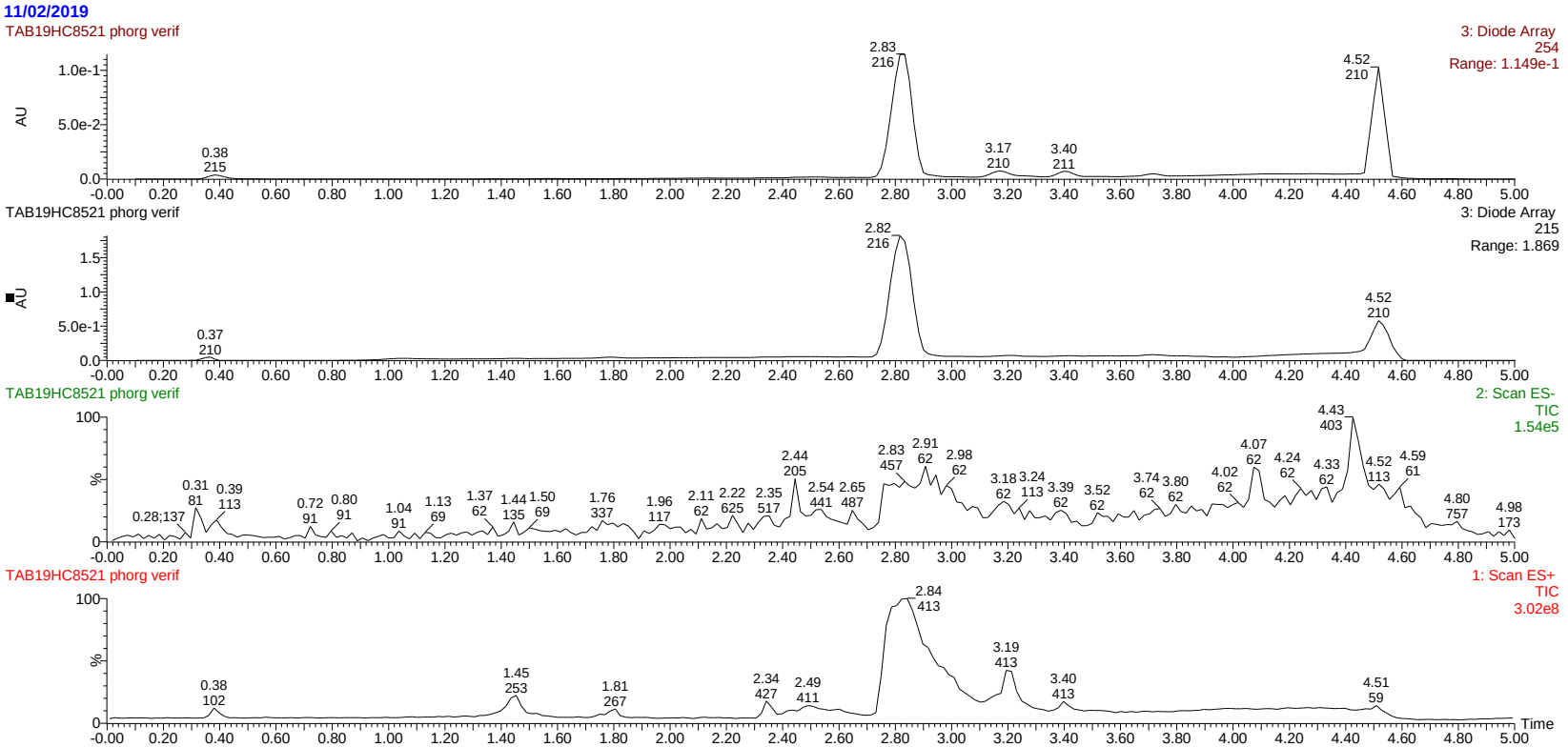

11/02/2019

TAB19HC8521 phorg verif 153 (2.824)

1: Scan ES+
1.47e8

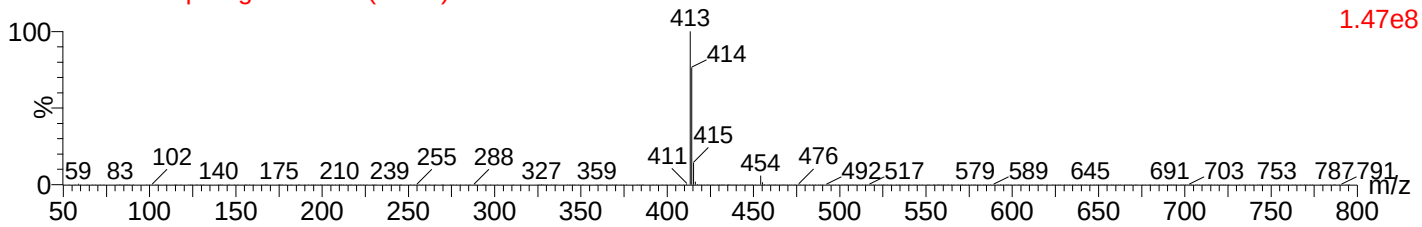

BDM89000 (Compound 13), ^{1}H NMR (300 MHz, $CDCl_3$)

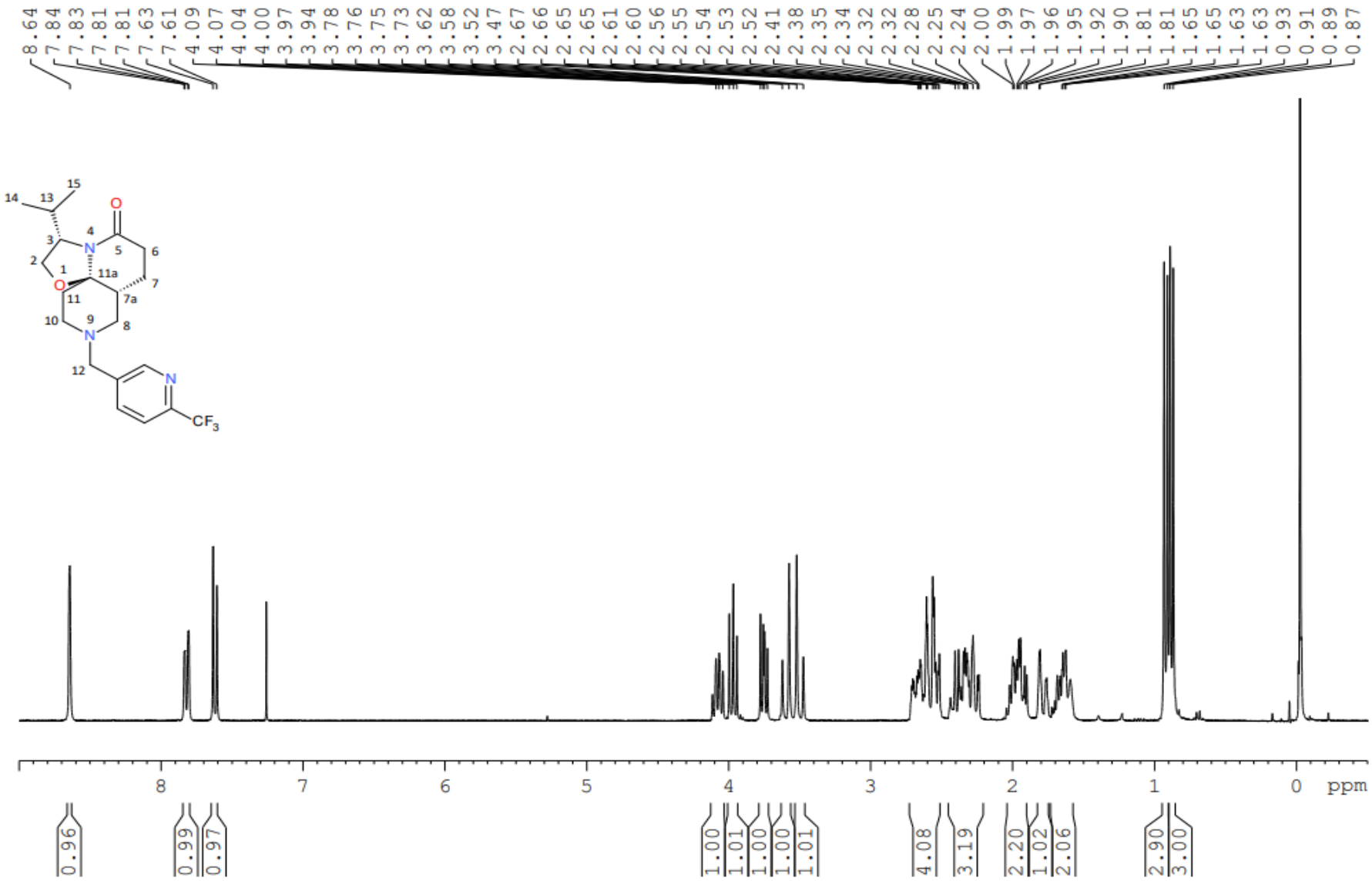

BDM89000 (Compound 13), ^{13}C NMR (75 MHz, $CDCl_3$)

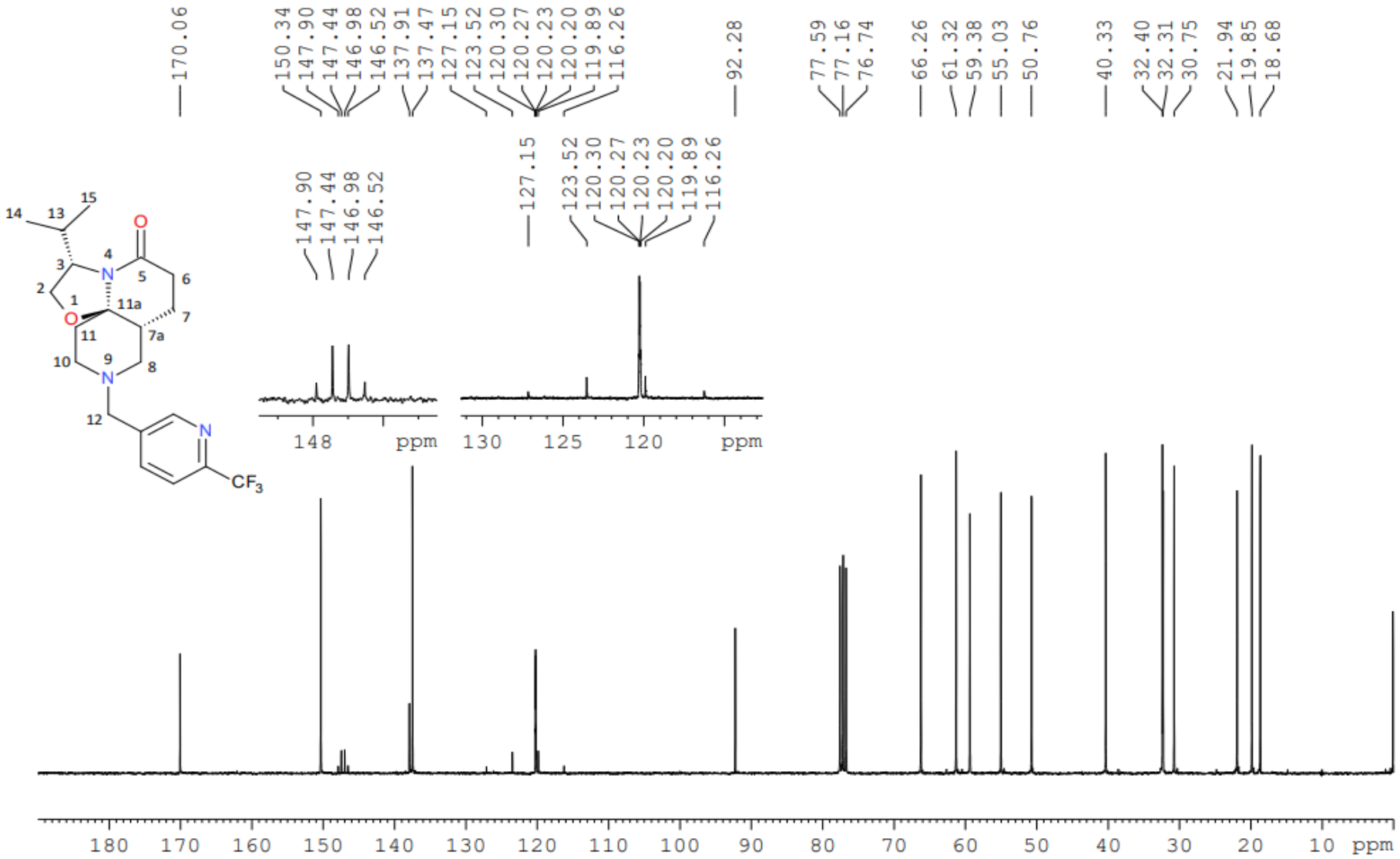

BDM89000 (Compound 13), COSY

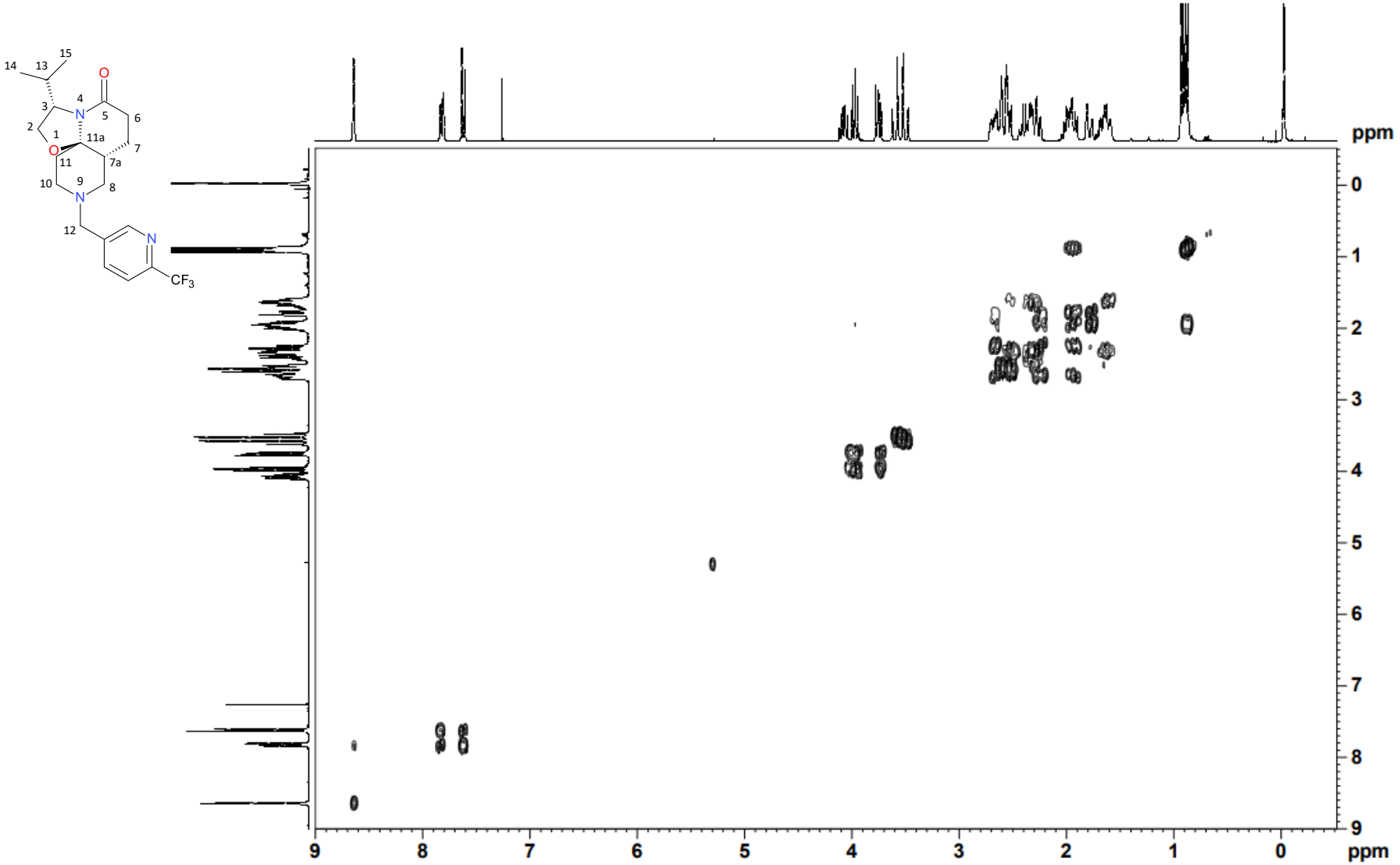

BDM89000 (Compound 13), HSQC

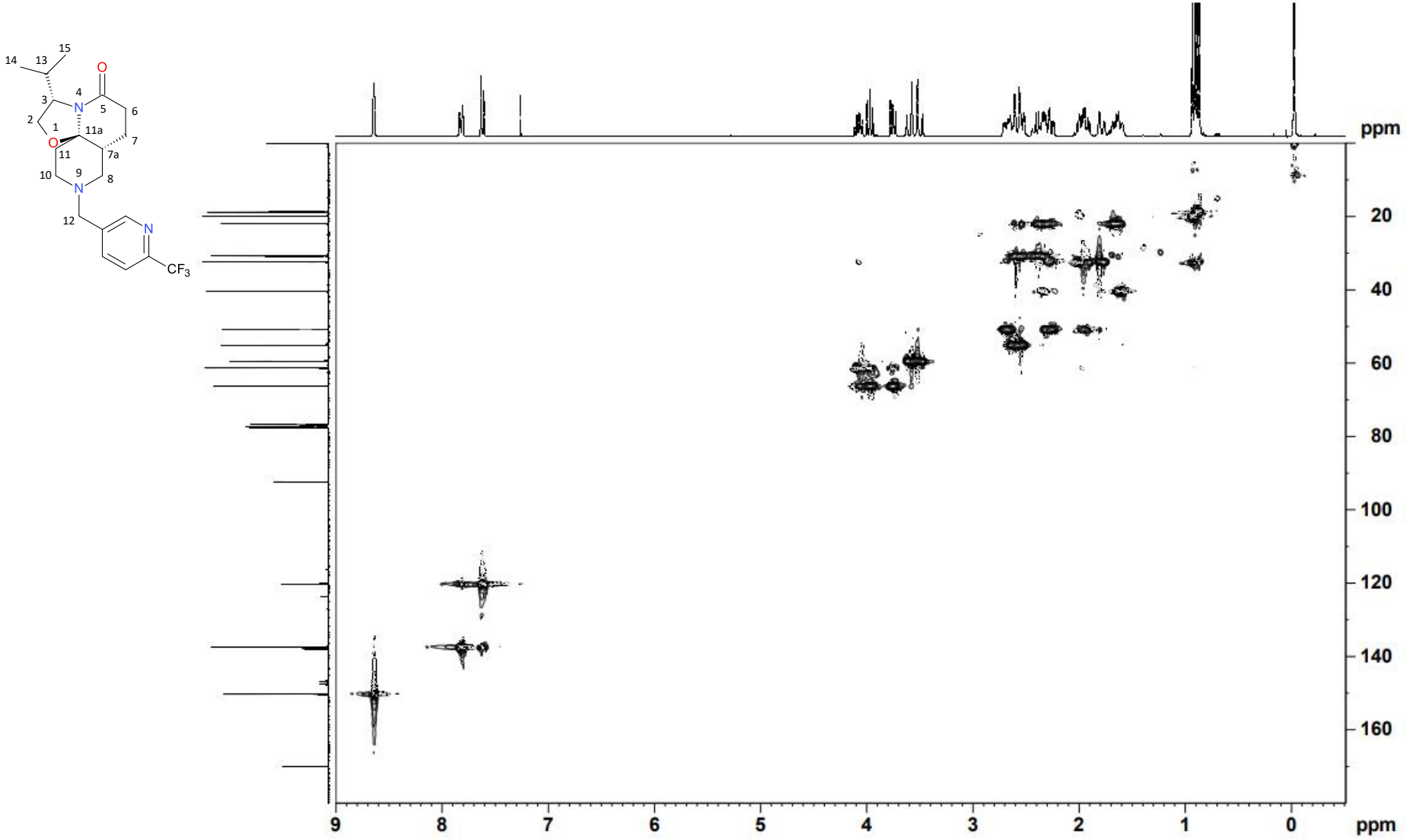

BDM9000 (Compound 13), HRMS

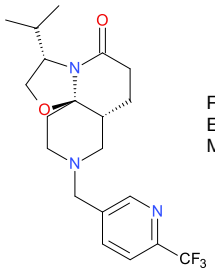

Formula Weight: 397,43454
Exact Mass: 397,197711702
Molecular Formula: $C_{20}H_{26}F_3N_3O_2$

Elemental Composition Report

Single Mass Analysis

Tolerance = 10.0 PPM / DBE: min = -1.5, max = 500.0
Element prediction: Off
Number of isotope peaks used for i-FIT = 3

Monoisotopic Mass, Even Electron Ions
509 formula(e) evaluated with 4 results within limits (up to 10 best isotopic matches for each mass)
Elements Used:
C: 0-40 H: 0-50 N: 0-4 O: 0-5 F: 0-3

BDM89000 121 (2.336) Cm (120:122-(91:115+126:144))

1: TOF MS ES+
7.45e+004

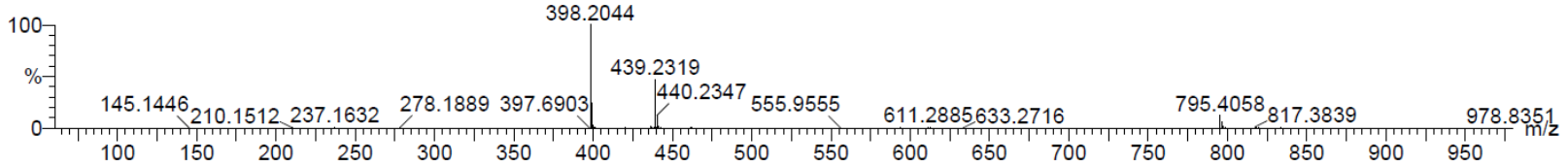

Mass	Calc. Mass	mDa	PPM	DBE	i-FIT	Formula
Minimum:				-1.5		
Maximum:		100.0	10.0	500.0		
398.2044	398.2055	-1.1	-2.8	7.5	10.8	C20 H27 N3 O2 F3
	398.2044	0.0	0.0	11.5	213.8	C23 H26 N3 O F2
	398.2080	-3.6	-9.0	10.5	255.0	C22 H28 N3 O4
	398.2033	1.1	2.8	15.5	727.9	C26 H25 N3 F

BDM89000 (Compound 13), LCMS

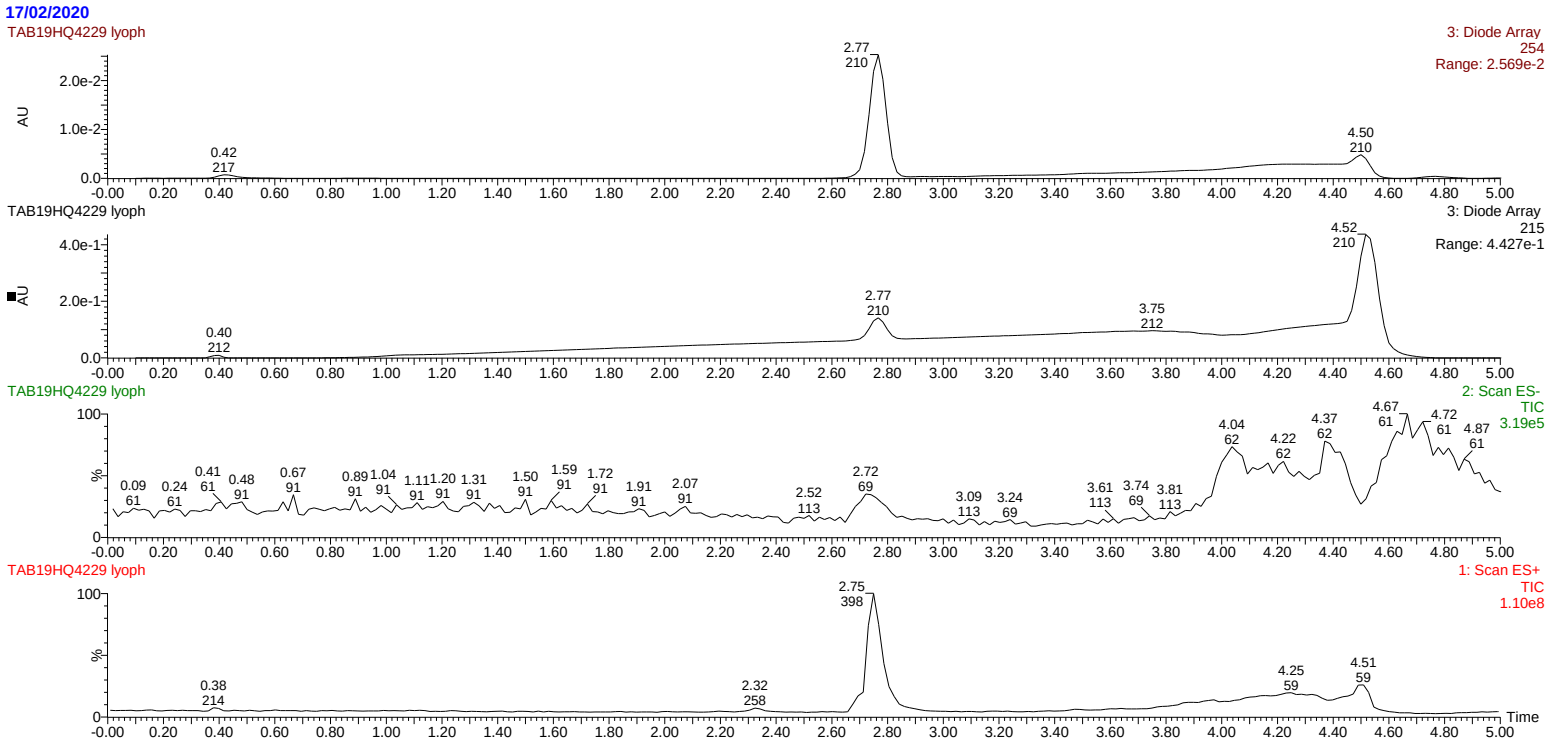

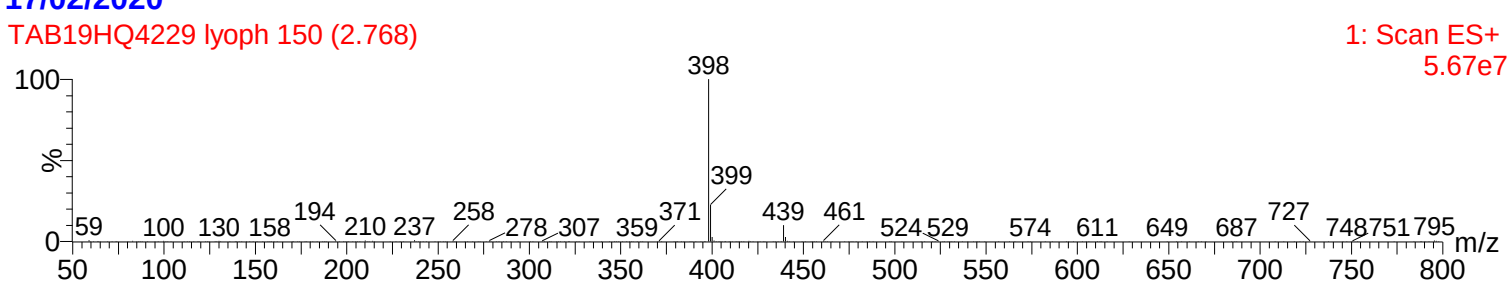

References

(1) Dolomanov, O. V.; Bourhis, L. J.; Gildea, R. J.; Howard, J. A. K.; Puschmann, H. OLEX2 : A Complete Structure Solution, Refinement and Analysis Program. *J. Appl. Crystallogr.* **2009**, *42* (2), 339–341. https://doi.org/10.1107/S0021889808042726.

(2) Palatinus, L.; Prathapa, S. J.; van Smaalen, S. EDMA : A Computer Program for Topological Analysis of Discrete Electron Densities. *J. Appl. Crystallogr.* **2012**, *45* (3), 575–580. https://doi.org/10.1107/S0021889812016068.

(3) Palatinus, L.; van der Lee, A. Symmetry Determination Following Structure Solution in P 1. *J. Appl. Crystallogr.* **2008**, *41* (6), 975–984. https://doi.org/10.1107/S0021889808028185.

(4) Palatinus, L.; Chapuis, G. SUPERFLIP – a Computer Program for the Solution of Crystal Structures by Charge Flipping in Arbitrary Dimensions. *J. Appl. Crystallogr.* **2007**, *40* (4), 786–790. https://doi.org/10.1107/S0021889807029238.

(5) Sheldrick, G. M. A Short History of SHELX. *Acta Crystallogr. Sect. A Found. Crystallogr.* **2008**, *64* (1), 112–122. https://doi.org/10.1107/S0108767307043930.

(6) Vocat, A.; Hartkoorn, R. C.; Lechartier, B.; Zhang, M.; Dhar, N.; Cole, S. T.; Sala, C. Bioluminescence for Assessing Drug Potency against Nonreplicating Mycobacterium Tuberculosis. *Antimicrob. Agents Chemother.* **2015**, *59* (7), 4012–4019. https://doi.org/10.1128/AAC.00528-15.

(7) Zhang, M.; Sala, C.; Hartkoorn, R. C.; Dhar, N.; Mendoza-Losana, A.; Cole, S. T. Streptomycin-Starved Mycobacterium Tuberculosis 18b, a Drug Discovery Tool for Latent Tuberculosis. *Antimicrob. Agents Chemother.* **2012**, *56* (11), 5782–5789. https://doi.org/10.1128/AAC.01125-12.

(8) Hartkoorn, R. C.; Chandler, B.; Owen, A.; Ward, S. A.; Bertel Squire, S.; Back, D. J.; Khoo, S. H. Differential Drug Susceptibility of Intracellular and Extracellular Tuberculosis, and the Impact of P-Glycoprotein. *Tuberculosis* **2007**, *87* (3), 248–255. https://doi.org/10.1016/j.tube.2006.12.001.

(9) Rybniker, J.; Chen, J. M.; Sala, C.; Hartkoorn, R. C.; Vocat, A.; Benjak, A.; Boy-Röttger, S.; Zhang, M.; Székely, R.; Greff, Z.; Őrfi, L.; Szabadkai, I.; Pató, J.; Kéri, G.; Cole, S. T. Anticytolytic Screen Identifies Inhibitors of Mycobacterial Virulence Protein Secretion. *Cell Host Microbe* **2014**, *16* (4), 538–548. https://doi.org/10.1016/j.chom.2014.09.008.

(10) Murugesan, D.; Ray, P. C.; Bayliss, T.; Prosser, G. A.; Harrison, J. R.; Green, K.; Soares de Melo, C.; Feng, T.-S.; Street, L. J.; Chibale, K.; Warner, D. F.; Mizrahi, V.; Epemolu, O.; Scullion, P.; Ellis, L.; Riley, J.; Shishikura, Y.; Ferguson, L.; Osuna-Cabello, M.; Read, K. D.; Green, S. R.; Lamprecht, D. A.; Finin, P. M.; Steyn, A. J. C.; Ioerger, T. R.; Sacchettini, J.; Rhee, K. Y.; Arora, K.; Barry, C. E.; Wyatt, P. G.; Boshoff, H. I. M. 2-Mercapto-Quinazolinones as Inhibitors of Type II NADH Dehydrogenase and Mycobacterium Tuberculosis : Structure–Activity Relationships, Mechanism of Action and Absorption, Distribution, Metabolism, and Excretion Characterization. *ACS Infect. Dis.* **2018**, *4* (6), 954–969. https://doi.org/10.1021/acsinfecdis.7b00275.

(11) Daugelat, S.; Kowall, J.; Mattow, J.; Bumann, D.; Winter, R.; Hurwitz, R.; Kaufmann, S. H. E. The RD1 Proteins of Mycobacterium Tuberculosis: Expression in Mycobacterium Smegmatis and Biochemical Characterization. *Microbes Infect.* **2003**, *5* (12), 1082–1095. https://doi.org/10.1016/S1286-4579(03)00205-3.

(12) Beites, T.; O'Brien, K.; Tiwari, D.; Engelhart, C. A.; Walters, S.; Andrews, J.; Yang, H.-J.; Sutphen, M. L.; Weiner, D. M.; Dayao, E. K.; Zimmerman, M.; Prideaux, B.; Desai, P. V.; Masquelin, T.; Via, L. E.; Dartois, V.; Boshoff, H. I.; Barry, C. E.; Ehrt, S.; Schnappinger, D. Plasticity of the

Mycobacterium Tuberculosis Respiratory Chain and Its Impact on Tuberculosis Drug Development. *Nat. Commun.* **2019**, *10* (1), 4970. https://doi.org/10.1038/s41467-019-12956-2.

(13) Stinear, T. P.; Seemann, T.; Harrison, P. F.; Jenkin, G. A.; Davies, J. K.; Johnson, P. D. R.; Abdellah, Z.; Arrowsmith, C.; Chillingworth, T.; Churcher, C.; Clarke, K.; Cronin, A.; Davis, P.; Goodhead, I.; Holroyd, N.; Jagels, K.; Lord, A.; Moule, S.; Mungall, K.; Norbertczak, H.; Quail, M. A.; Rabbinowitsch, E.; Walker, D.; White, B.; Whitehead, S.; Small, P. L. C.; Brosch, R.; Ramakrishnan, L.; Fischbach, M. A.; Parkhill, J.; Cole, S. T. Insights from the Complete Genome Sequence of Mycobacterium Marinum on the Evolution of Mycobacterium Tuberculosis. *Genome Res.* **2008**, *18* (5), 729–741. https://doi.org/10.1101/gr.075069.107.

(14) Takaki, K.; Davis, J. M.; Winglee, K.; Ramakrishnan, L. Evaluation of the Pathogenesis and Treatment of Mycobacterium Marinum Infection in Zebrafish. *Nat. Protoc.* **2013**, *8* (6), 1114–1124. https://doi.org/10.1038/nprot.2013.068.

(15) Bernut, A.; Dupont, C.; Sahuquet, A.; Herrmann, J.-L.; Lutfalla, G.; Kremer, L. Deciphering and Imaging Pathogenesis and Cording of Mycobacterium Abscessus</Em> in Zebrafish Embryos. *J. Vis. Exp.* **2015**, *2015* (103), 1–13. https://doi.org/10.3791/53130.

(16) Lamason, R. L.; Mohideen, M.-A. P. K.; Mest, J. R.; Wong, A. C.; Norton, H. L.; Aros, M. C.; Jurynec, M. J.; Mao, X.; Humphreville, V. R.; Humbert, J. E.; Sinha, S.; Moore, J. L.; Jagadeeswaran, P.; Zhao, W.; Ning, G.; Makalowska, I.; McKeigue, P. M.; O'Donnell, D.; Kittles, R.; Parra, E. J.; Mangini, N. J.; Grunwald, D. J.; Shriver, M. D.; Canfield, V. A.; Cheng, K. C. SLC24A5, a Putative Cation Exchanger, Affects Pigmentation in Zebrafish and Humans. *Science (80-.).* **2005**, *310* (5755), 1782–1786. https://doi.org/10.1126/science.1116238.

(17) Bernut, A.; Herrmann, J.-L.; Kissa, K.; Dubremetz, J.-F.; Gaillard, J.-L.; Lutfalla, G.; Kremer, L. Mycobacterium Abscessus Cording Prevents Phagocytosis and Promotes Abscess Formation. *Proc. Natl. Acad. Sci.* **2014**, *111* (10). https://doi.org/10.1073/pnas.1321390111.

(18) Sander, T.; Freyss, J.; von Korff, M.; Rufener, C. DataWarrior: An Open-Source Program For Chemistry Aware Data Visualization And Analysis. *J. Chem. Inf. Model.* **2015**, *55* (2), 460–473. https://doi.org/10.1021/ci500588j.

(19) Madeira, F.; Park, Y. M.; Lee, J.; Buso, N.; Gur, T.; Madhusoodanan, N.; Basutkar, P.; Tivey, A. R. N.; Potter, S. C.; Finn, R. D.; Lopez, R. The EMBL-EBI Search and Sequence Analysis Tools APIs in 2019. *Nucleic Acids Res.* **2019**, *47* (W1), W636–W641. https://doi.org/10.1093/nar/gkz268.

(20) Waterhouse, A. M.; Procter, J. B.; Martin, D. M. A.; Clamp, M.; Barton, G. J. Jalview Version 2--a Multiple Sequence Alignment Editor and Analysis Workbench. *Bioinformatics* **2009**, *25* (9), 1189–1191. https://doi.org/10.1093/bioinformatics/btp033.

(21) Jumper, J.; Evans, R.; Pritzel, A.; Green, T.; Figurnov, M.; Ronneberger, O.; Tunyasuvunakool, K.; Bates, R.; Žídek, A.; Potapenko, A.; Bridgland, A.; Meyer, C.; Kohl, S. A. A.; Ballard, A. J.; Cowie, A.; Romera-Paredes, B.; Nikolov, S.; Jain, R.; Adler, J.; Back, T.; Petersen, S.; Reiman, D.; Clancy, E.; Zielinski, M.; Steinegger, M.; Pacholska, M.; Berghammer, T.; Bodenstein, S.; Silver, D.; Vinyals, O.; Senior, A. W.; Kavukcuoglu, K.; Kohli, P.; Hassabis, D. Highly Accurate Protein Structure Prediction with AlphaFold. *Nature* **2021**, *596* (7873), 583–589. https://doi.org/10.1038/s41586-021-03819-2.

(22) Varadi, M.; Anyango, S.; Deshpande, M.; Nair, S.; Natassia, C.; Yordanova, G.; Yuan, D.; Stroe, O.; Wood, G.; Laydon, A.; Žídek, A.; Green, T.; Tunyasuvunakool, K.; Petersen, S.; Jumper, J.; Clancy, E.; Green, R.; Vora, A.; Lutfi, M.; Figurnov, M.; Cowie, A.; Hobbs, N.; Kohli, P.; Kleywegt, G.; Birney, E.; Hassabis, D.; Velankar, S. AlphaFold Protein Structure Database: Massively Expanding the Structural Coverage of Protein-Sequence Space with High-Accuracy Models. *Nucleic Acids Res.* **2021**, 1–6. https://doi.org/10.1093/nar/gkab1061.